



GEOLOGICAL SURVEY OF CANADA
COMMISSION GÉOLOGIQUE DU CANADA

This document was produced
by scanning the original publication.

Ce document est le produit d'une
numérisation par balayage
de la publication originale.

BULLETIN 323

**GLACIAL DISPERSAL OF ROCKS AND MINERALS
AT THE SOUTH END OF LAC MISTASSINI, QUEBEC,
WITH SPECIAL REFERENCE TO THE ICON
DISPERSAL TRAIN**

R.N.W. DiLabio



Energy, Mines and
Resources Canada

Énergie, Mines et
Ressources Canada

1981



**GEOLOGICAL SURVEY
BULLETIN 323**

**GLACIAL DISPERSAL OF ROCKS AND MINERALS
AT THE SOUTH END OF LAC MISTASSINI, QUEBEC,
WITH SPECIAL REFERENCE TO THE ICON
DISPERSAL TRAIN**

R.N.W. DiLabio

© Minister of Supply and Services Canada 1981

Available in Canada through

authorized bookstore agents
and other bookstores

or by mail from

Canadian Government Publishing Centre
Supply and Services Canada
Hull, Québec, Canada K1A 0S9

and from

Geological Survey of Canada
601 Booth Street
Ottawa, Canada K1A 0E8

A deposit copy of this publication is also available
for reference in public libraries across Canada

Cat. No. M42-323E Canada: \$4.00
ISBN 0-660-10817-8 Other countries: \$4.80

Price subject to change without notice

Critical Reader

J-S. Vincent

Original manuscript submitted: 1977 - 05 - 24

Approved for publication: 1979 - 05 - 25

Preface

In order to assist in the discovery of mineral resources, the Geological Survey of Canada develops and assesses mineral exploration techniques. One technique is the use of glacial deposits for mineral tracing. To be successful this technique requires a thorough knowledge of all aspects of the local glacial history and of the processes that have been operative.

In this report the results of a study of glacial dispersal in central Quebec are presented. Included are detailed descriptions of the shape and origin of dispersal trains of till eroded from the Icon Sullivan Joint Venture copper deposit. These trains aided the Icon Syndicate in the discovery of the ore deposit. Till is the most common surficial sediment in the glaciated portions of Canada and this and similar studies are necessary if ways are to be found whereby dispersal trains in till may be used in mineral exploration.

Ottawa, June 1979

D.J. McLaren
Director General
Geological Survey of Canada

CONTENTS

| | |
|----|--|
| 1 | Abstract/Résumé |
| 2 | Introduction |
| 2 | Purpose and scope of investigation |
| 2 | Acknowledgments |
| 3 | Location and access |
| 3 | Previous work |
| 3 | History of exploration |
| 4 | Methods of study |
| 5 | Bedrock geology |
| 5 | Stratigraphy |
| 5 | Archean |
| 5 | Proterozoic |
| 5 | Chibougamau Formation |
| 6 | Mistassini Group |
| 6 | Southeastern gneisses |
| 6 | Structure |
| 7 | Mineral deposits |
| 7 | Copper |
| 9 | Lead and zinc |
| 9 | Quaternary geology |
| 9 | Surficial geology |
| 9 | Physiography and drainage |
| 10 | Bedrock-controlled landscapes |
| 10 | Drumlinoid landforms |
| 10 | Eskers and ice-disintegration landforms |
| 10 | Lacustrine plains and terraces |
| 11 | Regional glacial flow patterns |
| 11 | Stratigraphy and provenance |
| 12 | Unit A |
| 14 | Unit B |
| 14 | Unit C |
| 18 | Unit D |
| 19 | Unit E |
| 19 | Unit F |
| 19 | Quaternary history |
| 20 | Dispersal trains at Icon mine |
| 20 | The North train |
| 20 | Morphology |
| 21 | Origin |
| 21 | The Icon train |
| 21 | Morphology and structure |
| 24 | Origin |
| 25 | Depth of erosion |
| 25 | Comparison of prospecting methods |
| 26 | Comparison of units A, B, C, and D as sampling media |
| 28 | Sampling density versus size of dispersal train |
| 29 | Glacial comminution of chalcopyrite |
| 29 | Unoxidized till |
| 30 | Weathering of chalcopyrite-bearing till |
| 31 | Conclusions and recommendations |
| 31 | Conclusions |
| 32 | Recommendations for future research |
| 32 | References |
| | Appendices |
| 37 | 1. Methods and results of textural, carbonate, and lithological analyses of Quaternary units |
| 43 | 2. True distribution of chalcopyrite in unoxidized till |
| 45 | 3. Distribution of heavy minerals and chalcopyrite in oxidized till |
| | Tables |
| 4 | 1. Bedrock units in the Mistassini basin |
| 12 | 2. Quaternary units in the study area |
| 12 | 3. Median values of variables used to estimate the textural and lithological properties of tills in the study area |
| 28 | 4. Selected sulphide-bearing glacial dispersal trains |
| 29 | 5. Samples used for determinations of chalcopyrite abundance in till |

Figures

- 2 1. Location map
- 3 2. Schematic diagram of a failed attempt to discover the source of
chalcopyrite-bearing boulders on the west bank of Waconichi River
- 5 3. Generalized bedrock geology of the Lac Mistassini area
- 6 4. Bedrock geology of the study area
- 7 5. Bedrock geology of the Icon mine
- 8 6. View to east along strike of number one ore zone at Icon mine
- 8 7. Quartz crystals in chalcopyrite in the number one ore zone at Icon mine
- 9 8. A) Physiographic regions of the Lac Mistassini-Lac Waconichi area
B) Drainage basins of the same area
- 9 9. Surficial geology of the Lac Mistassini-Lac Waconichi area
- 10 10. Glacial landforms near Waconichi River
- 11 11. Mirror-image rose diagrams of till pebble fabrics (unit A) in the study area
- 11 12. Ternary diagram of the texture of units A, B, C, and E
- 13 13. Vertical exposure of unit A 2 km east of Icon mine showing the
fissile structure and texture of the till
- 13 14. Exposure of unit B (sand with till interbeds) about 30 m down-ice
from the western part of the subcrop of the number one ore zone
- 13 15. Folded interbedded pebbly sand and till of unit B overlain by
a thin layer of unit C
- 14 16. Ternary diagram of the texture of units A, B, and C
- 15 17. Particle size distributions of the less than -2ϕ (4 mm)
fraction of unit A and till from unit B
- 15 18. Abundance of distal rock types versus abundance of igneous and
gneissic rock types in the 4 to 64 mm fraction of unit B from
Icon mine and unit A from Icon mine and the surrounding area
- 15 19. Rain-washed surface of unit C showing its coarse rubbly texture
- 16 20. West side of groove filled with unit C cut into the number one
ore zone at Icon mine
- 16 21. Angular blocks of unit A in unit C overlying in situ unit A
- 17 22. Oblique section through light coloured lens of sand (unit B) in unit C
- 17 23. Interbedded sand and till of unit B in sharp contact with overlying unit C
- 17 24. Horizontal exposure of unit C filling oval groove in surface of unit A
- 18 25. Mining till (unit C) from the up-ice end of the Icon train
- 19 26. Boulder of chalcopyrite-bearing quartz-carbonate vein rock
in coarse gravel of unit D
- 19 27. Unoxidized varved clayey silt of unit E draped over chalcopyrite-
rich boulder in unoxidized unit C
- 20 28. Perspective plot of the abundance of copper in the <0.177 mm
fraction of the B horizon of the soil profile at Icon mine
- 21 29. Abundance of copper in the <0.177 mm fraction of the B horizon
of the soil profile over the Icon train
- 22 30. Abundance of vein rock types in the 4 to 64 mm fraction of
unit C in the Icon train
- 22 31. Perspective plot of the abundance of vein rock types in the
4 to 64 mm fraction of unit C in the Icon train
- 23 32. Longitudinal and transverse sections of the Icon dispersal train
- 24 33. Mirror-image rose diagrams of till pebble fabrics in unit C
in the northeast part of the Icon train
- 24 34. Bedrock topography of Icon mine
- 25 35. Abundance of chalcopyrite-bearing pebbles (4 to 64 mm) in unit C
in the Icon train
- 26 36. Striae and mirror-image rose diagrams of till pebble fabrics in
units A and B under the Icon train
- 27 37. A. Abundance of vein rock types in the 4 to 64 mm fraction of units A,
B, C, and D in sections on the east side of the Icon train
B. Abundance of vein rock types in the 4 to 64 mm fraction of units B
and C in sections on the west side of the Icon train
- 30 38. True chalcopyrite distributions in till samples 73-56, 73-57, 73-58, and 73-74
- 31 39. Apparent heavy mineral and chalcopyrite distributions in till
sample 72-12EU56
- 31 40. True chalcopyrite distributions in till samples 72-12EU56 and 72-12EU46

GLACIAL DISPERSAL OF ROCKS AND MINERALS AT THE SOUTH END OF LAC MISTASSINI, QUEBEC, WITH SPECIAL REFERENCE TO THE ICON DISPERSAL TRAIN

Abstract

This project was undertaken to study the patterns and processes of glacial dispersal on local and regional scales in the Lac Mistassini-Lac Waconichi area of Quebec. The following Quaternary units were mapped: unit A, lodgment till of regional extent; unit B, ice contact stratified drift and ablation till; unit C, lodgment till restricted to Waconichi Valley; unit D, ice contact or outwash gravel; unit E, varved clayey silt; and unit F, alluvium and peat. They were deposited during the Wisconsin and Holocene as the products of a simple glacial cycle of: major southward advance – recession – minor southward readvance – completed recession – glaciofluvial sedimentation – glaciolacustrine sedimentation – postglacial organic sedimentation. Lodgment tills (units A and C) were found to reflect the local bedrock lithology better than ablation till, ice contact stratified drift, outwash gravel, and postglacial lake or stream sediments.

The dispersal trains at the Icon mine are three-dimensional bodies in unit C; the North train is 1650 m long by 75 m wide, and the Icon train is 570 m long by 250 m wide. The trains have high geochemical and lithological contrast with the surrounding till. They were formed by glacial erosion (mainly quarrying), transport, and deposition during the readvance that deposited unit C. These processes were orderly, not chaotic. The mapping of dispersal trains at a detailed scale provides guidelines for mineral exploration in glaciated terrain and aids in the interpretation of glacial processes.

In various samples of unoxidized unit C, chalcopyrite has a clast mode between 8 and 1 mm and a matrix mode from 0.063 to 0.016 mm. The clast mode developed after short glacial transport, but the matrix mode required at least 100 m of transport to develop. When samples are collected during mineral exploration from an unoxidized till similar to unit C, the size range to be analyzed for copper should include the matrix mode, the size range in which glacially comminuted chalcopyrite is most abundant. Chalcopyrite is most abundant in the range 32 to 8 mm, and malachite is most abundant in the range 0.5 to 0.037 mm in strongly oxidized unit C. Sampling of oxidized carbonate-bearing copper-rich till for geochemical analysis for copper should include the malachite-bearing size range so that a representative portion of malachite is analyzed.

Mapping the abundance of chalcopyrite-bearing pebbles in the Icon train is a more efficient guide to the location of the ore in place than analysis for copper in the soil developed on the train. Therefore, when clasts containing economically interesting minerals are found in a till, the abundance of those clasts should be mapped.

Résumé

Ce projet a été entrepris afin d'étudier les modes et processus de la dispersion glaciaire aux échelles locale et régionale dans la région des lacs Mistassini et Waconichi, au Québec. On a cartographié les unités quaternaires suivantes: unité A, till de fond à l'échelle de la région; unité B, matériaux stratifiés contenant des dépôts de contact et du till d'ablation; unité C, till de fond dans la vallée de la Waconichi uniquement; unité D, dépôt de contact ou graviers proglaciaires; unité E, silt argileux à varves; et unité F, alluvions et tourbe. Ces matériaux ont été déposés pendant le Wisconsin et l'Holocène et sont les produits d'un simple cycle glaciaire: avance principale vers le sud – récession – nouvelle avance mineure vers le sud – achèvement de la récession – sédimentation fluvio-glaciaire – sédimentation glaciolacustre – sédimentation organique postglaciaire. On a découvert que le till de fond (unités A et C) reflète mieux la lithologie locale de la roche en place que le till d'ablation, les matériaux stratifiés contenant des dépôts de contact, les graviers proglaciaires, et les sédiments postglaciaires lacustres ou fluviaux.

Les traînées de débris de la mine Icon sont des masses à trois dimensions correspondant à l'unité C; la traînée Nord a 1650 m de long sur 75 m de large et la traînée de la mine Icon a 570 m de long sur 250 m de large. Les traînées présentent de forts contrastes géochimiques et lithologiques avec le till avoisinant. Elles ont été formées par érosion glaciaire (essentiellement arrachement), transport et dépôt pendant la nouvelle avance qui a déposé l'unité C. Ces processus ont été ordonnés et non pas chaotiques. La cartographie des traînées de débris à l'échelle détaillée a fourni des lignes directrices pour l'exploration minérale des terrains glaciaires et aide à interpréter les processus glaciaires.

Dans divers échantillons non oxydés de l'unité C, la chalcopryrite se présente sous forme clastique de 8 à 1 mm et en matrice de 0,063 à 0,016 mm. Le mode clastique s'est développé après un bref transport glaciaire, mais la formation de la matrice a demandé un transport sur au moins 100 m. Lorsque des échantillons sont prélevés pendant l'exploration minérale dans le till non oxydé semblable à celui de l'unité C, la gamme de dimensions à analyser doit inclure de la cas du cuivre, soit la gamme dans laquelle la chalcopryrite amenuisée est la plus abondante. La chalcopryrite est très abondante dans la gamme de 32 à 8 mm, et la malachite est très fréquente dans la gamme de 0,5 à 0,037 mm dans les matériaux fortement oxydés de l'unité C. L'échantillonnage du till à cuivre carbonifère oxydé pour l'analyse géochimique du cuivre doit inclure la gamme de dimensions contenant de la malachite de façon à permettre l'analyse d'une partie représentatif de malachite.

C'est en cartographiant l'abondance des cailloux contenant de la chalcopryrite dans la traînée Icon au lieu d'analyser le cuivre du sol qui s'est formé dans la coulée que l'on obtient de meilleures indications sur l'emplacement du minerai en place. Par conséquent, lorsque l'on découvre dans le till des roches clastiques contenant des minerais d'intérêt économique, il faudrait cartographier l'abondance de ces roches.

INTRODUCTION

Purpose and Scope of Investigation

This project was undertaken to investigate Quaternary glacial dispersal of rock and mineral particles in the Lac Mistassini - Lac Waconichi area of Quebec (DiLabio, 1976). The area was selected on the advice of Mr. A.J. Troop, formerly of Icon Sullivan Joint Venture, because that organization's property at the south end of Lac Mistassini contained a copper ore deposit with which two dispersal trains were associated. One of these, the Icon train, was well exposed, which facilitated its sampling and measurement.

The primary objectives of this project were (1) to determine the shape and size of the dispersal trains, (2) to determine their mode of origin, and (3) to find the down-ice abundance trends of their components in order to arrive at a general model of the style of glacial dispersal that might be found while prospecting in other areas. Related objectives were (1) to compare traditional soil geochemical analytical surveys with surveys involving the tracing of mineralized pebbles both as to the quality of results and costs, (2) to compare lodgment till to ablation till and ice contact stratified drift as sampling media in prospecting, and (3) to determine the grain size distribution produced by the glacial comminution of chalcopryrite in order to suggest size ranges for sampling unoxidized till by overburden drilling in other areas. Secondary objectives were (1) to compare unoxidized copper and carbonate-bearing till to its oxidized equivalent as sampling media in geochemical prospecting and (2) to estimate the depth of erosion resulting from the last glacial overriding of the copper ore deposit.

This report presents a detailed study of the stratigraphy, structure, and origin of the drift units at and near the Icon mine and provides guidelines for exploration projects in other glaciated areas.

Acknowledgments

The research for this study was carried out at the University of Western Ontario while I held a National Research Council of Canada Scholarship. Financial support was provided from National Research Council of Canada grant A4215 to Dr. A. Dreimanis, University of Western Ontario.

The following contributed to the investigation: J.N. Botsford and E.W. Watt, Icon Sullivan Joint Venture, gave permission to work on the Icon mine property; G. Darcy, mine geologist, loaned geological maps and soil geochemistry data; A.J. Troop, Icon Syndicate, suggested the project and sponsored the initial field work; A.O. Grins, University of Western Ontario, performed carbonate and textural analyses; and Dr. D.G.F. Long, Geological Survey of Canada, loaned unpublished data on the Chibougamau Formation.

Fieldwork was aided by discussions with Dr. G.O. Allard, University of Georgia; Dr. J-L. Caty and Dr. E.H. Chown, Université du Québec à Chicoutimi; and B. Warren, Ministère des richesses naturelles du Québec.

The manuscript was improved by the critical reading of Drs. A. Dreimanis, R.W. Hutchinson, G.M. Young, P.G. Sutterlin, and R.H. King, University of Western Ontario; J.A. Westgate, University of Toronto; W.W. Shilts, and J-S. Vincent, Geological Survey of Canada.

I thank Sharon DiLabio for providing able field assistance.

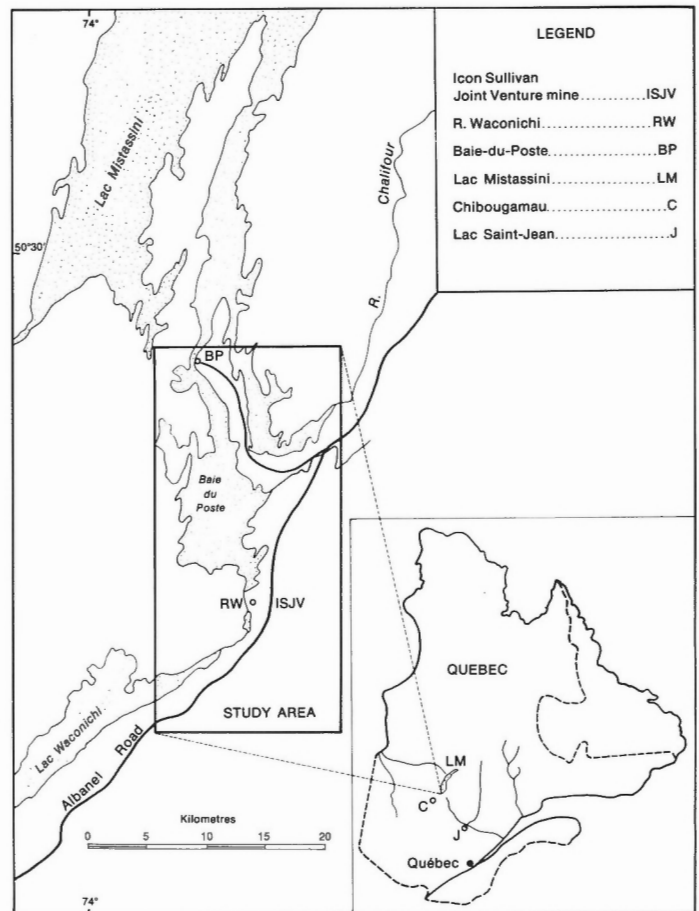


Figure 1. Location map

Location and Access

The study area comprises parts of Bignell, O'Sullivan, Gauvin, McOuatt, and Duquet townships. Detailed work centred around the Icon Sullivan Joint Venture property, which is located at the south end of Lac Mistassini (50°14'15"N, 73°48'20"W, Fig. 1). Access to the mine is via the Albanel Road from Chibougamau, 64 km to the southwest. Albanel Road is an all-weather gravel road traversing the region, and its branches and roadcuts provide good access to the Quaternary sediments and bedrock, with reduced access to the west and north parts of the study area.

Previous Work

The most comprehensive early geological observations in the Chibougamau – Lac Mistassini region are those of Richardson (1872), Low (1885, 1896, 1906), and Faribault et al. (1911). Norman (1940) described the Mistassini fault, a major feature now believed to be a sector of the boundary between the Superior and Grenville structural provinces of the Canadian Shield. Bergeron (1957) studied the stratigraphy of the Mistassini Group, which he divided into five formations. The upper unit of the Mistassini Group, the Temiscamie Formation, was studied by Quirke et al. (1960) and Neilson (1953, 1963) as a possible source of iron ore. Gilbert (1958), Deland and Sater (1967), Guilloux (1969), Duquette (1970), Chown and Caty (1973), Caty and Chown (1973), Gros (1975), and Caty (1976) described the lower units of the Mistassini Group as well as the adjacent crystalline rocks. The most detailed study of the Chibougamau Formation is that of Long (1973). Base metal mineral deposits have been described by Guilloux (1972), Troop and Darcy (1973), Caty and Chown (1973), Collins et al. (1974), and Gros (1975). Radiometric ages for the Temiscamie Formation have been determined by Quirke et al. (1960) and Fryer (1972) and for greenstones and gneisses of the Superior Province in areas south and west of the Mistassini basin, by Jones et al. (1974) and Dallmeyer (1974).

Concerning the Quaternary geology of the region, Low (1885, p. 32) made a perceptive early observation of glacial dispersal: "In the vicinity of Lake Mistassini, no rounded boulders of limestone were met with in directions to the east and north-west of the lake, and the probability is that the drift there was from north-east to south-west". Low (1896) postulated that the central névé for the Laurentide Ice Sheet was between 53° and 55°N, midway between the coasts of the Quebec-Labrador peninsula, because of the lack of glacial features in this area and the radiating pattern of striae around it. He stated that the depth of glacial erosion was not greater than 60 m and described the drumlins, eskers, and terraces of the region. Faribault et al. (1911) added a description of the crag and tail hills near Lac Waconichi and commented on the coarse texture of the tills outside the Mistassini basin.

Norman (1938) surveyed the Lake Barlow-Ojibway beaches near Lac Opémisca, 45 km west of Lac Waconichi. He also postulated a mode of origin for the De Geer moraines found below the elevations of the beaches. Norman's (1939) contention that a remnant ice cap advanced from the southeast to form an end moraine in the north end of the Mistassini basin was disputed by Ignatius (1958), who showed Norman's end moraine to be part of an outwash complex. Both authors agreed on a general deglaciation pattern of ice recession towards the northeast. Prest (1970, p. 737) gave an age of 6960 ± 90 radiocarbon years for basal organic sediments in the Chibougamau area.

Allard and Cimon (1974) suggested that only a small amount of glacial erosion may have taken place in the Chibougamau mining camp because of the presence of caps of deeply lateritized rocks on some of the ore deposits.

They suggested that this may have been due to ice stagnation at the high elevations of the camp and/or deflection of the most actively advancing parts of the ice sheet by high hills of resistant rock upglacier from the camp.

Warren (1974) mapped 1250 km², including the area of the present study; his surficial units were hummocky moraine-bedrock complex, flutings, drumlins, glaciofluvial sand and gravel, and esker sand and gravel. The project was specifically designed to provide background information for prospecting parties working in this glaciated area where bedrock outcrops are not abundant. Gros (1975) collected stream sediment samples within the same area to test the usefulness of stream sediment geochemistry as a prospecting tool.

Studies of glacial dispersal trains for prospecting purposes have taken place mostly in Fennoscandia, and many papers on such studies are found in Kvalheim (1967), in the proceedings of the conferences on prospecting in areas of glaciated terrain (Jones, 1973, 1975; IMM, 1977, 1979), in Bradshaw (1975), and in Kauranne (1976). Canadian dispersal trains that have been mapped include the Steep Rock iron ore train (Dreimanis, 1956); the train of sphalerite-bearing boulders at George Lake, Saskatchewan (Karup-Moller and Brummer, 1970); the trains derived from the ultramafic rocks at Thetford Mines, Quebec (Shilts, 1973); the Kidd Creek, Ontario train (Skinner, 1972); the train related to the Gullbridge ore deposit in Newfoundland (O'Donnell, 1973); and the Mount Pleasant train in New Brunswick (Szabo et al., 1975). Dreimanis (1958), O'Donnell (1973, p. 51-67) and Shilts (1976) provided literature reviews on the types of dispersal trains and the sediments found in them and how such trains may be used in exploration.

History of Exploration

The history of exploration of the Chibougamau-Lac Mistassini region prior to discovery of the Icon Sullivan Joint Venture copper deposit provides an example of how circumstances and inadequate understanding of local geology may combine to inhibit the discovery of an important ore deposit.

Two ore zones were present at the bedrock surface under the bed of Waconichi River at the second and third rapids downstream from Lac Waconichi on the canoe route to Lac Mistassini. A glacial dispersal train containing chalcopyrite-bearing boulders was associated with the subcrop of each ore zone on the west bank of the river. For more than 300 years Waconichi River has been the main canoe route for traders and explorers between southern points such as Chibougamau and Lac Saint-Jean and the Lac Mistassini area (Fig. 1). Low (1906) reported that

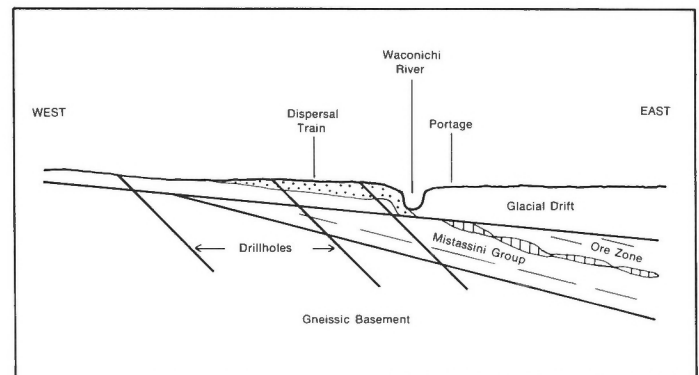


Figure 2. Schematic diagram of a failed attempt to discover the source of chalcopyrite-bearing boulders on the west bank of Waconichi River. Diagram is not to scale.

Table 1
Bedrock units in the Mistassini basin
(after Duquette, 1970; Long, 1973; Caty and Chown, 1973)

| | | |
|------------------------|---|---|
| PROTEROZOIC | Southeastern gneisses | Biotite, hornblende gneisses, and granitic gneisses. May include remobilized older units |
| | — TECTONISM — | |
| | Mistassini Group Temiscamie Formation | Sideritic iron-formation, ferruginous slate |
| | — DISCONFORMITY — | |
| | Upper Albabel Formation | Pink and buff massive dolostone |
| | Lower Albabel Formation Member F Member E Member D Member C Member B Member A | Pale grey to white dolostone Brown laminated dolostone Grey dolostone, intraformational breccias Laminated dolostone Grey argillaceous dolostone, graphitic argillite Stromatolitic and arenaceous dolostone |
| | Cheno Formation | Black to grey quartz sandstone and subarkose, arenaceous dolostone |
| Papaskwasati Formation | Green, grey, yellow quartz sandstone and subarkose | |
| — UNCONFORMITY — | | |
| Chibougamau Formation | Granitoid conglomerate, arkose, graded laminites, mixtites | |
| — UNCONFORMITY — | | |
| ARCHEAN | Granitic intrusions | Hornblende syenite to hornblende biotite diorite, granite |
| | Gneissic complex | Hornblende and biotite gneisses |
| | Roy Group Waconichi Formation | Pillowed basalt, basaltic flows, felsic pyroclastic rocks |

disseminated chalcopyrite had been seen in 1905 in arkose of the Chibougamau Formation 2 km upstream from the then undiscovered ore zones, and in 1911 Faribault et al. reported galena and sphalerite in dolostone of the Mistassini Group at the Hudson Bay Company post, 24 km downstream, both showings being on the canoe route. These discoveries undoubtedly spurred interest in the area, but because portages around the rapids had been made on the east bank of the river, the dispersal trains on the west bank went unnoticed.

In 1956, Stratmat Ltd. discovered the copper-bearing dispersal trains but was unable to locate the bedrock source of the mineralized boulders because of misunderstandings concerning the local geology. Apparently believing that the dispersal trains directly overlay steeply dipping mineralized zones like those present in greenstone belts of Superior Province, Stratmat drilled six diamond drillholes at 45 degrees through the centre of the trains (Fig. 2). The drilling results were negative partly because the trains were formed by glacial action, not by in situ weathering, and therefore were displaced from their bedrock sources, and partly because the mineralization was conformable with

gently dipping rocks of the Mistassini Group. All the drillholes were collared in the footwall rocks (G. Darcy, personal communication, 1973).

On June 4, 1965, the Icon Syndicate began ground checking of electromagnetic conductors found in its airborne survey in order to distinguish mineralized zones in the area from barren graphitic argillite beds. Only two days later, after the discovery of chalcopyrite-bearing boulders in till on the west bank of Waconichi River at the second rapids by prospector P. Bedard, the entire field party was involved in a systematic search for additional boulders in an attempt to define the source of the dispersal train. Seven trenches were excavated exposing the copper-rich till. Drilling up-ice from the train confirmed the presence of an ore deposit, and mining began May 24, 1967 (Troop and Darcy, 1973).

Methods of Study

Samples of glacial drift were collected from natural and man-made exposures near Albabel Road covering a distance of 25 km parallel with ice flow direction. Sections were measured where strata were well exposed. Pebble

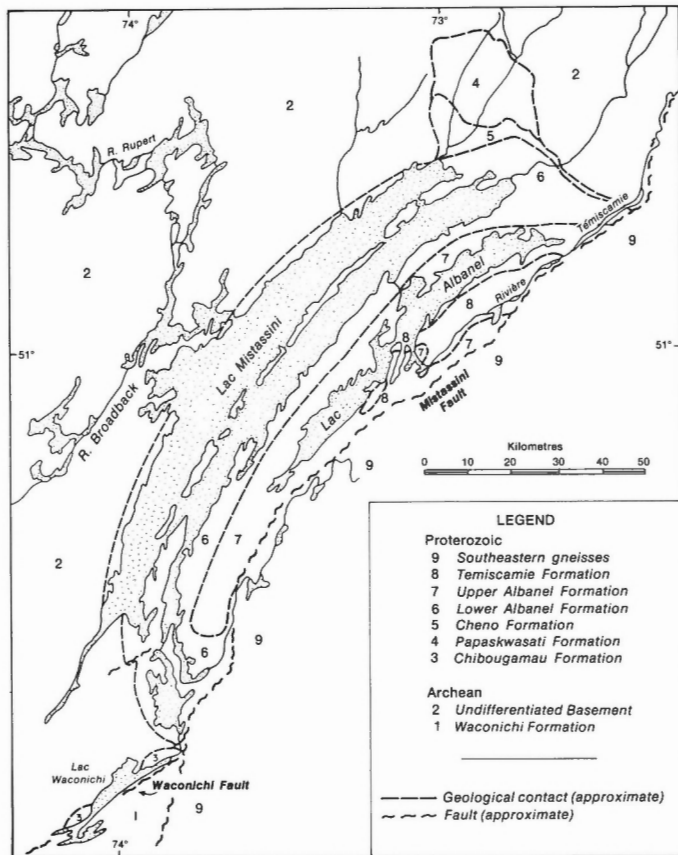


Figure 3. Generalized bedrock geology of the Lac Mistassini area. Compilation from Wahl (1953), Gilbert (1958), Neilson (1963, 1966), Deland and Sater (1967), Duquette (1970), Long (1973), Chown and Caty (1973), Caty and Chown (1973), and Caty (1976).

fabrics were measured at sites where till was found in an undisturbed state, following the procedure outlined in Appendix 1.

At the Icon mine, a base line oriented subparallel to the local striae was cut through the forest west of the Icon dispersal train and eleven crosslines were cut in the train at 61 m intervals. Samples were collected from test pits at 30.5 m spacings along the crosslines. Sequential samples were collected from sections exposed by mining. Pebble fabrics in till and striae were measured to determine ice movement directions at several localities at the mine. Four bulk samples of approximately 50 to 60 L were collected from unoxidized chalcopyrite-bearing till to determine the grain size distribution of glacially comminuted chalcopyrite.

The types of laboratory analyses that were routinely performed were: (1) textural analysis of the <4 mm fraction; (2) lithologic analysis of the 4 to 64 mm fraction; and (3) carbonate analysis of the <0.063 mm fraction. Most samples analyzed were till. Textural analysis was by hydrometer and sieve methods using a modified form of the American Society for Testing and Materials (ASTM, 1964) procedure. A modified form of the gasometric method of Dreimanis (1962) was used in the carbonate analyses to determine the amount of calcite and dolomite in the samples. The pebble fabrics were plotted as mirror-image rose diagrams using a modified version of the computer plotting program of Starkey (1970). The four bulk samples of till were examined at 1 phi intervals from -7 to 9 phi, and for each

fraction the abundance of chalcopyrite was determined volumetrically or by point counting. More detailed descriptions of the laboratory methods are in Appendix 1.

BEDROCK GEOLOGY

Stratigraphy

A study of the provenance of glacial drift units must include descriptions of the rock types present in the bedrock of the area and in the region up-ice from it. In the Lac Mistassini – Lac Waconichi area, distinctive bedrock types in and up-ice from the study area were selected as indicator rock types (Table 1). All of these units occur within the study area except for the Papaskwasati, Cheno, Upper Albanel, and Temiscamie formations, which are found up-ice from it in the Mistassini basin.

Archean

The oldest rock in the area is the Waconichi Formation, the lowest unit in the Roy Group (Duquette, 1970), which underlies the wedge-shaped area between Waconichi and Mistassini faults (Fig. 3). The rocks are dark green amphibolites derived from pillowed basalts, basaltic flows, and felsic pyroclastic rocks. Metamorphic rank of the amphibolite increases towards the Mistassini fault. Jones et al. (1974) gave a rubidium-strontium whole-rock age for the Roy Group of 2206 ± 85 Ma which is post-Archean, but may be too young because of the proximity of some of their sample sites to the Grenville Front. A few small bodies of metagabbro are found within the Waconichi Formation.

A large area north of Lac Waconichi and west of Lac Mistassini is underlain by quartzofeldspathic granitic gneisses with biotite, hornblende, and garnet as the dominant accessory minerals. Dallmeyer (1974) determined the $^{40}\text{Ar}/^{39}\text{Ar}$ incremental release ages for two samples of hornblende from these gneisses as 2517 ± 40 and 2610 ± 40 Ma. The corresponding potassium-argon ages are 2504 ± 56 and 2607 ± 62 Ma. These rocks therefore are thought to have been last metamorphosed during the Kenoran Orogeny.

A late intrusive body of plagioclase-rich hornblende syenite extends westward from the northwest shore of Lac Waconichi.

Proterozoic

Chibougamau Formation

The clastic rocks of the Chibougamau Formation (Long, 1973, 1974) unconformably overlie the Archean rocks around the eastern shores of Lac Waconichi (Fig. 3). In terms of thickness and subcrop areas, the formation is dominated by varicoloured arkoses. Thick granitoid conglomerates cap the Lac Waconichi sections. Mixtites and laminated slaty argillites with dropstones are intercalated with the arkoses in the lower portion of the succession. The metamorphic rank of these rocks is lower greenschist, and they are thought to be early Aphebian in age (McGlynn, 1970, p. 59). An age of approximately 1000 Ma for argillites from the Chibougamau Formation was determined by the rubidium-strontium whole-rock age method. The age is interpreted as a resetting of the rubidium and strontium abundances in the rocks by alkali metasomatism during the Grenvillian Orogeny (B.J. Fryer, personal communication, 1974). Because no dolostone clasts have been found in the Chibougamau Formation around Lac Waconichi, this formation is believed to be older than the adjacent Mistassini Group (Fig. 3).

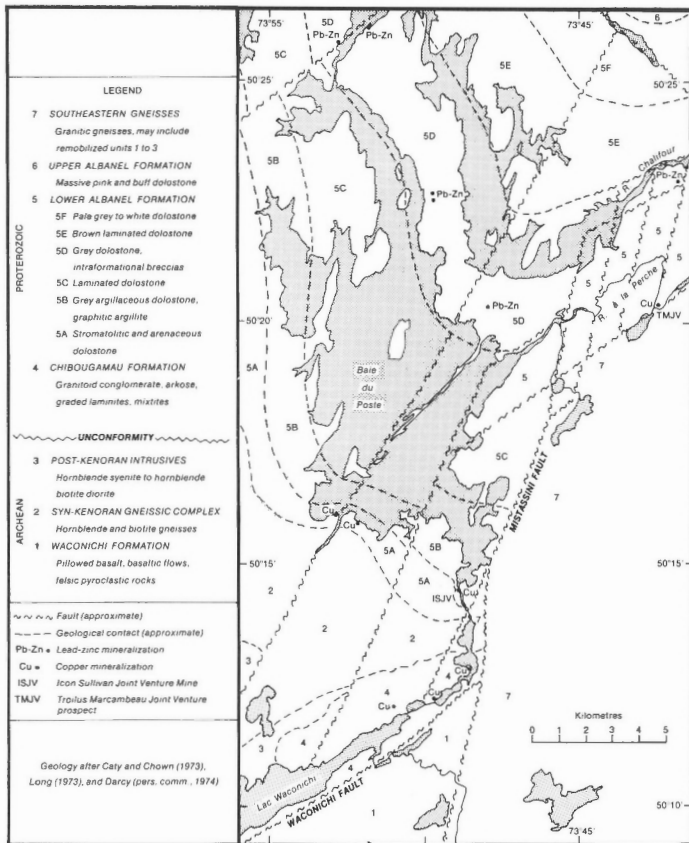


Figure 4. Bedrock geology of the study area

Mistassini Group

The stratigraphy of the Mistassini Group was first described by Bergeron (1957), but modifications and more detailed descriptions have since been provided by Neilson (1963, 1966), Deland and Sater (1967), Chown and Caty (1973), and Caty and Chown (1973). The group consists of five formations, from base to top: Papaskwasati, Cheno, Lower Albanel, Upper Albanel, and Temiscamie (Fig. 3).

As described by Neilson (1966), Chown and Caty (1973), and Caty (1976), the Papaskwasati Formation is a basal clastic unit up to 490 m thick found only around the northeast end of Lac Mistassini. The dominant rock types are pale green to greyish white arkose, subarkose, and conglomeratic arkose. Because of similarity of rock types, thicknesses, and internal stratigraphy, the Papaskwasati Formation is said by Chown and Caty (1973) to be correlative with the Indicator Formation of the Otish Group, which is exposed 40 km northeast of the Papaskwasati.

The Cheno Formation (Chown and Caty, 1973) is also restricted in distribution to the northeast end of Lac Mistassini and is a clastic rock, laterally transitional between the Papaskwasati and Lower Albanel formations. Its lower member consists of sandstone similar to that of the Papaskwasati Formation, but with a dark grey to black matrix caused by fine sericite, chlorite, iron oxides, and graphite. Black sandy dolostone and black sandstone comprise the upper member.

Caty and Chown (1973) subdivided the Lower Albanel Formation into six members (Fig. 4) which can be traced along the length of the Mistassini basin. A discontinuous

regolith separates this formation from the underlying Archean rocks on the west and south sides of the basin. Two samples of the regolith from its southern limit at the Icon Sullivan Joint Venture operation consist of pebble-sized fragments of angular, exfoliated weathered gneiss cemented by dolomite and silica. The lowest member of the Lower Albanel Formation, member A, is a thin grey arenaceous dolostone containing small stromatolites. Member B is made up of laminated argillaceous grey dolostone intercalated with five graphitic argillite beds, the lowest of which is the host for the Icon Sullivan Joint Venture ore deposit (Fig. 5). Member C is a thick grey flaggy-bedded argillaceous laminated dolostone. Member D is characterized by many intraformational breccias and black chert lenses in grey dolostone. Rusty-weathering laminated grey dolostones make up member E. Member F is transitional between the Lower and Upper Albanel formations, changing from grey argillaceous laminated dolostone at the base to pink-weathering white massive dolostone at the top. Because the Lower Albanel Formation has a large subcrop area which is parallel to the glacial trend (Fig. 3), none of its rock types is distinctive of local or distant provenance when found in glacial sediments in the study area.

In contrast to the underlying argillaceous grey dolostones, the rocks of the Upper Albanel Formation are mainly pink and buff massive dolostones (Deland and Sater, 1967). These hard and dense rocks cap a prominent cuesta between Lac Albanel and Lac Mistassini.

The work of Wahl (1953), Neilson (1953, 1963), and Quirke et al. (1960) showed that the Temiscamie Formation is made up mostly of sideritic iron-formation and ferruginous slate. Its subcrop is between Lac Albanel and the Mistassini fault, and it disconformably overlies the Lower Albanel Formation. Quirke et al. (1960) determined a potassium-argon age for argillite from the Temiscamie Formation of 1290 Ma, but they stated that this age could only approximate the time of lithification of the rock because the sample was of uncertain origin and composition. Fryer (1972) found a rubidium-strontium whole-rock age of 1787 ± 55 Ma for the Temiscamie Formation.

Southeastern Gneisses

Most metamorphic rocks of Grenville Province in this region are lithologically indistinguishable from the gneissic rocks of Superior Province. The rock types are dominantly plagioclase-quartz gneisses with hornblende, biotite, and garnet as accessory minerals. Using the potassium-argon method, Quirke et al. (1960) determined the age of biotite from Grenville Province gneiss at the northeast end of the Mistassini basin to be 1000 Ma.

Structure

The gneisses and metavolcanic rocks of Superior Province generally strike east-northeast with moderate to steep dips, whereas the metamorphic rocks of Grenville Province have a strong north-northeasterly strike.

The rocks of the Chibougamau Formation are found in an asymmetric, canoe-shaped synform on the downthrown (northwest) side of Waconichi fault. Beds in the northwestern limb dip at between 5 and 25°, whereas the southeastern limb dips 75 to 90°. Shearing extends up to 400 m from the fault (Long, 1973).

Deland and Sater (1967) stated that the rocks of the Mistassini Group form a gently north-plunging syncline, the axis of which strikes north-northeast. The folding of the group was de-emphasized by Caty and Chown (1973), who thought faults were the most important structures affecting the Mistassini Group. Stockwell (1970, p. 52) placed the

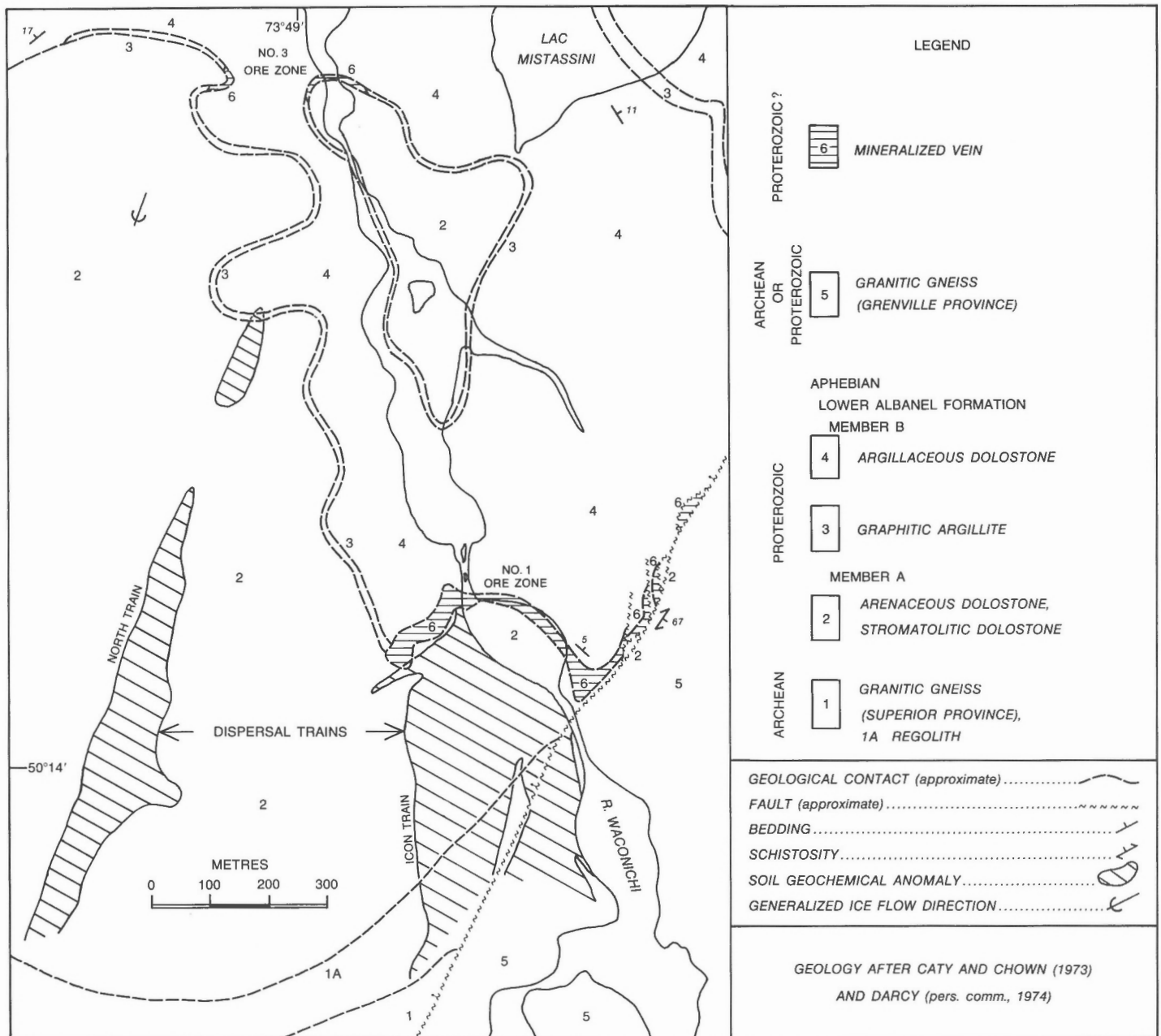


Figure 5. Bedrock geology of the Icon mine. Also shown are copper anomalies in soil over the dispersal trains.

rocks of the Mistassini Group, Otish Group, and Chibougamau Formation in the Mistassini Homocline, a subprovince of Superior Province.

In general, the rocks of the Mistassini Group strike northeast and dip at low angles towards the southeast. Near the Mistassini Fault, the attitude of the beds changes abruptly to strike northeast and dip steeply northwestward. The Mistassini fault is an east-dipping thrust (Norman, 1940) which has been interpreted as the position of the Grenville Front in this region (Laurin, 1969). Many faults in the Mistassini basin are parallel or en echelon to the Mistassini fault. Waconichi fault is the northeastward extension of the Gwillim Lake fault, which has a minimum strike length of 100 km (Duquette, 1972).

Mineral Deposits

Copper

Occurrences of copper mineralization in the Chibougamau Formation (Fig. 4) have been known for many years (Low, 1906; Faribault et al., 1911, p. 212). The Portage showing (Guilloux, 1969) is found at the foot of the falls at the outlet of Lac Waconichi. Chalcopyrite occurs there in a narrow, northeasterly trending quartz-carbonate lens and disseminated in the enclosing arkose. The Bouzan showing (Guilloux, 1969) is found near the northern limit of the Chibougamau Formation outcrop on the west bank of Waconichi River and is similar to, and probably an extension of, the Portage showing (Gilbert, 1958, p. 34). The Blondeau showing (Guilloux, 1969) is located 1200 m west of the outlet



Figure 6

View to east along strike of number one ore zone at Icon mine. The vein is the light-toned unit at the base of the section. North-dipping lens of sulphides (dark) is in the white quartz-carbonate gangue on the right side of the vein exposure. GSC 203266-P

Figure 7

Quartz crystals in chalcopyrite in the number one ore zone at Icon mine. GSC 203518-A



of Lac Waconichi, where large chalcopyrite grains occur with quartz and calcite in small fractures. Although repeatedly drilled, none of these showings has proved to be economic.

Caty and Chown (1973) and Gros (1975) reported two showings of chalcopyrite with quartz-carbonate in brecciated dolostone of member A of the Lower Albnel Formation on the south shore of Lac Mistassini west of the Icon Sullivan Joint Venture property (Fig. 4). When these showings were drilled, low copper abundances were found over narrow widths.

The geology of the Icon Sullivan Joint Venture copper deposit (Fig. 5) has been described by Troop and Darcy (1973), Guilloux (1972), and Gros (1975). The ore is in a coarse grained quartz-carbonate vein ranging in vertical thickness from 0.3 to 13 m which occurs with the lowest of the five graphitic argillite beds in member B of the Lower Albnel Formation. This concordant vein dips at about 6° to the northeast, except where it has been upturned along the Mistassini fault. The richest ore is found on the north limbs

of wallrock monoclines, the axial planes of which strike east-west and dip south (Fig. 6). These monoclines reflect undulations in the bedding of member A of the Lower Albnel Formation caused by the presence of stromatolitic mounds (Troop and Darcy, 1973; Collins et al., 1974).

The mineralogy of the vein is simple; quartz and ferroan dolomite are the most common minerals. The quartz is white and coarse grained; terminated quartz crystals up to 3 m long and 0.6 m in basal diameter have been found (Fig. 7). The ferroan dolomite is ankeritic, rusty weathering, and medium to coarse grained. A few large calcite crystals have been found with the sulphides. Chalcopyrite, pyrite, marcasite, pyrrhotite, sphalerite, bornite, and millerite constitute the sulphide minerals; chalcopyrite, commonly coarse grained, is by far the most abundant.

Most workers agree that this vein is of low-temperature hydrothermal origin, emplaced in dilatent openings on a bedding-plane thrust fault associated with the Mistassini fault (Troop and Darcy, 1973; Guilloux, 1972; Collins et al., 1974; Gros, 1975).

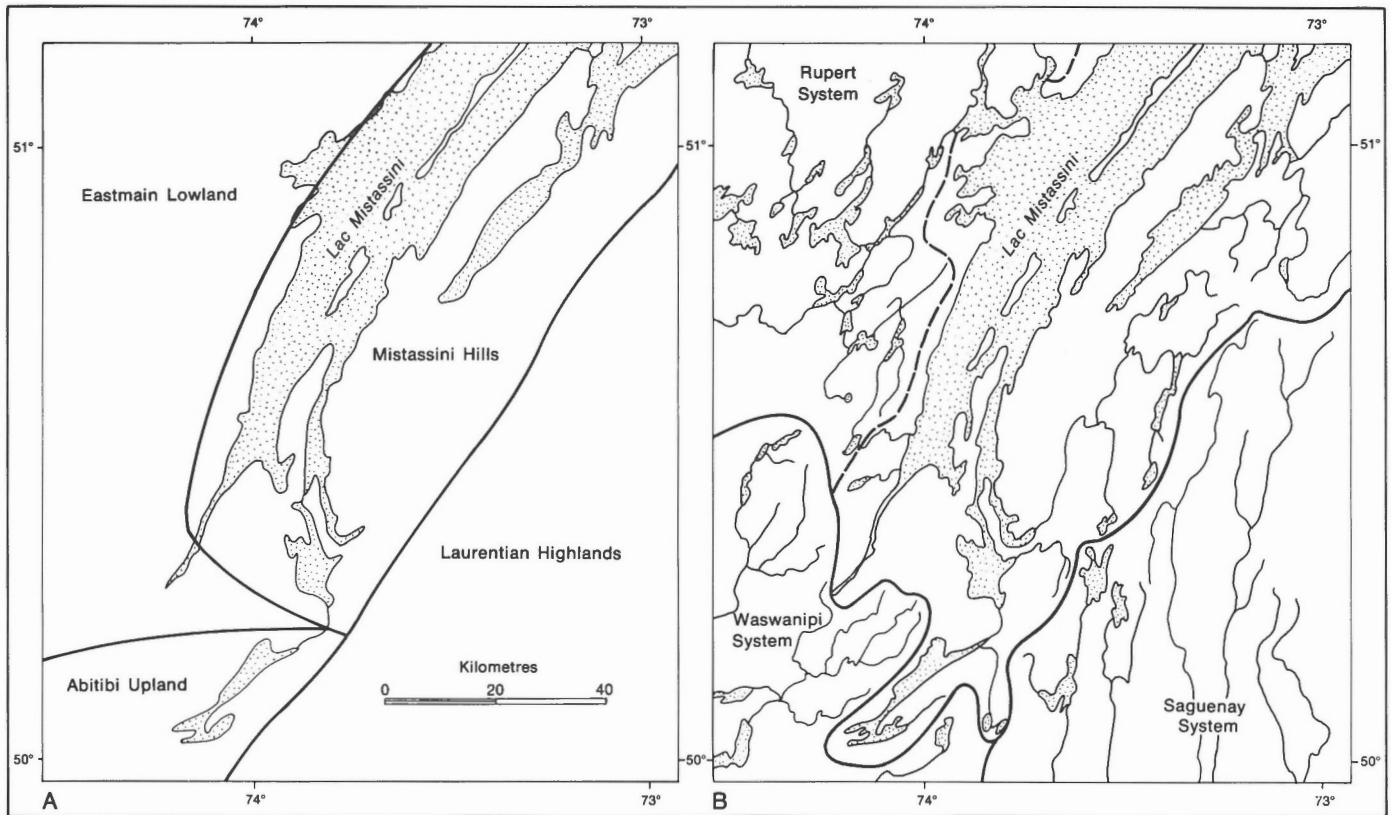


Figure 8. A) Physiographic regions of the Lac Mistassini – Lac Waconichi area (after Bostock, 1969, 1970). B) Drainage basins of the same area. The drainage divide between the Rupert River system and Lac Mistassini is shown by a dashed line.

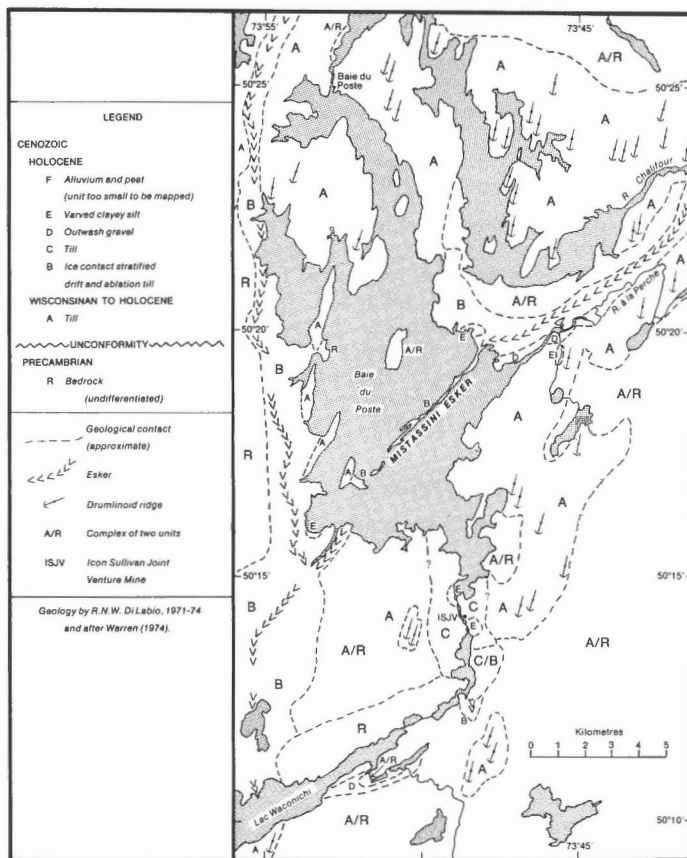


Figure 9. Surficial geology of the study area

Between May 1967, when production began, and June 1975, the mine produced 43 000 t of copper from 2 132 700 t of ore containing an average of 1.96 per cent copper. The ore was exhausted, and the mine closed in June 1975 (Fielder, 1976, p. 158).

The Troilus Marcambeau Joint Venture copper prospect is located 13 km north-northeast of the Icon Mine (Fig. 4). The mineralized zone is the fifth and uppermost graphitic argillite bed of member B of the Lower Albnel Formation. This deposit is mineralogically similar to the Icon deposit, except that quartz and chalcopryrite are less abundant. The mineralized zone has the same stratabound morphology, and its relationship to the Mistassini fault is the same as that of the Icon deposit (Forgeron, 1971; Gros, 1975).

Lead and Zinc

Caty and Chown (1973) described several occurrences of galena-sphalerite mineralization in the area (Fig. 4). All these showings are within concordant, intraformational breccias of member D of the Lower Albnel Formation in the fractured hinges of folds near minor faults. The mineralization consists of coarse grained galena, sphalerite, and carbonates between intraclasts and in fractures in the breccias. Anthraxolite is commonly found as globules with the sulphides.

QUATERNARY GEOLOGY

Surficial Geology

Physiography and Drainage

The study area includes the junction of four physiographic divisions of the Canadian Shield as defined by Bostock (1970) (Fig. 8A). The Abitibi Upland and Eastmain



Figure 10. Glacial landforms near Waconichi River (cf. Fig. 9). Drumlinoid ridges (1) are dominant; an esker segment (2) and ice-disintegration complex (3) are also present. EMR A15266-41

Lowland are underlain by Archean rocks of the Superior Structural Province; they are areas of low relief and poor drainage. The Mistassini Hills are subparallel hills and valleys partly inundated by Lac Mistassini. Most of the hills are subdued, north-facing cuestas formed of the rocks of the Mistassini Group. The Laurentian Highlands, an upland peneplain of moderate relief, are underlain by the southeastern gneisses of the Grenville Province.

The divide separating drainage into James Bay from that into St. Lawrence River follows the Grenville Front over much of its length (Fig. 8B). The drainage basin that feeds Lac Mistassini corresponds roughly with the area of the Mistassini Homocline. The lake drains into James Bay via the Rupert River system. Westward drainage of the Lac Mistassini – Lac Waconichi area is blocked by a divide having broad cols at about 440 m.

Bedrock-controlled Landscapes

Although the bedrock of the region is almost completely covered by drift, there are a few areas of abundant outcrops (Fig. 9). Chibougamau Formation conglomerates are well exposed on top of the hills north of Lac Waconichi, and the more resistant units of the Mistassini Group are exposed in the Mistassini basin.

Within the study area, no large exposures of bedrock are present except those of the Chibougamau Formation.

Drift cover is generally thick (5 to 35 m), except near drainage divides, where the bedrock surface rises to higher elevations and drift cover gradually becomes thin (less than 5 m) but continuous.

Drumlinoid Landforms

Most of the area is a drumlinized till plain (Fig. 9, 10). Flutings and drumlinoid ridges (Prest, 1968) are the most common landforms; "ideal" drumlins (Flint, 1971, p. 101) shaped like the inverted bowl of a spoon are rare. The drumlinoid ridges are up to 3 km long, 500 m wide, and 50 m high, with straight sides and level crests. On the average, they are 1.8 km long and 200 m wide (Warren, 1974), and their long axes trend north-northeast. These features are common in areas of thick drift cover over relatively soft bedrock such as the Lower Albnel and Waconichi formations. Most drumlinoid ridges are composed entirely of compact silty sand till, although some of those overlying the Waconichi Formation have bedrock bosses under their stoss ends.

Eskers and Ice-disintegration Landforms

Three eskers cross the area (Fig. 9). The south end of the generally northeast-southwest trending Mistassini esker (Ignatius, 1958) forms a long narrow peninsula in Baie du Poste of Lac Mistassini and terminates in Lac Waconichi. This large esker was first described by Norman (1939), who mapped 115 km of it to the northeastern end of Lac Mistassini. The esker and its associated flanking sand deposits are up to 3 km wide. Many steep-sided kettles adjoin the sharp-crested central ridge which is up to 40 m higher than the surrounding terrain. The southward dip of bedding and crossbedding of the esker sediments in gravel pits indicate that those sediments were deposited by southward-flowing currents. A smaller esker to the west (Fig. 9) trends southward from the settlement of Baie-du-Poste to join the Mistassini esker at the southwest end of Baie du Poste.

A small esker segment was found 3.5 km south of the Icon mine and 2.4 km east of the outlet of Lac Waconichi (Fig. 9). The sharp-crested esker trends north-south and is about 300 m long, 25 m wide, and 15 m high. Its southern end overlaps the drumlinized till plain, and its northern end disappears in an area of knob-and-kettle topography (Fig. 10). The kames and kettles in this hummocky area are interpreted as ice-disintegration deposits. No other large areas of hummocky drift were found.

Lacustrine Plains and Terraces

Several authors (Coleman, 1909; Antevs, 1925; Norman, 1938, 1939; Shaw, 1944; Ignatius, 1958; Gillett, 1962; Prest, 1970; Vincent and Hardy, 1979) have described and attempted to explain the glacial lake phases in central Quebec. The simplistic view of Norman (1939) that only one lake, Barlow-Ojibway, formed there in front of the wasting Laurentide Ice Sheet is basically correct. Prest (1970) disputed Norman's claim that this lake extended into the Mistassini basin as a single body of water. Prest (1970, p. 723-725) offered an alternative explanation by postulating that there were several overlapping lake phases between 8400 and 7500 years ago in central Quebec, having different outlets depending on the position of the ice margin during its retreat.

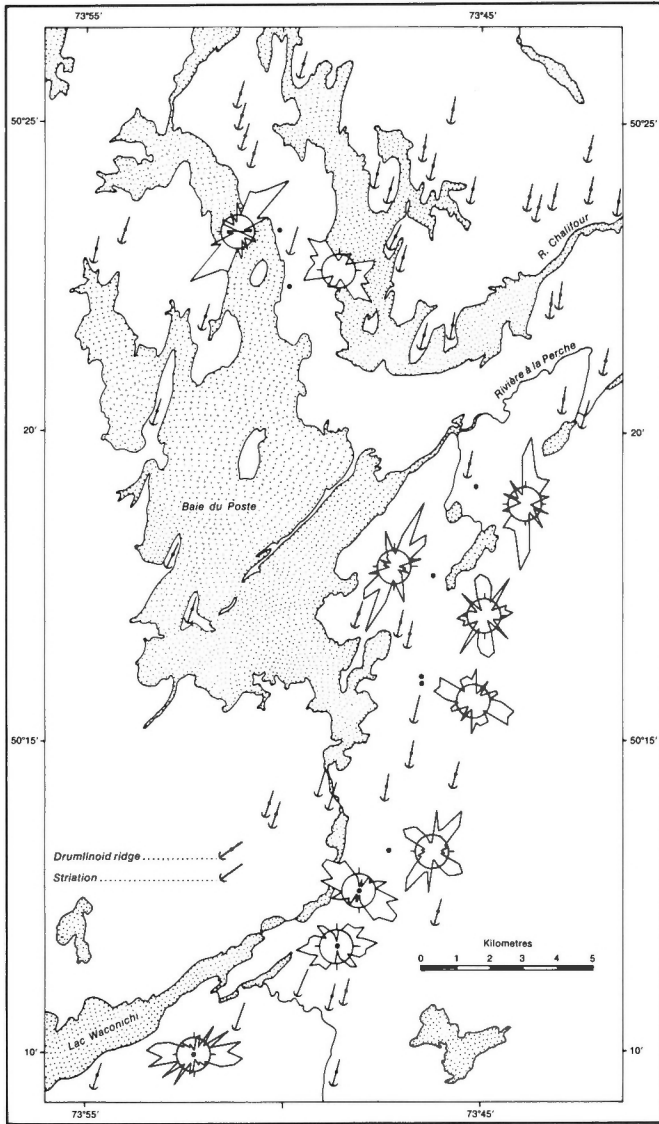


Figure 11. Mirror-image rose diagrams of till pebble fabrics (unit A, Fig. 9) in the study area. Each diagram has a scale circle at 8%. Dots represent the sample sites.

Vincent and Hardy (1979) postulated that only one lake phase existed north of the Hudson Bay - St. Lawrence drainage divide after it had emerged. This lake, Ojibway, continually drained southwards via upper Kinojevis River, and it did not undergo water level fluctuations related to the Cochrane advances. Lake Ojibway rapidly drained northward when New Quebec and Hudson Bay ice separated at the latitude of Hudson Bay about 7900 years ago.

Following this event, a small glacial lake remained in the Mistassini basin. Vincent and Hardy (1979) postulated that this lake drained towards the Tyrrell Sea initially via the Rupert River system and finally via the Eastmain system. Wave-cut terraces noted by Low (1896) around Lac Waconichi at an elevation of 393 m and by Neilson (1953) and Wahl (1953) around Lac Albanel at an elevation of 404 m probably were built by this glacial lake. Vincent and Hardy (1979) showed that the maximum elevation attained by Lake Ojibway, just before its final drainage, was about 450 m in

the southern part of the Mistassini basin. The smaller lake which persisted there after drainage of Lake Ojibway reached elevations of about 395 m at its southern end and 410 m at its northern end.

Lacustrine plains in the study area are small peat-covered areas at low elevations; one of the highest, at 381 m elevation, is at the Icon mine. Several occurrences of lacustrine silt have been mapped by Warren (1974) near the present elevation of Lac Mistassini (375 m). Undoubtedly, many other small lacustrine plains will be found under low-level bogs. Lacustrine reworking of sand on the flanks of the Mistassini esker near Baie du Poste extends to an elevation of about 395 m.

Regional Glacial Flow Patterns

The regional glacial flow patterns are best defined by the orientation of the long axes of drumlinoid ridges, striae, and pebble fabrics in till (Fig. 11). The drumlinoid ridges have little variation in their orientation within the map area, apparently being controlled by the general flow path of the glacier. On the other hand, striae on the bedrock surface vary through 40°, glacial flow being redirected locally by irregularities in the bedrock topography. There is no evidence from orientations of the drumlinoid ridges, till pebbles, or striae to indicate that the regional glacial movement occurred in more than one direction.

Stratigraphy and Provenance

Many authors have stressed the importance of understanding the stratigraphy and history of Quaternary sediments when mineral exploration projects are undertaken in glaciated terrain. Studies by Dreimanis (1960), Skinner (1972), Shilts (1971, 1973, 1976), Kokkola (1975), and others have shown conclusively that differences in provenance and transport direction, mode of transport, and depositional style will produce basic differences in the properties of the glacial drift units at a single site. Thus the units must be identified and their history deciphered so that they may be used sensibly in mineral exploration.

This section contains descriptions and interpretations of the Quaternary lithostratigraphic units (Table 2) in the study area. The interpretations are based on outcrop tracing, stratigraphic position, internal structure, geomorphology, texture of the <4 mm fraction, carbonate content of the <0.063 mm fraction, and lithology of the 4 to 64 mm fraction of samples of the units. Data from these analyses are tabulated in Appendix 1 and summarized in Table 3.

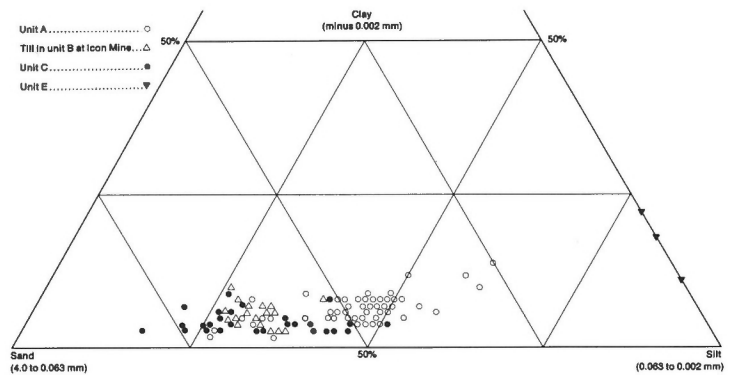


Figure 12. Ternary diagram of the texture of units A, B, C, and E.

Table 2
Quaternary units in the study area

| Time-stratigraphic unit | Lithostratigraphic unit | Materials | Distribution | Landforms | Provenance | Depositional Processes |
|-------------------------|-------------------------|--|---------------------------|-----------------------------|--------------------|--|
| HOLOCENE | Unit F | Alluvium and peat | Discontinuous, widespread | Bogs and stream beds | Local | Postglacial stream and organic sedimentation |
| | Unit E | Varved clayey silt | Discontinuous, widespread | Lacustrine plains | Regional | Glaciolacustrine sedimentation |
| | Unit D | Ice contact or outwash gravel | Discontinuous, widespread | Valley fills | Regional to local | Glaciofluvial sedimentation |
| | Unit C | Lodgment till | Waconichi Valley | Veneer on units A and B | Local | Glacial sedimentation |
| | Unit B | Ice contact stratified drift and ablation till | Discontinuous, widespread | Eskers and hummocks | Regional to distal | Ice-wastage sedimentation |
| WISCONSIN TO HOLOCENE | Unit A | Lodgment till | Widespread | Drumlinoid ridges, flutings | Regional | Glacial sedimentation |

Table 3

Median values of variables used to estimate the textural and lithological properties of tills in the study area, highly weathered sampled excluded.

Samples of units B and C are from Icon mine sites.
Data from Appendix 1.

| Unit | A | B | C |
|--|------|-------|-------|
| Number of samples | 44 | 21 | 16 |
| % clasts >4 mm | 10 | 10 | 20-35 |
| Texture of <4 mm fraction | | | |
| % sand | 45 | 62 | 60 |
| % silt | 49 | 33 | 35 |
| % clay | 6 | 5 | 5 |
| % carbonates in <0.063 mm fraction | 19 | 21 | 24 |
| Lithology of pebble fraction | | | |
| Number of samples | 44 | 24 | 22 |
| % vein rock types | 0.5 | 0.4 | 54.2 |
| % Papaskwasati and Cheno formations | 1.4 | 7.4 | 0.1 |
| % Temiscamie Formation | 0.1 | 0.1 | < 0.1 |
| % Lower Albanel Formation | 60.6 | 62.2 | 43.2 |
| % Upper Albanel Formation | 9.3 | 8.4 | 0.1 |
| % Chibougamau Formation | 0.1 | < 0.1 | 0.0 |
| % igneous and metamorphic crystallines | 27.3 | 18.5 | 0.3 |

Because access to the west and north parts of the area was limited, the mapping and sampling of the units on a regional scale must be considered as reconnaissance. This applies in particular to the distribution of units C and D (Fig. 9). A shortage of deep exposures prevented the detection of old Quaternary sediments which may be present in the area, although no old sediments were seen in the deep exposures that were available.

Unit A

This unit is the oldest and most widespread of the Quaternary units (Fig. 9). It is a hard, massive till containing about 10% of clasts larger than 4 mm. The clasts are well abraded and striated. The <4 mm fraction (matrix) of the till is a sandy silt (Fig. 12), according to Elson's (1961) classification. The <0.063 mm fraction of this till usually contains between 15 and 22% carbonates (Appendix 1), almost all of which is dolomite. The till quickly develops a subhorizontal fissility during freeze-thaw cycles above the frost line (Fig. 13). The moist colour of the till matrix ranges from dark grey (5Y 4/1; Munsell, 1971) to dark olive-grey (5Y 3/2) when unoxidized, to olive-grey (5Y 5/2) when oxidized. Oxidation reaches 5 m below surface at well drained sites. Its massive structure, poor sorting, striated clasts, and its occurrence in drumlinoid ridges indicate that unit A is a lodgment till. The orientation of drumlinoid ridges and striae, and stoss-and-lee relationships on the bedrock surface suggest that the till was deposited by a glacier that advanced from the north-northeast.

No older Quaternary units were found underlying unit A. Its maximum exposed thickness is 15 m, at the Troilus Marcambeau Joint Venture prospect. At the Icon mine, thin lenses of unit A were found between the bedrock

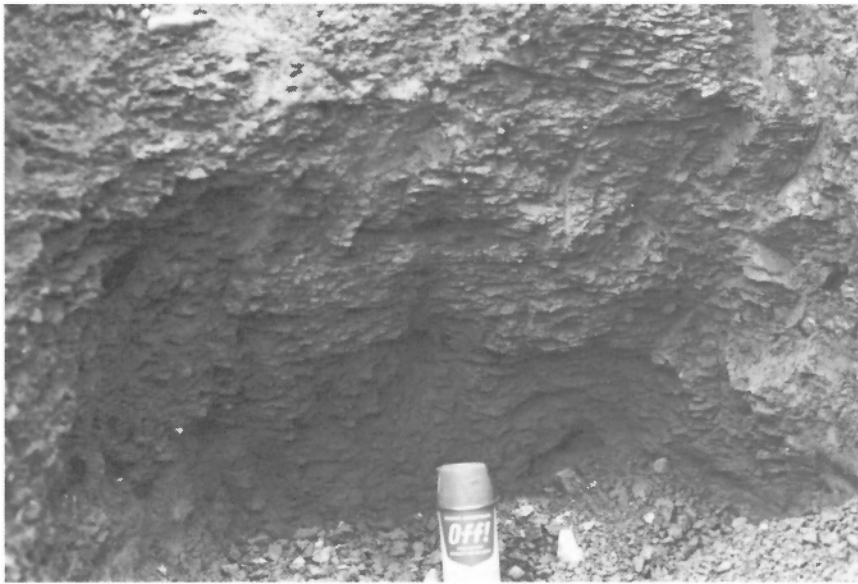


Figure 13

Vertical exposure of unit A 2 km east of Icon mine showing the fissile structure and texture of the till. GSC 203266-W

Figure 14

Exposure of unit B (sand with till interbeds) about 30 m down-ice from the western part of the subcrop of the number one ore zone at Icon mine (cf. Fig. 5). Less than 0.5 m of unit C overlies unit B in this section. The glacier that deposited unit C advanced away from the viewer. GSC 203266-O

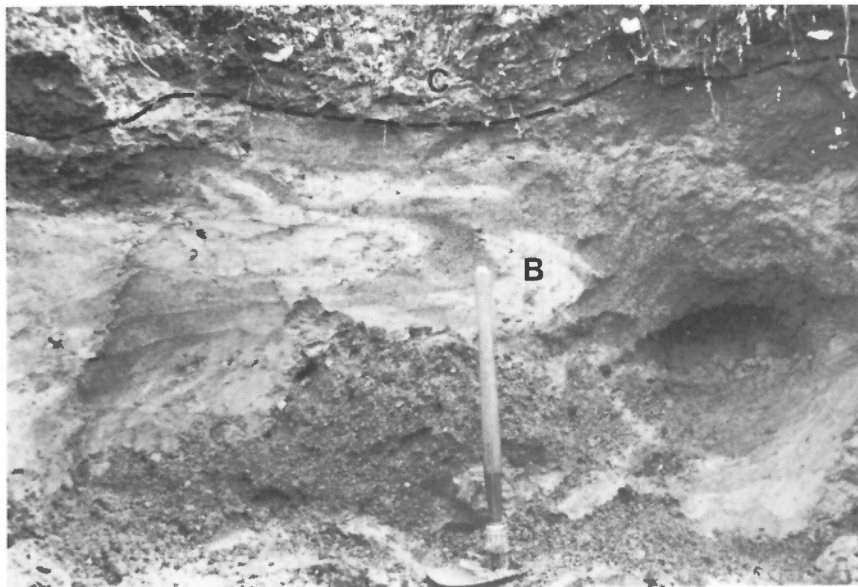


Figure 15

Folded interbedded pebbly sand and till of unit B overlain by a thin layer of unit C. The glacier that deposited unit C advanced away from the viewer. Location 1+50S, 7+20E, Figure 30. GSC 203266-R

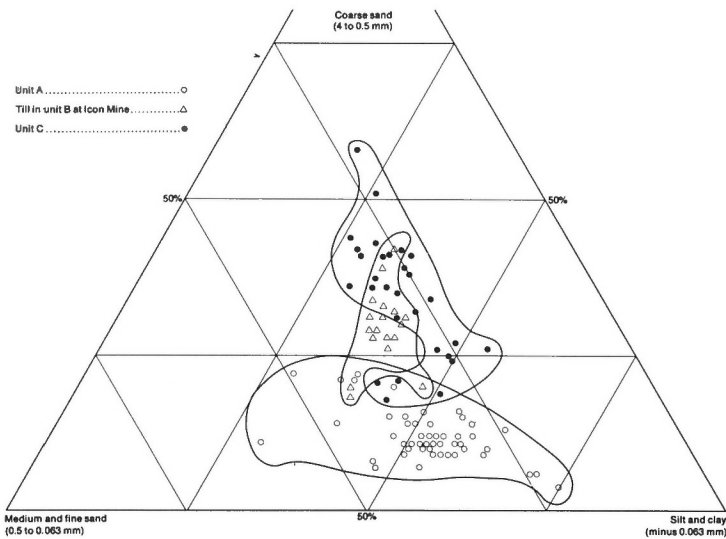


Figure 16. Ternary diagram of the texture of units A, B, and C.

and the younger Quaternary units, and blocks and slabs of unit A were found within unit C. The lithology of unit A in relation to the Icon ore deposit is discussed in the section dealing with dispersal trains.

Unit B

Unit B consists of sand, gravel, and till. It forms the eskers of the area, with sand and gravel being predominant. The esker sediments are unbedded to bedded, and normal faults are common. The grain size of adjacent beds ranges from fine sand to boulder gravel. The attitude of bedding and crossbedding is consistent with a southward-flowing depositional current.

The till in unit B occurs in two forms: as irregular bodies interfingering with the esker sediments and as a discontinuous cover over unit A. Where the till occurs as surficial material over unit A, its properties are variable. It is usually a loose, weathered bouldery sand till containing 20 to 50% of clasts larger than 4 mm. The clasts are weakly striated. Lithologically, the till is similar to unit A. The <0.063 mm fraction of three samples contains between 16 and 28% carbonates. Crude bedding exists in some exposures, and interbeds of sand and gravel are commonly so numerous that the sediment is a poorly sorted gravelly sand. Unit B is found in hummocky landforms which mask the streamlined landforms of unit A.

Unit B forms a large part of the Quaternary sequence at the Icon mine. At the mine, unit B is a convex-upward lens of sand, gravel, and till beds with a maximum exposed thickness of 7 m (Fig. 14). It is overlain by unit C, and its structures are truncated along a well defined contact. Thin patches of unit A underlie unit B. The matrix of the till beds in unit B is a loose silty sand which is dark grey (N 4/) when unoxidized and light olive-grey (5Y 6/2) when oxidized. The <0.063 mm fraction usually contains between 17 and 25% carbonates (Appendix I). The pebble content is about 10%, and many pebbles are striated. The stratified drift is mainly massive fine sand; a few lenses of poorly sorted pebble to boulder gravel occur in it. Hairpin-shaped folds in the sand and gravel are associated with till lenses; their closures are convex to the west and south, and their axial planes dip downslope relative to the surface of the unit (Fig. 15). The till beds show a gradational contact with the sand and gravel,

and they interfinger with the sand as tongues 2 to 5 cm thick. The bedding of the sand is contorted or absent near the till. These field relations and structures support an interpretation of unit B as ice contact stratified drift and ablation till deposited during wastage of the glacier that deposited unit A.

The matrix of an ablation till should be coarser than that of its associated lodgment till (Goldthwait, 1971, p. 17). Comparison of till from unit B to unit A, its most probable associated lodgment till (Fig. 12), shows that the till is coarser in unit B, but the separation of fields is poor. Using different particle size ranges in order to emphasize the coarse sand and granule (4 to 0.5 mm) fraction improves the separation of fields (Fig. 16). Another approach to this problem is to compare the cumulative curves of the tills (Fig. 17). The envelopes for the units show that the till in unit B is coarser than in unit A, and the overall similarity of the particle size distributions suggests that the tills are derived from similar glacial debris loads with the addition of relatively coarse debris to unit B.

Ablation tills are formed at and near the glacier margin during ice wastage. The debris from melting ice slides or flows off the glacier and/or gradually subsides onto the substrate. The sediments produced by these processes may contain more of the debris that was held englacially than the associated lodgment till, which is derived largely from the basal debris load of the glacier. Debris becomes part of the englacial load by compressive flow at obstructions and by erosion of bedrock bosses which protrude above the basal part of the glacier. In this way even soft debris can be transported for long distances with only minor comminution, deposition occurring by wastage in the terminal zone of the glacier. Tills that have been interpreted as ablation tills on other grounds (internal structure, texture, and geomorphology) have been found to contain more far-travelled rock types than the associated lodgment tills (Dreimanis, 1976; Shilts, 1973). Transportation as englacial debris and deposition by downmelting may be the best way to explain the presence of erratics derived from distant sources which are found near the Wisconsin glacial limit in North America (Flint, 1971, p. 176, 183).

If the till in unit B at the Icon mine is ablation till, it may contain more distal rock types than unit A. The rock types of three formations were selected as indicators of transport over great distances. The iron formation of the Temiscamie Formation and the sandstones of the Papaskwasati and Cheno formations outcrop 85 and 150 km up-ice from the Icon mine (Fig. 3). The combined abundance of these rock types was plotted against the total abundance of igneous and gneissic rock types (common rock types both locally and distally) in samples of about 400 pebbles (4 to 64 mm) from units A and B (Fig. 18). It is obvious that unit B contains much more of the distal rock types than does unit A. The unit B field overlaps that part of the unit A field which contains the points for samples of unit A from the Icon mine.

This is interpreted to mean that both units were formed from the same glacier: unit A from basal debris and unit B from basal and englacial debris. Together the two units make up a lodgment till - ablation till "couple", displaying structural, textural, and lithologic differences resulting from different provenances and modes of deposition.

Unit C

Unit C has a small outcrop area, but because it contains the copper-bearing dispersal trains at the Icon mine, it is the most important of the Quaternary units for this study. Unit C is restricted to Waconichi Valley.

Unit C is a till, the properties of which are determined by the lithology of the local up-ice substrate. Where the till was derived from the bedrock, it contains 20 to 35% of clasts

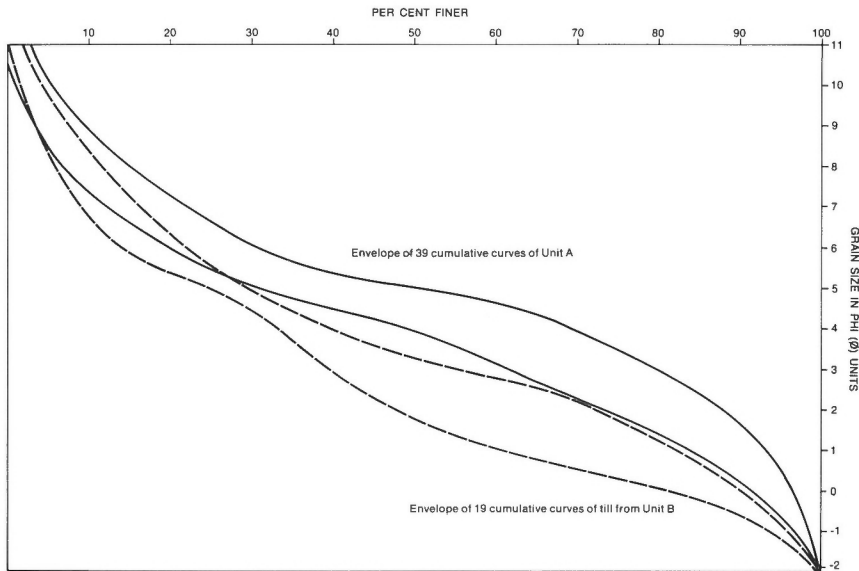


Figure 17
Particle size distributions of the less than -2ϕ (4 mm) fraction of unit A and till from unit B.

Figure 18
Abundance of distal rock types versus abundance of igneous and gneissic rock types in the 4 to 64 mm fraction of unit B from Icon mine and unit A from Icon mine and the surrounding area.

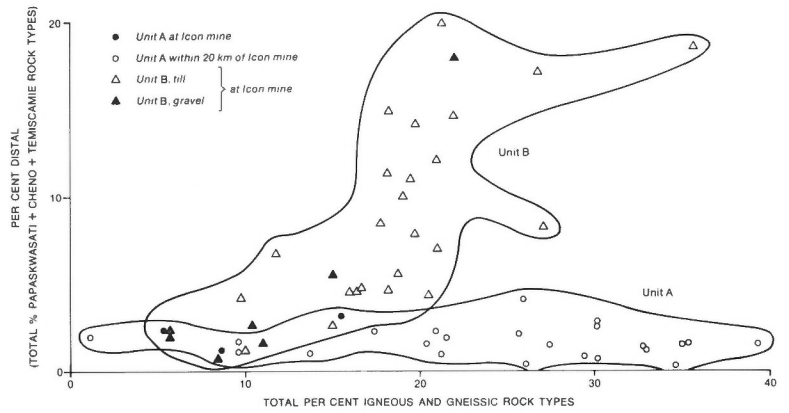


Figure 19
Rain-washed surface of unit C showing its coarse rubbly texture. Child for scale is 75 cm tall. GSC 203266-M

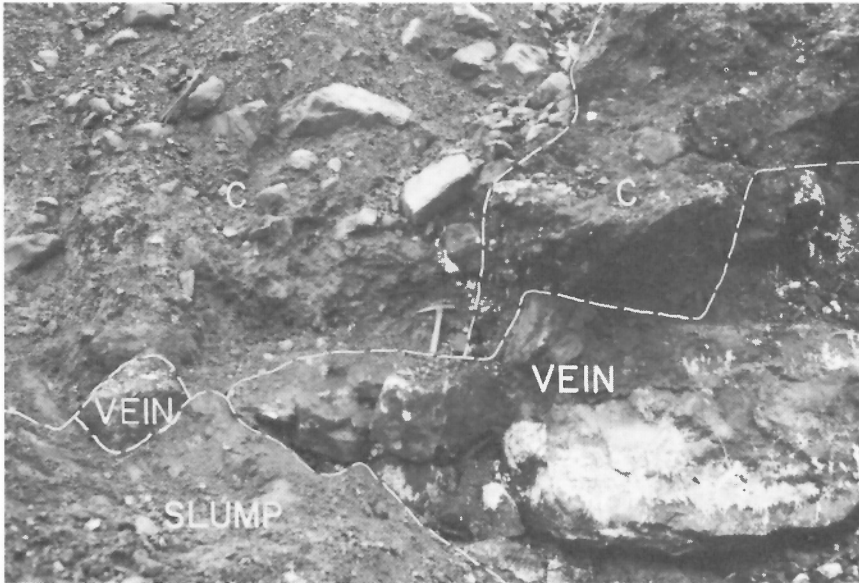
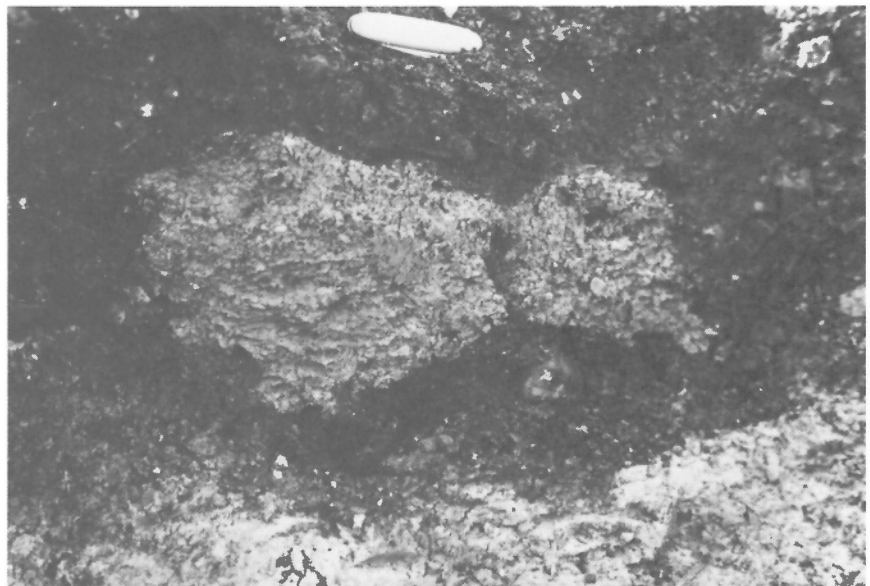


Figure 20

West side of groove filled with unit C cut into the number one ore zone at Icon mine. Note angular bedrock surface and dark lens of cemented unit C (upper right) in contact with the vein. Glacier advanced away from the viewer. GSC 203266-ZZ

Figure 21

Angular blocks of unit A in unit C overlying in situ unit A. Glacier that deposited unit C advanced from right to left. Location 2+80S, 9+20E, Figure 30. GSC 203266-Q



larger than 4 mm. Boulders up to 2 by 3 by 4 m were seen in this till. The clasts are angular and nonstriated. Clast-to-clast contacts are abundant, giving the till a rubbly appearance (Fig. 19). Clasts of soft graphitic argillite are found in the part of the till that was derived from the Icon orebody. These features, together with the presence of the dispersal trains in unit C, are consistent with a short distance of transport for most of the debris and with the domination of crushing over abrasion during transport.

The till matrix is compact and sandy. Coarse sand is more abundant in unit C than in units A or B (Fig. 16). Samples of unit C containing debris incorporated from units A and B plot in the fine end of the unit C field shown in Figure 16. Samples containing abundant vein debris plot in the centre of the field if they are unoxidized and in the coarse end of the field if oxidized.

Unit C is weathered to varying degrees. This is evident in the carbonate contents of the <0.063 mm fractions of the oxidized samples (Appendix 1) which vary from nil to 29%. The unoxidized samples (Appendix 1) contain 13 to 35% carbonates.

Where the till matrix contains abundant sand derived from unit B, it is grey (5Y 5/1) when unoxidized and light olive-grey (5Y 6/2) when oxidized. If the dominant debris was derived from member B of the Lower Alanel Formation, which constitutes the rocks overlying the vein, the oxidized colour is olive-brown (2.5Y 4/4). In the dispersal trains, graphitic argillite from the vein colours the unoxidized till black (N 2.5/); iron-rich vein minerals give the oxidized till a dark brown (7.5YR 3/2) colour. Lenses of till cemented by malachite are pale green (5G 6/2); those cemented by limonite are yellowish brown (10YR 5/8).

Where unit C overlies bedrock, striae showing an ice flow direction between 190 and 200° are found on the bedrock surface, although most of the bedrock surface is angular and nonstriated (Fig. 20). The contact between unit C and units A and B is marked by deformations in the sediments. Angular, fractured blocks and slabs of unit A, up to 40 by 20 by 20 cm, are displaced up to 80 cm vertically from their original position and are found as isolated 'boulders' in unit C (Fig. 21). They probably were transported down ice as well as vertically. Folded, stretched lenses of

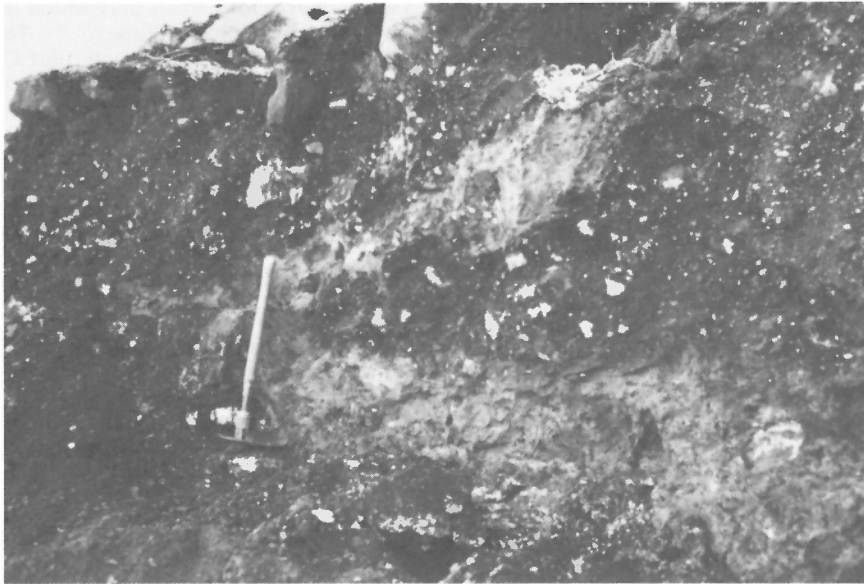


Figure 22

Oblique section through light coloured lens of sand (unit B) in unit C. Direction of glacial advance was away from the viewer. Location 2+20S, 8+20E, Figure 30. GSC 203266-S



Figure 23

Interbedded sand and till of unit B in sharp contact with overlying unit C. Glacier that deposited unit C advanced away from the viewer. Location 2+50S, 8+20E, Figure 30. GSC 203266-X

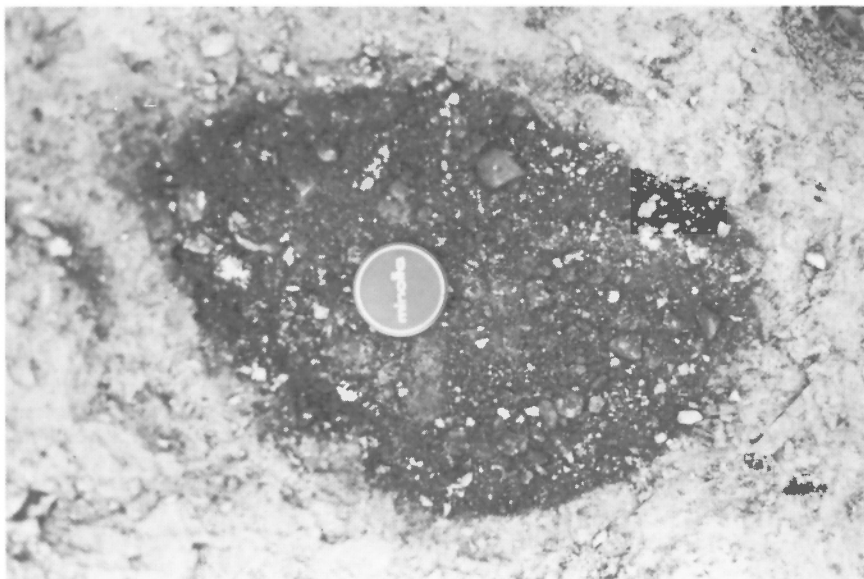


Figure 24

Horizontal exposure of unit C filling oval groove in surface of unit A. Glacier that deposited unit C advanced from right to left. Location 3+20S, 10+50E, Figure 30. GSC 203266-L



Figure 25. Mining till (unit C) from the up-ice end of the Icon train. Mound of unit B is light-toned area exposed by stripping in left background. Glacier that deposited unit C advanced away from the viewer. GSC 203518

massive sand from unit B are found in unit C. One 25 cm thick sand lens is in a tight, asymmetrical overturned antiform, the axial plane of which dips north at about 10° (Fig. 22); its wavelength is about 1 m, and its amplitude is 2 m. The contacts of the sand with the enclosing till are diffuse. Thrust faults in sand of unit B extend from the contact with unit C to 40 cm vertically below the contact; the faults dip north at 15° . The bedding of unit B is cleanly truncated everywhere along the contact, which is sharp and clearly defined by the textural and lithologic differences between the two units (Fig. 23). Numerous grooves are found on the surface of units A and B where they are overlain by unit C. The grooves are up to 5 cm deep, 20 cm wide, and 40 cm long; they are oval in plan with major axis orientations showing an ice flow direction of 190 to 200° (Fig. 24). One anomalously large groove was found at the west end of the number one ore zone (Fig. 20); it is 5 m deep and 8 m wide and is cut into the vein on its west side and unit B on its east side. The base of this groove rises rapidly to where it is only 1.5 m below the surface at a distance of 50 m south of its deepest point.

Unit C, which is interpreted as a lodgment till, is generally less than 1 m thick. At many sites it is so thin that it is entirely above the C horizon of the soil profile, and at others it is found only in the upper half of the B horizon. It has a maximum thickness of up to 6 m (i.e., in the aforementioned large groove), but this measurement is exceptional; the true maximum thickness is about 3 m. Most measurements of thickness are vertical and not true because unit C generally was deposited on pre-existing sloping surfaces (Fig. 25).

Unit C is usually found at the surface. It is overlapped by units D, E, and F in small areas near Waconichi River. The transition from unit C to the younger units marks a change from glacial sedimentation to fluvial and lacustrine sedimentation.

Although unit C can be seen to overlie units A and B in sections at the Icon mine, the genetic relationship between unit C and the older Quaternary units is unclear. It is believed that units A and B are a basal till – ablation till "couple" and that they are glacial deposits of regional extent.

Unit C is a volumetrically small unit which is found only in Waconichi Valley. To determine the relationship between unit C and older units, exposures were examined near the subcrop of the number three ore zone at the Icon mine (Fig. 5). Unit C is present there as a bouldery silt till containing contorted lenses of silt, and as crushed and deformed pebble gravel which is possibly the result of glacial reworking of glaciolacustrine silt and ice contact gravel. Neither older unit could be identified. Sections north of Baie du Poste contain only units A and B.

The southern edge of unit C is difficult to determine. Unit C thins rapidly south of the mine, and it is not found in sections outside Waconichi Valley. The esker segment 3.5 km south of the mine (Fig. 9) is interpreted as unit B. If the associated ice-disintegration complex is interpreted as unit B, which the glacier that deposited unit C overrode and upon which it stagnated, the ice-disintegration complex is the terminal position for the glacial advance that deposited unit C. The thinning of unit C south of the mine may have been caused by flotation of the ice margin in glacial Lake Ojibway.

Unit C thus is interpreted as a lodgment till deposited during a southward readvance of a small tongue of ice out of Baie du Poste into glacial Lake Ojibway. Unit C is probably part of the drift unit containing units A and B; they are the products of a major advance (unit A), retreat (unit B), and minor readvance (unit C) of the same ice sheet.

Unit D

Unit D is bouldery gravel which fills Waconichi Valley. The sediment has an intact framework and is loose and crudely crossbedded; the crossbedding is variable in attitude but is consistent with a southward-flowing depositional current. The clasts are generally well rounded, and some are striated; they make up 20 to 50% of the sediment volume. The matrix consists of compact coarse sand with a low content of fine sediment. Seven samples of the unit D matrix have averages of 59% sand (4.0 to 0.063 mm), 38% silt (0.063 to 0.002 mm), and 3% clay (<0.002 mm). The <0.063 mm fraction of these samples contains an average of 21 per cent carbonates. The unit fills a north-south trough in the bedrock surface to a maximum thickness of 6 m at the Icon mine under the bed of Waconichi River.

Unit D overlies unit C at the north end of the Icon dispersal train. The contact between the units is sharp and may be erosional. Unit D is the Quaternary unit that overlies most of the subcrop of the number one ore zone at the mine. Nevertheless, only two boulders and nine pebbles derived from the vein were found in about 2000 m² of its exposure. Both boulders were well rounded quartz-carbonate gangue containing traces of chalcopyrite (Fig. 26). The transport distance from the source area was probably less than 400 m.

The crudely crossbedded nature of this unit, its geometry, and the lack of vein rock types indicative of local erosion support the conclusion that unit D is ice contact or proximal outwash gravel which was deposited in Waconichi Valley during final deglaciation. Similar units of sand and gravelly sand were found filling other valleys (Fig. 9).



Figure 26. Boulder of chalcopyrite-bearing quartz-carbonate vein rock in coarse gravel of unit D. Boulder is 1 m above the contact between unit D and down-ice subcrop edge of the number one ore zone. Location 3+50S, 12+50E, Figure 30. GSC 203266-Z



Figure 27. Unoxidized varved clayey silt of unit E draped over chalcopyrite-rich boulder in unoxidized unit C. Boulder is about 2 m below present land surface. Location 2+00S, 8+50E, Figure 30. GSC 203266-U

Unit E

Unit E consists of silty varves which fill depressions in the older units up to about 381 m elevation. It has been found overlying units C (Fig. 27) and D at the Icon mine and overlies units A and B at lower elevations near Lac Mistassini. Unit E, which is up to 5 m thick, has a lake plain landform.

The varves are usually about 1 cm thick and are dominated by the silty (summer) layer. In a section overlying the eastern end of the number one ore zone of the Icon mine (Fig. 5), 210 varves were counted in an interval 2 m thick. Because of their thinness and the lack of dropstones, current bedding, and sand, they are interpreted as distal varves. Three channel samples of unit E have averages of 17% clay, 83% silt, and no sand; the same samples contain an average of 10% carbonates.

Unit F

Unit F consists of alluvium and peat. The alluvium has a high content of cones, twigs, and pelecypod shells. It is up to 2 m thick on the bed of Waconichi River but also was seen as a thin (2 cm) sand layer supporting large articulated pelecypod shells overlying unoxidized chalcopyrite-bearing unit C on the riverbank. One sample from the thickest section of alluvium contained 91% silt and traces of sand and clay; the sample contained 7% carbonates in the <0.063 mm fraction.

Peat is found in poorly drained sites and commonly directly overlies unit E to a maximum thickness of 1 m. It is well stratified, compressed, woody, and fibrous. Prest (1970, p. 737) gave a radiocarbon date of 6960 ± 90 years for gyttja beneath peat near Chibougamau, 65 km south of the study area. This date indicates the onset of organic growth and not the time of deglaciation, which probably occurred several hundred years before the development of the peat. Revegetation began after the glacial Lake Ojibway episode.

Quaternary History

Stratigraphic evidence presented by McDonald (1971), McDonald and Shilts (1971), Gadd (1971), Skinner (1973), and Grant (1975) supports a conclusion that the study area was covered by the Laurentide Ice Sheet from the start of the Wisconsin Stage until deglaciation during the Holocene. The study area is near the presumed starting position of the Laurentide Ice Sheet, central New Quebec, and it would have been deglaciated early in the history of the ice sheet. There is no evidence in the area to support a concept of glacial retreat to the north during either the St. Pierre or Port Talbot Interstadial. All Quaternary units therefore are Wisconsin to Holocene in age; moreover, most are relatively young, the products of deglaciation. Prest's (1970) postulated deglaciation sequence showed that the Lac Waconichi - Lac Mistassini area became ice free between 7800 and 7500 years ago, whereas Vincent and Hardy (1979) showed that the area became ice free as early as about 8100 years ago, so all units deposited during deglaciation (units B to F) are Holocene, that is, less than 10 000 years old (Hageman, 1971).

Glaciation by the Laurentide Ice Sheet began in the early Wisconsin, and through a series of oscillations, eventually culminated during the Nissouri Stadial (Dreimanis and Karrow, 1972) when the ice margin reached southern Ohio. Unit A was deposited during this glaciation, but it is not known whether the till was deposited during the advance or recession, or both. Unit A forms the drumlinoid ridges of the area, which because of their streamlined morphology are thought to have formed during active phases of glaciation,

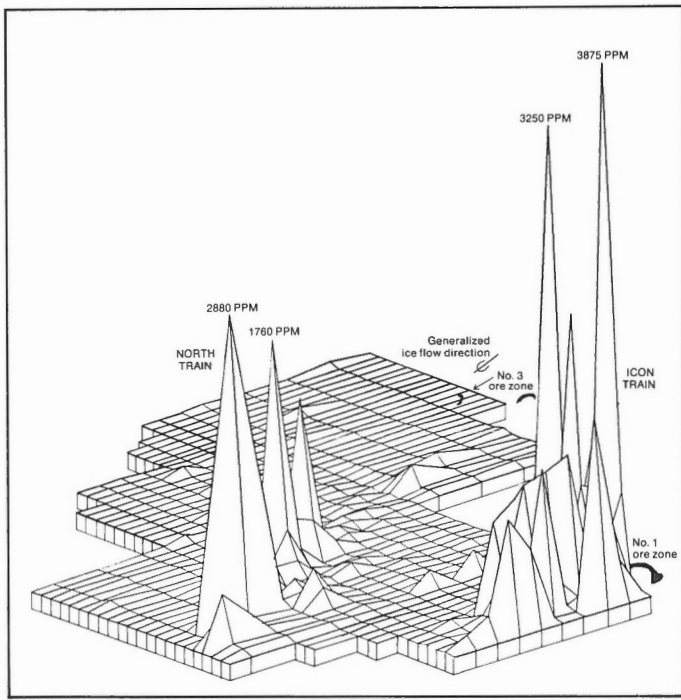


Figure 28. Perspective plot of the abundance of copper in the <0.177 mm fraction of the B horizon of the soil profile at Icon mine, viewed from the southeast. Small grid rectangles represent 100 by 200 ft. (30.5 by 61 m). Plot produced at the University of Western Ontario computer centre by program called PLT3DI from data supplied by Icon Syndicate and Icon Sullivan Joint Venture.

but the glacier probably was active during deglaciation, a process noted along this ice margin near James Bay (Vincent, 1977). Because these landforms were ice covered until about 7900 years ago (Vincent and Hardy, 1979), the age of unit A can be defined no more narrowly than Wisconsin to Holocene.

During deglaciation, with the ice margin in glacial Lake Ojibway, unit B was deposited as eskers and ablation drift. It is a diachronous unit of Holocene age.

After a short stillstand, the ice front readvanced from Baie du Poste up Waconichi Valley to 3.5 km south of the Icon mine, depositing unit C. The readvance eroded the older Quaternary units and the Icon vein, resulting in the formation of dispersal trains in unit C. Based on the deglaciation sequence of Vincent and Hardy (1979), unit C probably was deposited after 8200 years and before the drainage of Lake Ojibway, about 7900 years ago (Hardy, 1977).

Glaciofluvial activity followed, with meltwater streams flowing south from the receding glacier margin and producing the coarse ice contact or proximal gravel of unit D.

During late Lake Ojibway time, low-level varved sediments of unit E were deposited. At least 210 years of deposition took place, as recorded by varve counts. After drainage of Lake Ojibway about 7900 years ago, a small proglacial lake persisted in the Mistassini basin. The level of this lake was a few metres above the present level of Lac Mistassini, with successive outlets via the Broadback, Rupert, and Eastmain river systems. The lake is interpreted to have existed about 7500 years ago (Prest, 1970, Fig. 16w). The establishment of organic growth and modern streams in the area produced unit F.

An alternative explanation of the Quaternary history is that units A and B in sections at the Icon mine are pre-Wisconsin in age. In this scheme, unit C would be a

lithologically anomalous part of what has been mapped as unit A in the drumlinized till plain around the south end of Lac Mistassini. On the other hand, although there is an unconformity between unit C and the older units at the mine, no evidence (weathering profiles, fossils, nonglacial sediments) was found to indicate that the older units had undergone a nonglacial interval. The unconformity is believed to be an erosional one (Fig. 21-24), caused by the glacial readvance that deposited unit C.

DISPERSAL TRAINS AT ICON MINE

Two dispersal trains were discovered by the Icon Syndicate and Icon Sullivan Joint Venture by boulder and pebble prospecting and by traditional geochemical analyses for copper in the <0.177 m fraction of the B horizon of the soil (Fig. 28). Soil samples were taken every 31 m along lines spaced 62 or 124 m apart, so that the boundaries of the trains may be defined accurately. Of the 666 samples taken in the soil survey, 96 were judged to contain anomalously high amounts of copper (that is, their copper contents were above the 85th percentile of the cumulative frequency distribution). The anomalous samples contained at least 60 ppm copper. Troop and Darcy (1973) stated that background for copper in the soil is about 12 ppm. The boundaries of the trains (Fig. 5) are placed at the 60 ppm contour of copper in the soil.

For purposes of discussion, the trains are called the "North train" and the "Icon train". The Icon train was traced to its source in the exploration program that discovered the mine, but the North train was mapped late in the life of the mine.

The North Train

Morphology

The North train first reaches the surface 430 m down-ice from the eastern subcrop of the number three ore zone (Fig. 5). Soil geochemistry indicates that the train is not recognizable up-ice from that point, and unfortunately, no information exists concerning the nature of the till-ore contact because of mining disturbances. If the train exists closer to the ore subcrop in the subsurface, it is masked by the varved silt and clay of unit E, which is the surficial sediment down-ice from the ore subcrop (Fig. 9). The train is exposed discontinuously for at least 1220 m. The down-ice end of this train is outside the limit of the geochemical survey, but it is at least 1650 m down-ice from the ore zone. The train is narrow, about 75 m wide, but it locally reaches a width of 185 m. It is linear or ribbon shaped, as detailed mapping of Fennoscandinavian trains has shown (Wennervirta, 1968), not fan shaped as most glacial dispersal trains have been thought to be (Hawkes and Webb, 1962, p. 186-188; Levinson, 1974, p. 455-458). The train points directly up-ice to the eastern subcrop of the number three ore zone (Fig. 5, 28) and is oriented south-southwest (195°).

Pits and trenches excavated in the North train exposed unit C containing quartz-carbonate clasts derived from the vein. The vein clasts were larger and more abundant in the up-ice part of the train than they were in the down-ice part, although their abundance was not mapped. A few of these pebbles and boulders contained traces of chalcopyrite. Quaternary unit C is 1 to 2 m thick and directly overlies barren member A of the Lower Albnel Formation.

The B horizon of the soil developed on the till contains up to 2880 ppm copper. Six of the 35 anomalous samples in the train contained more than 300 ppm copper, and these high copper abundances were found in the down-ice part of the train (Fig. 28). The contrast is great between the copper abundances outside the train and those within it; that is, the boundaries of the train are sharp and the abundances of

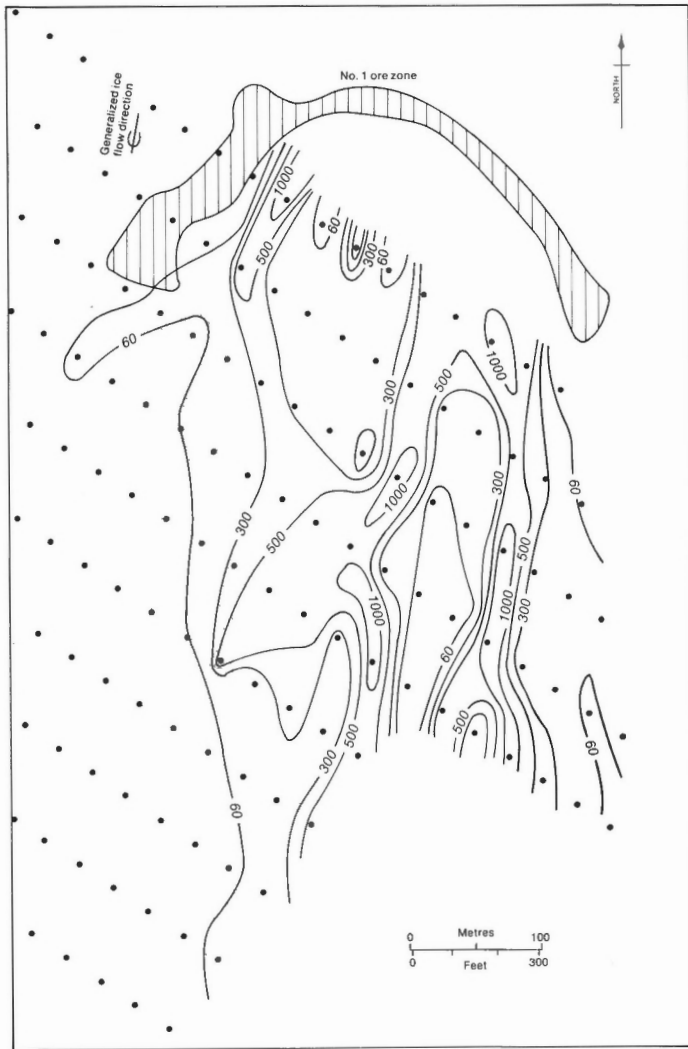


Figure 29. Abundance of copper in the <0.177 mm fraction of the B horizon of the soil profile over the Icon train. Dots represent sample sites. Contours are labelled in parts per million copper. Data supplied by Icon Syndicate.

copper in the soil commonly changes from background outside the train to 10 or 100 times background within the 31 m distance in which the boundary exists. When viewed as a perspective plot of the soil copper results (Fig. 28), the North train appears as a sawtoothed ridge standing high above a flat background plain.

Comparison of the elevation of the top of number three ore zone to the highest known elevation of till in the train indicates that debris derived from the ore zone was transported upslope by the glacier through a vertical distance of 55 m in a horizontal path length of 1280 m. Therefore, glacial debris was transported upslope at a gradient of up to 43 m/km. This gradient is similar to the steepest ones listed by Flint (1971, p. 111) for much longer transport distances.

Origin

The North train was formed by erosion of the eastern subcrop of the number three ore zone by the glacial readvance that deposited unit C. The subcrop is now small and arcuate (Fig. 5), and assuming its size and shape are similar to what they were before erosion, the glacier

traversed an arcuate subcrop width of up to 30 m (mostly about 10 m) along a strike length of 100 m, measured at right angles to the direction of glacier flow. This part of the ore zone contained abundant copper; a steeply north-dipping lens of massive chalcopyrite up to 3 m in subcrop width was found in it. The entire number three ore zone, including weakly mineralized parts, contained 144 041 t of ore with an average copper content of 7.28% (Troop and Darcy, 1973).

The strong linearity and sharp edges of the train are evidence of consistent glacial flow in one direction, towards 195°, as indicated by the orientation of striae and the train. There apparently were no major obstacles to glacial flow because the train does not bend or broaden markedly. The glacier transported the debris in an orderly manner, and it was impeded only by the gradient of the bedrock surface. It is interesting to note that the train is usually narrower than the strike length of its source (100 m). This may mean that the train, as defined by the copper anomaly in the soil, was derived from the subcrop of the small lens of massive chalcopyrite in the eastern part of the number three ore zone, rather than from the entire mineralized subcrop.

The apparent down-ice decrease in the abundance of vein pebbles and increase in copper content of the soil may indicate that comminution of the clasts proceeded during transport. Older Quaternary units do not underlie unit C in the train, and assuming that older units were removed by the advance, dilution from such sources of debris was possible. The Lower Albanel Formation also could have supplied debris (Fig. 5).

The high copper content of a few of the soil samples was caused by the presence of malachite, a product of the fixation as a carbonate of copper released during the oxidation of chalcopyrite. No hydromorphic anomaly, however, was produced downslope from the train. The copper was fixed near its source in the soil because carbonates were abundant there. Pyrite and marcasite, which on weathering would produce acidic groundwater to remove copper in solution, were rare in the till.

One unexplained problem is the apparent lack of a dispersal train derived from the western subcrop of the number three ore zone (Fig. 5, 28). No dispersal train, which should lie within the limits of the geochemical soil survey, was detected. The western subcrop of the ore zone however is smaller than the eastern one; the glacier traversed an arcuate subcrop width of up to 50 m along a strike length of 40 m. In addition, the orebody here is only about 0.4 m thick and is weakly mineralized. The small size and low chalcopyrite content of the western subcrop of the number three ore zone may explain the absence of a related soil anomaly. A few boulders of barren quartz-carbonate vein material are found in unit C where the train should be, but no systematic search for the boulders was conducted. If it exists, this train probably would contain only barren quartz-carbonate clasts.

The Icon Train

Morphology and Structure

The geochemical soil survey conducted by the Icon Syndicate revealed 61 anomalous samples in the Icon train, down-ice from the subcrop of the number one ore zone (Fig. 5, 29). Twenty-eight of the samples contained more than 300 ppm copper. When defined by the soil anomaly (Fig. 29), the train is a broad flame-shaped body having two bands of high copper abundance oriented parallel to the glacial transport direction as determined from striae, indicating an ice flow direction towards 195°. The train does not vary greatly in width; it is 260 to 330 m wide, measured at right angles to the glacial transport direction. It is at least 630 m long because anomalous sites are found this

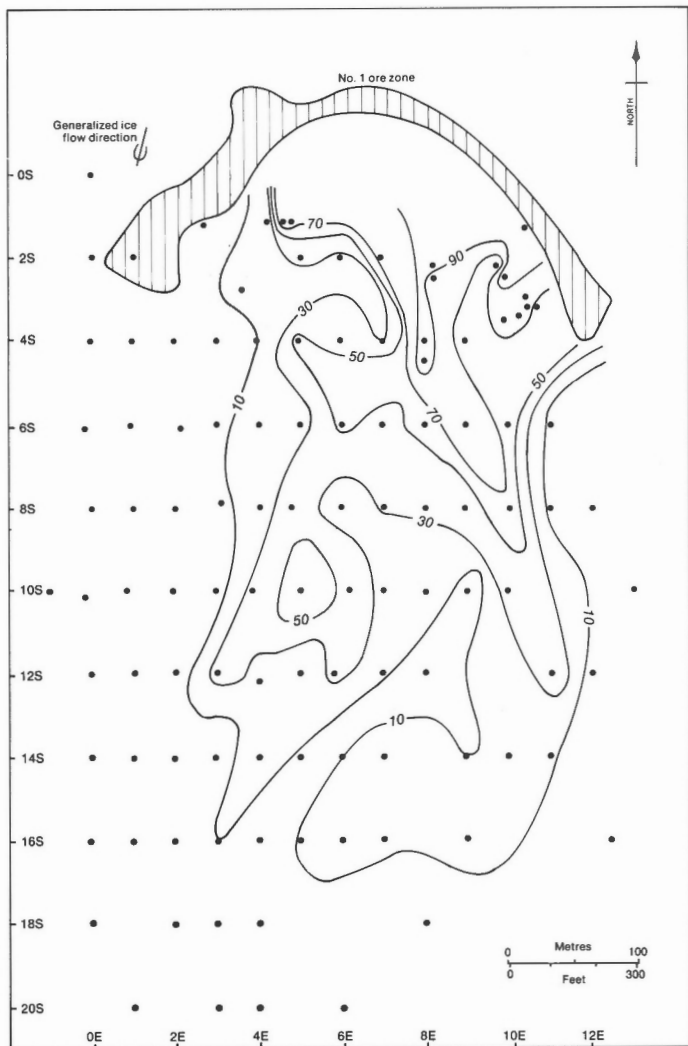


Figure 30. Abundance of vein rock types in the 4 to 64 mm fraction of unit C in the Icon train. Dots represent samples sites. Contours are labelled in per cent vein rock types. Grid is labelled in hundreds of feet.

distance down ice from the ore subcrop, and the sampled area does not include the down ice extremity of the train. When viewed as a perspective plot (Fig. 28), the soil anomaly of the Icon train appears as a cluster of high peaks and ridges rising abruptly out of the flat background plain.

Eight soil samples contained more than 1000 ppm copper; the highest abundance recorded was 3875 ppm (0.39%) copper. These high copper abundances were caused by the presence of chalcopyrite grains, malachite, and azurite. Malachite and azurite occur as discrete sand-sized grains, as coatings on all sizes of other grains, and as cement in the soil. The presence of these minerals as the weathering products of chalcopyrite indicates that fixation of copper has taken place during pedogenesis.

Based on information provided by the geochemical soil survey of the approximate location, size, and shape of the Icon train, the train then was mapped by determining the abundance of pebbles of vein rock types in the till in the train (unit C). This procedure was adopted in order to map a parameter (percentage of vein pebbles) which would be controlled primarily by glacial (clastic) dispersal and not by hydromorphic dispersion or copper fixation during weathering.

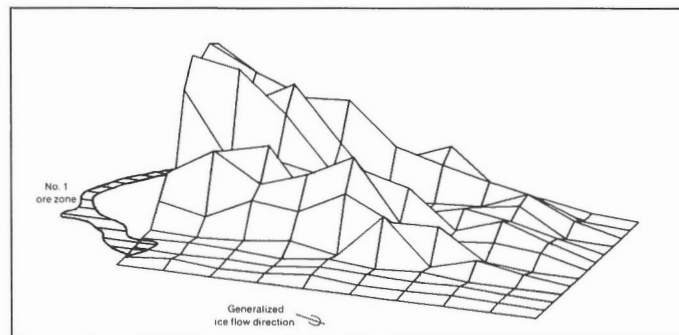


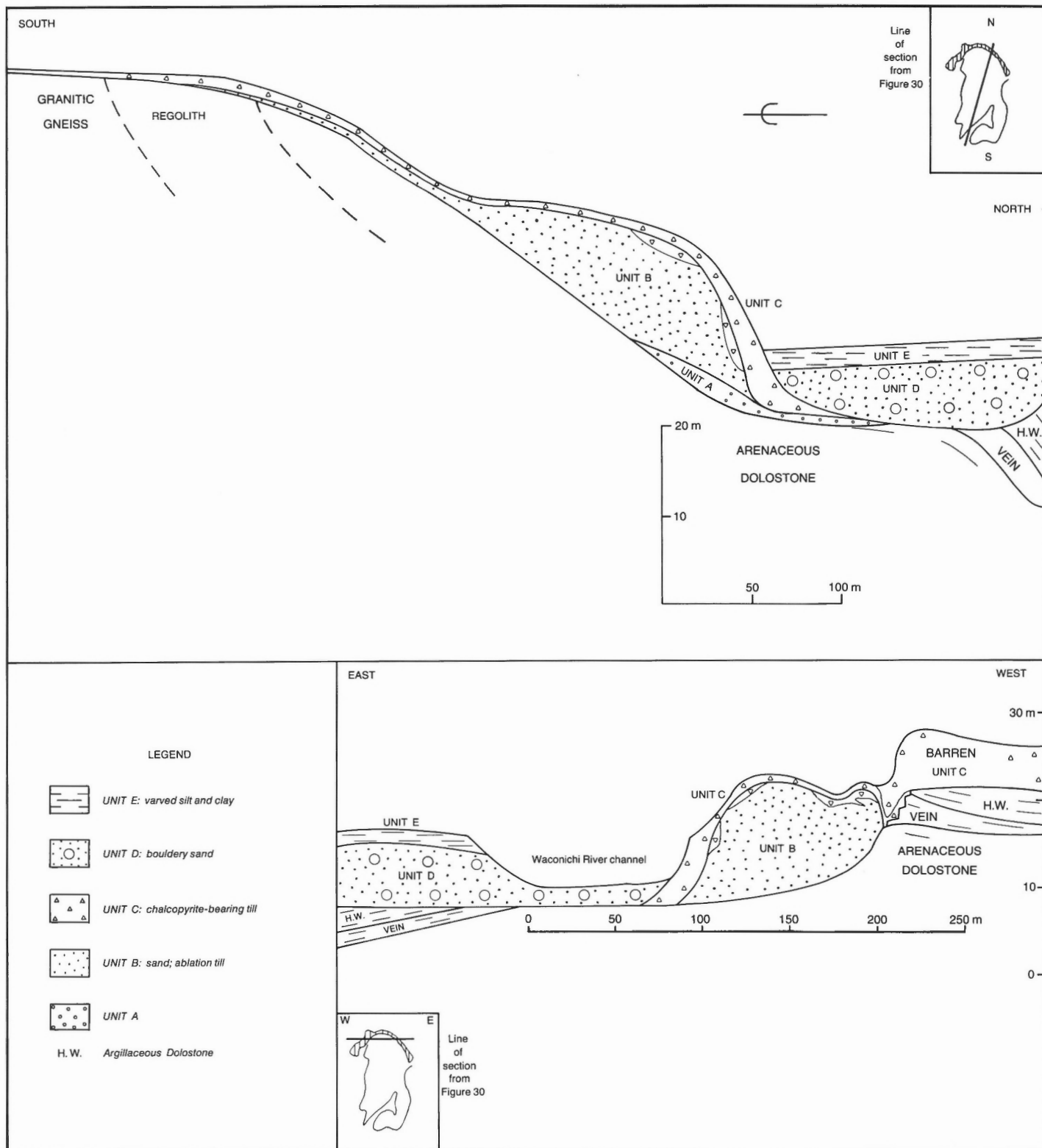
Figure 31. Perspective plot of the abundance of vein rock types in the 4 to 64 mm fraction of unit C in the Icon train, viewed from the west. Grid rectangles represent 100 by 200 ft. (30.5 by 61 m). The highest peak represents 99 per cent. Plot produced at the University of Western Ontario computer centre by program called PLT3DI.

Till at sites outside the train usually contains less than 5% of vein pebbles, and a 5% contour would almost coincide with the 10% contour; thus the edge of the train is placed at the 10% contour (Fig. 30). Defined in this way, the train is 570 m long and 240 to 270 m wide. It is flame-shaped, not fan-shaped, and is oriented parallel to the glacial transport direction, 195°. A belt of high abundances of vein pebbles that trends at about 345° within the train that will be considered in the discussion of the origin of the train.

A perspective plot of the same pebble data (Fig. 31) shows the contrast between the low abundances outside the train (flat areas) and the high abundances within it. The lateral edges of the train are sharp. The down-ice decay curve of abundance of vein pebbles is nonlinear and similar to a negative exponential curve. In the up-ice half of the train, the abundances decline steeply from above 90% to about 30%; down-ice they decline more gradually to below 5% (Fig. 30, 31).

The test pits and mining faces which were excavated in the Icon train allowed examination of its third dimension. It was then possible to describe the train as a three-dimensional body and to suggest ways in which its morphology and lithology have been influenced by the substrate. Its up-ice end overlies a convex-upward lens of sand and ablation till belonging to unit B (Fig. 14, 25). The till that forms the train, unit C, is up to 6 m thick and dips steeply northward on the up-ice side of the mass of unit B (Fig. 32A). The attitude of unit C conforms to the attitude of the bedrock surface in the down-ice part of the train where unit C is less than 1 m thick. In a transverse section across the up-ice end of the train (Fig. 32B), unit C appears to be "draped" over unit B and bedrock. Examination of the contact between these units shows that unit C fills grooves cut in unit B and bedrock. Where unit C is thickest, on the west side of the train, only the lowest 1 m contains abundant sediment derived from the vein. It grades upward into physically similar till, the lithology of which is dominated by another local rock type, the argillaceous dolostone of member B of the Lower Albanel Formation which is the rock overlying and forming the hanging wall of the vein.

In summary, the Icon train is a portion of unit C and is a lithologically distinct part of this till because it contains abundant debris derived from the subcrop of the number one ore zone at the mine. The three-dimensional shape of the train is similar to the shape of the inverted bowl of a spoon: convex upward, concave downward, with a thicker steeply north-dipping up-ice end and a thinner, gently north-dipping down-ice end.



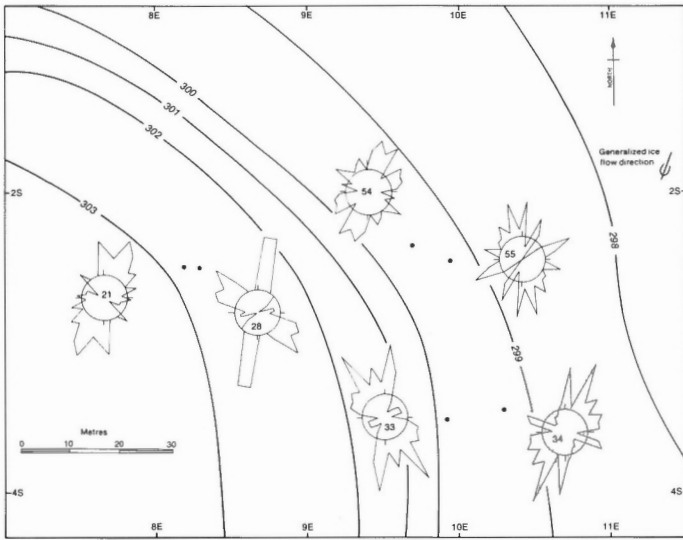


Figure 33. Mirror-image rose diagrams of till pebble fabrics in unit C in the northeast part of the Icon train. Dots represent the sample sites. The sampling grid from Figure 30 is shown for reference. Each diagram has its site number inside an 8% scale circle. The present topography of the contact of unit C with older units is shown by contours at 1 m intervals, based on mine datum of 305 m.

Origin

Obviously, the Icon train was formed by the glacial erosion of the subcrop of the number one ore zone followed by deposition of the debris as lodgment till a short distance down-ice from its source. Assuming the size and shape of the subcrop are similar to what they were before erosion, the glacier traversed a subcrop width of 20 to 80 m along a strike length of 370 m, measured at right angles to the direction of glacial flow (Fig. 30).

The till containing the train (unit C) includes undeformed or folded blocks and slabs of the underlying Quaternary units, and the contact between unit C and the older units is marked by grooves and thrust faults which must be glacial in origin (Fig. 21, 22, 24). The till in the train is rubbly (Fig. 19) and contains several large vein boulders. Rock flour is scarce where the till was derived from the vein alone. The till is thickest (vertically) on the lateral and up-ice edges of a mound of older drift (Fig. 32). Measurements of the pebble fabric in unit C in the train (Fig. 33) indicate that the till was transported towards the south-southwest (sites 21, 34, and 54) and south-southeast (sites 28 and 33). The map of abundance of vein pebbles in the till (Fig. 30) shows a belt of high percentages with a south-southeast trend within the train, which contrasts with the general south-southwest trend of the train. The vein subcrop from which the train was derived lay on the top and on the down-ice side of a slight bedrock structural ridge (Fig. 34). The down-ice and lateral faces of the vein subcrop are ragged and rubbly (Fig. 20). All striae on the bedrock under unit C are oriented south-southwest. If the interpretation of the glacial history of the area is correct, the train was formed by a minor glacial readvance up Waconichi Valley. The glacier was probably thin, and the formation of the Icon train occurred near its margin.

The coarse rubbly texture of the till and the ragged faces of the vein subcrop indicate that quarrying was the dominant erosive process. Thin, incompetent graphitic argillite lenses within the vein and at its contacts with the wallrocks would facilitate the plucking of blocks of vein rock.

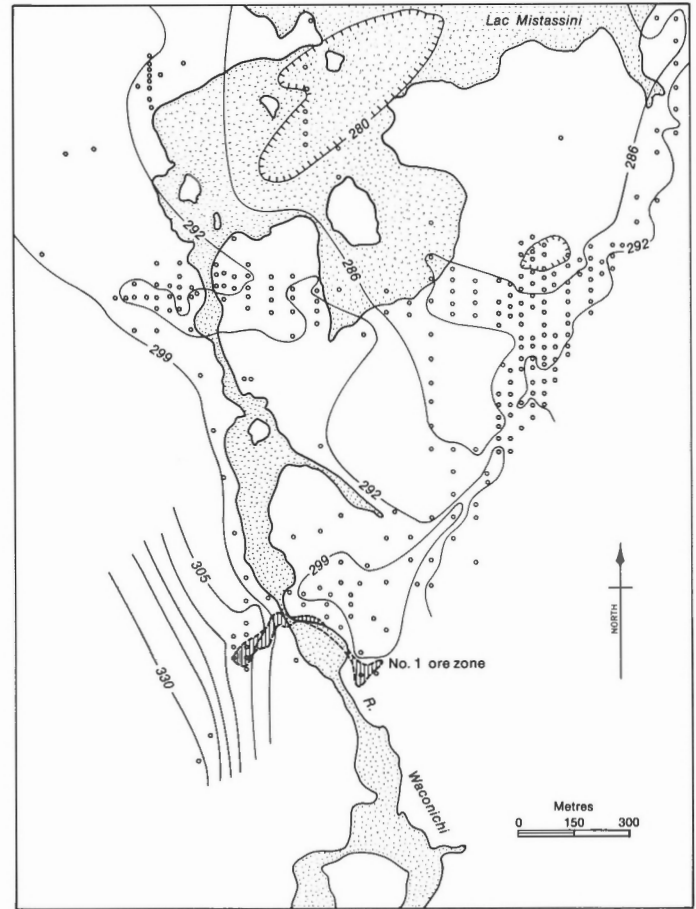


Figure 34. Bedrock topography of Icon mine, compiled from company drilling records. Each open circle is the site of a vertical drillhole. Contour interval is 6 m based on a mine datum of 305 m. The ridge on the east side of the contoured area is along the Mistassini fault.

The quartz masses and crystals in the vein are brittle and highly fractured; the carbonate minerals are easily cleaved. The contacts between quartz, carbonates, and sulphides are commonly large crystal faces with minor intergrowths, which would be planes of weakness. The position of the vein subcrop on the down-ice side of a bedrock ridge (Fig. 34) is analogous to the quarried lee side of whaleback bedrock landforms, except for the west end of the subcrop which is on a surface that rises down-ice. No conclusions can be reached concerning the exact mechanisms of quarrying, but it is believed that plucking dominated over crushing because the mineralogy and structure of the vein rock makes it amenable to plucking without much glacial crushing. The west end of the subcrop apparently was not strongly eroded because unit C contains low amounts of vein rock types down-ice from it (Fig. 30).

Less than 100 m down-ice from the vein subcrop, the glacier carrying the quarried debris met and overrode the older mound of units A and B (Fig. 25) which stood at least 7 m higher (Fig. 32B) than the substrate immediately up-ice from it. This mound of older drift apparently obstructed glacial flow, and the debris-rich ice was redirected locally around it, cutting grooves and infilling them with till. The fact that unit C is thickest on the up-ice end and sides of this mound and is in steep contact with the sediments in the mound supports this view. The south-southeast pebble fabrics (Fig. 33, sites 28, 33) on the east side of the train may reflect

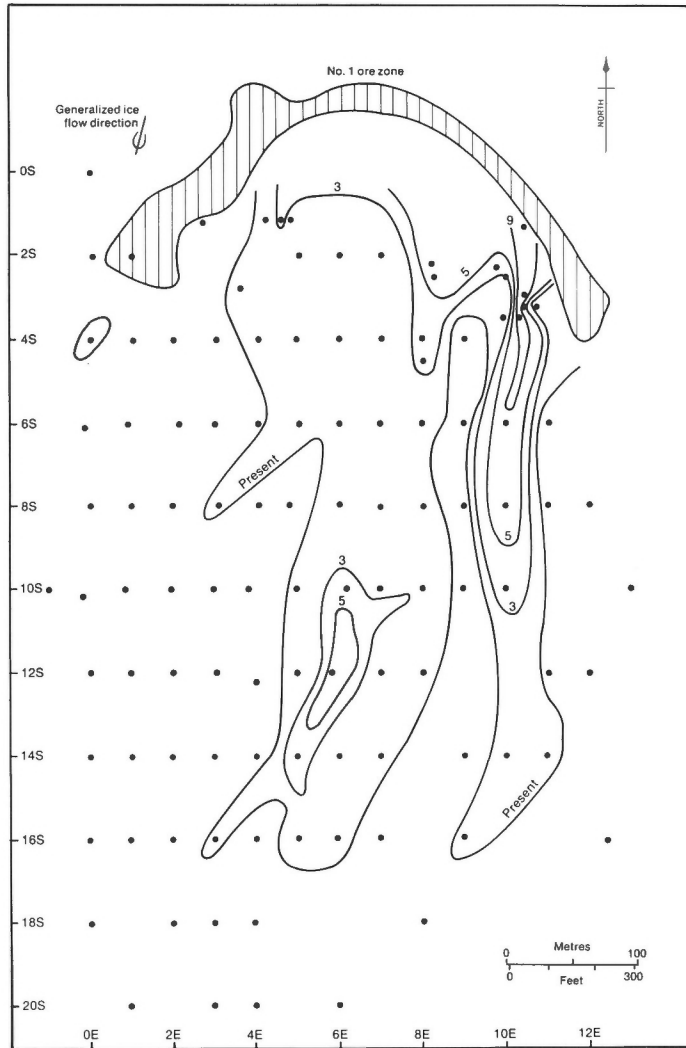


Figure 35. Abundance of chalcopyrite-bearing pebbles (4 to 64 mm) in unit C in the Icon train. Dots represent sample sites. Sampling grid is the same as that in Figure 30. Contour labelled "present" encloses sites where unit C contains any chalcopyrite-bearing pebbles. Other contours are labelled in per cent chalcopyrite-bearing pebbles.

local deflections of glacial flow, with the ice moving generally from the north-northeast (Fig. 33, sites 21, 34). The pebble fabrics, however, may simply reflect between-site variability in unit C. The abundance of vein pebbles in the train (Fig. 30) indicates that the normal transport of debris was from the north-northeast to south-southwest (outline of train), but the belt of high abundances on the east side of the train also shows that a large amount of the debris may have been redirected towards the south-southeast. The bedrock surface, the down-ice part of which the train overlies, dips to the east-northeast (Fig. 34). The combined effects of glacial motion from the north-northeast against this east-northeast-dipping slope may have increased the tendency for the glacial debris to be redirected parallel to the south-southeast strike of the bedrock surface. The down-ice decrease in abundance of vein pebbles in unit C was caused by comminution during transport and by dilution through incorporation of clasts from the older Quaternary units and other bedrock.

Depth of Erosion

Icon Sullivan Joint Venture mined the till in the train because of its high copper content and because it required very little blasting. The production figures for the till ore were tabulated separately from other ore, so it is possible to estimate the depth of erosion of the subcrop of the number one ore zone by the glacier that deposited the Icon train.

The company mined 60 823 t of till containing an average of 1.276% copper from the train (G. Darcy, personal communication, 1975). The total weight of the eroded vein rock would be 20 900 t, based on a copper content of 3.28% (Troop and Darcy, 1973) and a weight of 685 t of contained copper. Ore containing 3.28% copper would be about 10% sulphides and 90% gangue minerals by volume. The specific gravity of the ore is about 3.0 (Seguin and Laroche, 1975). An orebody with a mass of 20 900 t and specific gravity 3.0 would have a volume of 6967 m³. Assuming the till was abraded from the part of the subcrop that is up ice from the train (Fig. 30), it was derived from an area of 8000 m², indicating that the depth of erosion was 0.87 m.

The volume of eroded ore is a minimum estimate because only the relatively rich, up-ice end of the train was mined, and because the copper content of the ore in place used in the calculation (3.28%) is probably too high. The vein has an average copper content of only 0.29% in nine drillholes near the down-ice edge of the present subcrop, so a better estimate of the copper content of the ore in place would be about 2%. Based on the revised numbers, the volume of eroded ore was probably about 20 000 m³, which would indicate a depth of erosion of 2.6 m.

From the foregoing discussion of the origin of the Icon train, it can be seen that the till was derived from the vein mostly by quarrying and not by abrasion, so it is improper to consider the till as derived from an area the same size as the present subcrop. Using the minimum volume of 6967 m³ and a maximum of 20 000 m³, a calculation of the area of vein eroded may be performed for a given thickness of vein. The vein has an average thickness of 2.8 m in nine drillholes near the down-ice edge of the present subcrop; the area of the vein that was eroded therefore is between 2490 and 7140 m². The zone of erosion was probably a narrow band on the down-ice edge of the present subcrop. Regardless of the uncertainties involved in the foregoing calculations, the depth of erosion thus indicated due to a minor glacial readvance is significant.

Comparison of Prospecting Methods

The map showing copper content of the soil developed on the Icon train (Fig. 29) is a guide to the position of the number one ore zone. In general, however, soil analyses have limitations, and their results can be misleading. A soil that is developed on detrital material, with soil water having transported metal ions, will contain an anomaly which is partly clastic and partly hydromorphic. The field worker may sample soils developed on different sediments (e.g., till, glaciofluvial sands, glaciolacustrine silts, alluvium) without realizing that they are different. The shipping and analysis of the samples takes valuable time, and the laboratory is a further source of error.

Figure 35 shows the abundance of chalcopyrite-bearing pebbles (4 to 64 mm) in unit C in the Icon train. Chalcopyrite-bearing pebbles are found up to 540 m down ice from the subcrop. The area covered in Figure 35 is the same as that shown in Figure 29. In form and style the two mapped patterns are similar; both show two bands of high abundance parallel with the direction of glacial transport. The anomaly

of chalcopyrite-bearing pebbles is smaller because it is solely detrital in origin and because glacial comminution of sulphide-bearing pebbles produced finer debris which was detected farther down-ice in the soil survey. The two maps yield the same information about the position of the ore in place. Consideration of the procedures used in gathering the data for the maps allows a choice of the most useful map.

The abundance of chalcopyrite-bearing pebbles in the till is free of hydromorphic effects such as seepage anomalies and downslope distortion of the shape of the dispersal train. The pebble anomaly therefore can be interpreted more easily because it is a detrital one and can be traced directly up-ice to its source. The collection of pebbles from the till is less prone to sampling error because a pit must be dug to recover the pebbles, giving the sampler an opportunity to inspect the sediment and identify it.

Twenty man-days of fieldwork were required to collect the 111 samples of about 150 pebbles each shown in Figure 35. The same number of soil samples probably could be collected in about five man-days, unless difficulties were encountered in augering the clast-rich till. However, whereas soil samples must be shipped to a laboratory for an expensive form of analysis, the abundance of chalcopyrite-bearing pebbles can be determined easily in the field by someone with elementary geological training. Identification of the pebbles concurrent with sampling provides feedback to the sampler so that sample sites may be chosen efficiently and re-examined while in the field. In addition, identification of the pebbles yields data on the local bedrock types and economic mineral associations.

The conclusion that is drawn from this comparison is that wherever pebbles, cobbles, or boulders containing economically interesting minerals are found in till, the abundance of those clasts should be mapped. On-site and simultaneous analysis provides rapid return of information at low cost, and the abundance of the clasts in the till is a good guide to their bedrock source.

Drainage of surface water and groundwater into Waconichi River from the Icon train, which is part of the riverbed (Fig. 32B), could have supplied copper ions to the river water. In addition, fluvial erosion of the chalcopyrite-bearing till should have added chalcopyrite grains to the sediment load of the river.

The experimental stream sediment survey of Gros (1975) included most of the area of the Icon Sullivan Joint Venture property. Of the 137 stream sediment samples collected at a sampling density of about 2 samples/km², 14 were judged by Gros to be anomalous with respect to copper. None of the anomalous samples gives any indication about the location of the Icon ore zones; they are from streams in different drainage systems 8.4 to 10.8 km west of Waconichi River. The sample in the most favourable location, in Waconichi River 760 m downstream from the Icon train, did not detect the copper-bearing till.

Lake sediments have been suggested as sampling media for reconnaissance geochemical exploration in the Canadian Shield (Allan et al., 1973; Nicol et al., 1975). Samples are cored or dredged from the fine sediment in the deepest part of a lake on the assumption that the sediment at such a site best reflects the chemistry of the surrounding terrain. A core 25 cm long was collected from Baie du Poste, 17 km downstream from the Icon train (Allan and Timperley, 1975). Five samples taken at equal intervals down the core contained between 14 and 17 ppm copper, which gives no clue to the location of the Icon train.

Where chalcopyrite-bearing unit C in the Icon train forms the bed of Waconichi River, it is overlain by about 2 cm of fossiliferous oxidized sand of unit F (alluvium).

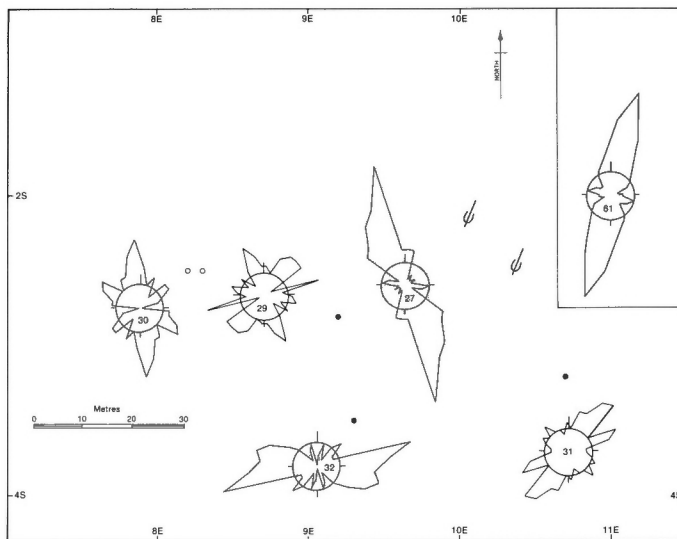


Figure 36. Striae and mirror-image rose diagrams of till pebble fabrics in unit A (sites marked by filled circles) and unit B (open circles) under the Icon train, mostly in the same area as shown in Figure 33. Sampling grid from Figure 30 is shown for reference. Each diagram has its site number inside an 8% scale circle. Inset: diagram for site 61, till in unit B at 1+10S, 4+25E on the grid.

Below the alluvium, the till is fresh and unoxidized, so relatively few copper ions could be moving from the till into the river water. This partly explains why the stream and lake sediments derived from the Icon train area do not contain anomalous amounts of copper.

Comparison of Units A, B, C, and D as Sampling Media

The Quaternary units near the subcrop of the number one ore zone at the Icon mine were examined in order to evaluate them as sampling media for prospecting by geochemical and lithological methods of analysis. Till pebble fabrics in units A and B and striae under unit B (Fig. 36) indicate that these sediments must have been transported across the vein subcrop along a path similar to that followed by the glacier that deposited unit C.

Figure 37 shows the abundance of vein pebbles and chalcopyrite-bearing pebbles in units A, B, C, and D in sections overlying and down ice from the subcrop of the number one ore zone. It is obvious that unit C is richer in pebbles derived from the vein than are the other Quaternary units. Unit B has been shown to be ice contact stratified drift and ablation till deposited from a wasting ice sheet. Lithologic analyses of its pebbles (Fig. 18) show that unit B has a high content of sediment derived from distant sources. The unit was deposited at the Icon mine site by streams running off the ice and by flows of till from the ice. Because deposition was the dominant local process, the lithology of unit B does not reflect the local bedrock. Unit D is a coarse, ice contact or proximal glaciofluvial gravel containing low percentages of vein pebbles. It is believed to have been deposited over the subcrop of the number one ore zone by a glacial stream in which the dominant local process was aggradation. Erosion of the vein subcrop was low because the subcrop was rapidly buried by unit D.

It remains to be explained why unit A, which is stratigraphically closer to bedrock than unit C, contains only low percentages of vein pebbles (Fig. 37). Unit A is a

Table 4
Selected sulphide-bearing glacial dispersal trains

| Name; Metals; Subcrop Size* | Sample Density (no./km ²) | Sampling Medium Component† | Anomaly Size (length by width) | Anomaly Shape | Reference |
|--|---|---|--|--------------------------|-----------------------------|
| Kidd Creek, Ont.; Cu, Zn, Ag; 600 by 30 m | 1.5 | Unoxidized lowest till, Zn and Cu | 8 by 1.6 km | Ribbon | Skinner, 1972 |
| Mount Pleasant, N.B. Mo, W, Bi, Cu, Sn, Zn; two large sources | 1.5 | Oxidized till, Cu and Zn Pb Ore host rock | 7-16 by 3.5 km 12-16 by 3.5 km 8 by 3 km | Flame | Szabo et al. 1975 |
| Spi Lake, N.W.T.; Zn, Pb, Cu; small, linear | 8 | Soil on till, Cu and Zn | 4 by 0.5-1 km | Ribbon | Shilts, 1975 |
| Noranda, Que.; Zn, Cu; 800 by 400 m | 9 | Soil on till Cu Zn | 2 by 2 km 1.5 by 1.5 km | Flame | Dreimanis, 1960 |
| Agricola Lake, N.W.T.; Pb, Cu; 50 by 400 m | 2320 | Soil on till, Cu and Pb | 500 by 250 m | Flame | Cameron and Durham, 1975 |
| Icon mine, Que.; Cu; 30 by 100 m 20 to 80 by 370 m 20 to 80 by 370 m | 580 580 580 | Soil on till, North train, Cu Icon train, Cu Icon train, vein pebbles | 1650 by 75 m 630 by 300 m 570 by 250 m | Ribbon Flame Flame | this study |
| Makola, Finland; Ni; 80 by 100 m | 9 | Soil on till, Ni | 1 by 0.25 km | Ribbon | Kauranne, 1959 |
| Korsnas, Finland; Pb; 450 by 100 m | 38 | Soil on till, Pb | 1.8 by 0.6 km | Ribbon | Hyvarinen, 1967 |
| *First number is length of subcrop parallel to direction of glacial flow, second number is length of subcrop at right angles to direction of glacial flow. | | | | | |
| †See references for explanations of methods of analysis. | | | | | |

lodgment till of regional extent which was deposited in a drumlinized till plain by an ice sheet advancing from the north-northeast. If the till pebble fabric at site 32 (Fig. 36) is assumed to be "transverse" to glacial flow as determined from striae, then all three measurements from this till (sites 27, 31, 32; Fig. 36) indicate that the glacier that deposited unit A advanced southward across the subcrop of the ore zone. Unit A, therefore, should contain large quantities of debris derived from the vein.

Very few vein pebbles are found in unit A; they are weathered, and weathering pits in the pebbles are packed with till matrix. The weathering may be pre-Wisconsin; the presence of the pebbles in unit A indicates that the vein was at least partly exposed to erosion at the onset of glaciation. The vein pebbles are distributed in the till in discontinuous bands, commonly only one pebble thick, which are interpreted as reflecting simultaneous glacial transport and comminution of the clasts along discrete planar paths.

One possible explanation for the low content of vein pebbles in unit A is that the vein subcrop was masked during deposition of unit A by an older drift unit that has since been

eroded from the vein subcrop. It is also possible that the vein subcrop was small or had an unfavourable geometry, which would inhibit glacial erosion of the vein. Another possible explanation is that the base of the ice sheet that deposited unit A was at its pressure-melting point; this would make abrasion and crushing the main erosional processes and lodgment of till the main depositional process at the base of the ice sheet (Boulton, 1972). Local inhomogeneities in subglacial water pressure would govern the distribution of zones of erosion and deposition. The fine grained texture of and the lack of rubble in unit A is evidence that quarried sediment is a minor local component of the till. It is believed that lodgment of till was the main process occurring at the Icon Sullivan Joint Venture property during deposition of unit A, but this hypothesis cannot yet be tested.

Sampling Density Versus Size of Dispersal Train

The Icon train is listed in Table 4 with other sulphide-bearing glacial dispersal trains (see Kauranne, 1976; Bradshaw, 1975, p. 104-107, 190-193 for additional examples). The trains are variable in size and methods of mapping, but they are generally ribbon shaped or flame shaped in plan, and

Table 5
Samples used for determinations of chalcopyrite abundance in till

| Sample Number | 73-56 | 73-57 | 73-58 | 73-74 | 72-12EU46 | 72-12EU56 |
|----------------------------|------------------------------|------------------------------|------------------------------|-------------------------------|------------------------------|------------------------------|
| Location | 1+25S, 3+15E (Fig. 30) | 1+20S, 3+20E (Fig. 30) | 2+35S, 9+70E (Fig. 33) | 3+05S, 10+70E (Fig. 33) | 2+50S, 8+20E (Fig. 33) | 2+50S, 8+20E (Fig. 33) |
| Median Diameter (ϕ) | 2.9 | 3.0 | -0.7 | -0.2 | -2.4 | -3.6 |
| Transport distance (m) | 10-50 | 10-50 | 90-125 | 110-150 | 90-125 | 90-125 |
| Provenance of clasts | Vein | Vein | Vein | Vein | Vein | Vein |
| Provenance of matrix | Unit B (Sand) | Unit B (Sand) | Vein | Vein | Vein | Vein |
| Chalcopyrite content (%) | 14.32 | 3.00 | 3.48 | 23.29 | 2.79 | 15.99 |
| Degree of oxidation | Nil | Nil | Nil | Nil | Moderate | High |

all have abrupt lateral edges. The large trains that were defined based on low sample densities, Kidd Creek and Mount Pleasant, are detectable by reconnaissance-scale sampling. Szabo et al. (1975) stated that a sample density of 0.2 samples/km² would be adequate to detect the Mount Pleasant train; small trains require a higher sample density, 8 to 10 samples/km². Increasing the sample density to 100 or even 2000 samples/km² is required for detailed tracing of trains.

The use of high sample densities, in spite of the high cost, provides information which guides other exploration methods. Detailed sampling more accurately defines the edge and shape of a train, and it facilitates location of the bedrock source of the metal or rock being traced. Once the source is known, study of the till in relation to its source may give detailed information on the processes of glacial erosion and deposition.

GLACIAL COMMINUTION OF CHALCOPYRITE

Unoxidized Till

Vagners (1969) and Dreimanis and Vagners (1971) have shown that minerals are glacially comminuted (crushed and abraded) so that the mineral species in lodgment till have peaks of abundance in specific particle size ranges. Near the source of a mineral, a clast-size mode dominates, whereas farther from the source, a matrix mode appears and the clast-size mode diminishes. With continued transport, the matrix mode does not become finer. The matrix modes may be analogous to the "equilibrium particle size distributions" observed by Bradshaw (1951), Theimer (1952), and Kelsall (1965) for artificially comminuted minerals.

The selection of the optimum particle size ranges for lithological or geochemical analyses of till for prospecting purposes should take into account the particle size ranges to which ore minerals are glacially comminuted. The selection of these size ranges becomes especially important when samples are collected by overburden drilling techniques, whereby small samples are recovered from subsurface tills that are difficult to identify.

An experiment was performed to determine the abundance of chalcopyrite in different particle size fractions of till. Four samples of 50 to 60 L of unoxidized lodgment till were collected from unit C, the till in the Icon train. The sample sites were selected to give a wide variety in distance of glacial transport, local provenance, texture, and total chalcopyrite content (Table 5). The laboratory procedures and calculations are similar to those of Vagners (1969, p. 14-41), except that volume or number percentages were used as much as possible instead of weight percentages to avoid biases resulting from the extreme differences between the specific gravities of chalcopyrite and the other minerals. The apparent percentage (Ap) of chalcopyrite was determined for each of 17 size fractions from 128 mm to 0.002 mm by separation and volumetric measurement of fractions coarser than 4 mm and by point counting of finer sizes. The abundance of sediment (all mineral species) in each size fraction (Gp) was determined from particle size analyses which were performed volumetrically for fractions coarser than 0.063 mm and from hydrometer analyses of finer fractions. Calculations of the true percentage (Tp) and true relative percentage (Trp) of chalcopyrite in each fraction are explained in Appendix 2. The Trp is the main variable considered in the following discussion.

The true relative percentages (Trp) of chalcopyrite in the four samples are presented as frequency polygons in Figure 38. All samples have a clast-size mode or modes in the 8 to 1 mm range, and three samples have matrix modes in the 0.25 to 0.016 mm range. The two samples with relatively short transport distances (73-56, 73-57, Table 5) have strong clast modes and weak or irregular matrix modes. The particle size range in the clast modes is believed to reflect the fracture pattern of the chalcopyrite in place, but this cannot be quantified. The samples with relatively long transport distances (73-58, 73-74, Table 5) have the strongest matrix modes even though these samples are relatively coarse grained.

The effect of incorporation of sand from unit B into the till can be seen in the frequency polygon for sample 73-57. An irregular peak occurs in the size range 0.25 to 0.032 mm; examination of the data for this sample (Appendix 2) shows that this peak is artificial and is caused by an abundance of

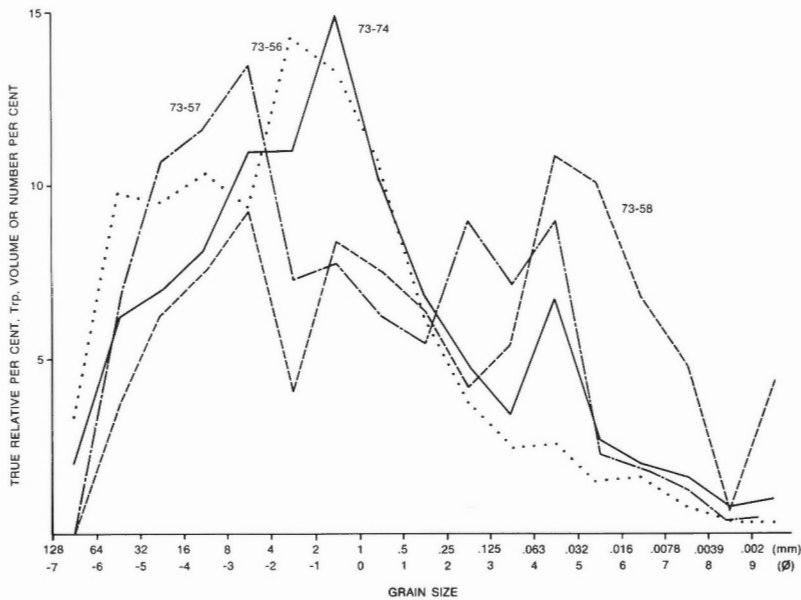


Figure 38. True chalcopyrite distributions in till samples 73-56, 73-57, 73-58, and 73-74.

sediment (high Gp) in this size range, not by abundant chalcopyrite (Ap). Hence, the true matrix modes in Figure 38 are between 0.063 and 0.016 mm (samples 73-58, 73-74).

Based on these four samples it can be seen that within 50 m of the source, chalcopyrite is glacially comminuted to produce a well defined clast mode in the 8 to 1 mm range. A matrix mode is not developed in less than 50 m of transport, but after more than 100 m, a matrix mode develops in the 0.063 to 0.016 mm range (Table 5). It is suggested, therefore, that 0.063 to 0.016 mm be considered for inclusion in the particle size range to be analyzed when unoxidized lodgment till is sampled for geochemical analysis, subject to the caveats given below. Analysis of the heavy mineral fraction of the particle size range chosen will remove unwanted light mineral contaminants and will enhance the geochemical response of the samples. Lithological analysis of the 8 to 1 mm fraction may provide useful information, especially near the source of the chalcopyrite.

The suggestions given above have limitations. It is obvious that chalcopyrite pebbles will never be found in till derived from fine grained or disseminated sulphides in which the maximum size of chalcopyrite grains is sand-sized or finer. All chalcopyrite clasts and grains seen in this study were angular, and chalcopyrite powder was rare, which agrees with the interpretation of the debris in unit C as crushed sediment derived from the vein by quarrying. In other glaciated areas where abrasion has been the main erosional process, the debris derived from an ore zone is fine grained. This type of study must be repeated for tills derived by abrasion of fine grained ores before definitive statements can be made about the optimum particle size ranges for geochemical analysis of unoxidized till. Other ore minerals should be investigated to broaden the scope of future studies.

Weathering of Chalcopyrite-bearing Till

Surficial weathering of unit C in the Icon train has changed the mineralogy of the till. Ferroan dolomite, pyrite, and chalcopyrite from the vein and marcasite from the graphitic argillite host rock all have been weathered; quartz is unaltered. Pyrite and marcasite are rare in the oxidized till. Ferroan dolomite is present as powdery limonitic pseudomorphs where the till is strongly oxidized and as soft, oxidized grains where the till is less weathered. The relative weathering resistances of chalcopyrite and ferroan dolomite were estimated by examining clasts containing these minerals and by comparing their relief relative to quartz crystals in the same clasts. Quartz crystals protrude 1 to 3 mm from massive chalcopyrite whereas ferroan dolomite is weathered 1 to 2 mm into the chalcopyrite; therefore, ferroan dolomite has weathered more rapidly than chalcopyrite. Weathered chalcopyrite clasts are brown to dark brown (7.5YR 4/2), coated with 0.5 to 2 mm of limonite. Limonite also occurs in fractures that are 0.5 to 1 mm wide in the chalcopyrite. Under the limonite, the chalcopyrite is fresh. It appears that a coating of limonite impedes further oxidation of the chalcopyrite.

Malachite and limonite are the main secondary minerals in the till. Limonite is present as cement, sand-sized grains, and coatings on chalcopyrite grains. Limonitic surfaces usually are coated with malachite. Malachite occurs as cement, sand-sized grains, and banded botryoidal masses in large interstices in the till. Azurite is found with the malachite, but it is much less common; it usually forms a finely crystalline coating on botryoidal malachite, and it is a cement stratigraphically below malachite in cemented sediments. Where oxidized unit C overlies unit B, malachite and azurite are cement in unit B up to 5 cm below the contact. Bornite and chalcocite form a tarnish on a few chalcopyrite grains only in the slightly oxidized parts of the till. A few dolostone pebbles plated with native copper were found near the surface of unit C.

An experiment was performed to estimate the amount of chalcopyrite destroyed during the weathering of unit C and to find the optimum grain size ranges for geochemical and lithological analyses of oxidized chalcopyrite-bearing till. Seven samples of 1 to 2 kg of oxidized till were collected from the B and C horizons of the soil profile developed on unit C. Each sample was split into 11 size fractions between 64 and 0.037 mm, and the weight percentage of heavy minerals (chalcopyrite, malachite, and limonite) was determined for each fraction after separation in tetrabromoethane (specific gravity, 2.96). Malachite and limonite were removed from the splits with a weak hydrochloric acid wash. The abundance of chalcopyrite in the remaining heavy minerals was converted to true relative percentage (Trp) for each split in the same way as for the unoxidized till samples already described, except that the data were weight percentages. The results of these analyses are tabulated in Appendix 3.

The abundances of heavy minerals (Hp) and chalcopyrite (Ap) in sample 72-12EU56 are shown in Figure 39. This sample is from the B horizon 0.3 m below the surface of the soil profile developed on unit C. The gap between the curves is the percentage of malachite plus limonite present, which is highest in the particle size range 0.5 to 0.037 mm. The true distribution of chalcopyrite (Trp) in the same sample (Fig. 40) shows a strong clast mode in the range 32 to 8 mm, and no

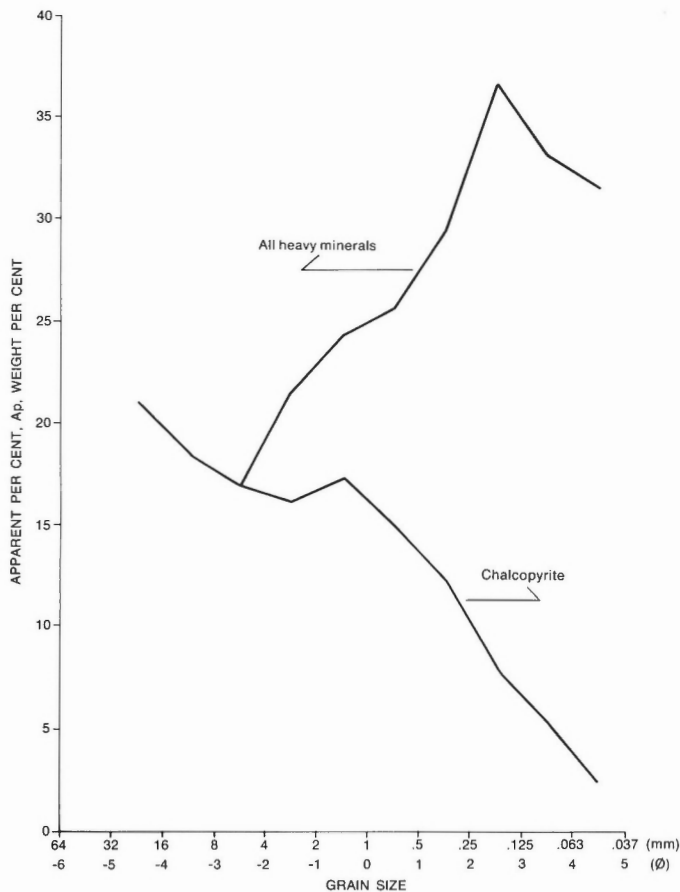


Figure 39. Apparent heavy mineral and chalcopyrite distributions in till sample 72-12EU56.

matrix mode is present. The sample is from till that was transported at least 100 m from its source (Table 5), so that modes were expected in the same particle size ranges that were found for unoxidized till samples 73-58 and 73-74 (Fig. 38). Either the till at site 72-12EU56 never had a matrix mode or the matrix mode was altered to malachite plus limonite and the clast mode shifted into coarser sizes in response to the removal of the finer chalcopyrite.

A sample of oxidized till (sample 72-12EU46) was collected 0.3 m below sample 72-12EU56 from the less strongly oxidized C horizon of the soil profile. The true distribution of chalcopyrite (Trp) in this sample (Fig. 40) has a clast mode in the range of 4 to 2 mm and a broad shoulder in the sand sizes. This indicates that the till did contain a matrix mode of chalcopyrite which has been partly or entirely removed depending on the degree of weathering. The finer chalcopyrite grains disappear first, and coarse grains are altered as weathering proceeds.

It should be noted that the seven samples are small, and many do not contain the full range of particle sizes (e.g., no chalcopyrite greater than 16 mm in sample 72-12EU46, Fig. 40), but the following consistent relationships are present from sample to sample (Appendix 3):

1. The abundance of chalcopyrite has an inverse relationship to the abundance of malachite plus limonite in the same size fraction.
2. The finer sizes contain the highest amounts of malachite plus limonite and the lowest amounts of chalcopyrite. This means that when samples of oxidized chalcopyrite-bearing till are collected for geochemical analysis, 0.5 to 0.037 mm is the optimum particle size range, because it is

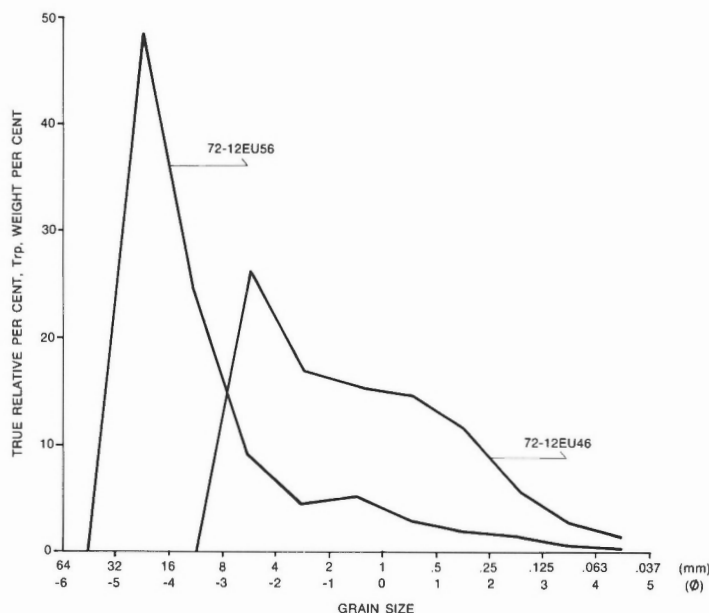


Figure 40. True chalcopyrite distributions in till samples 72-12EU56 and 72-12EU46.

in this range that most of the malachite is found (Fig. 39). This conclusion can only be made for tills that contain detrital carbonate minerals and have a low content of such sulphides as pyrite, pyrrhotite, and marcasite. Weathering of detrital carbonate minerals and rocks produces carbonate ions which fix copper ions as malachite. Without a source of carbonate ions, the copper ions from weathering chalcopyrite could be mobilized and would remain in the soil only as adsorbed ions. A high content of pyrite-like minerals might produce enough acid to mobilize both copper and carbonate ions. The importance of carbonate ions from other sources (e.g., rain, air) in malachite formation is unknown for this till.

About 7700 years have elapsed since unit C initially was exposed to significant weathering (Prest, 1970, p. 724-725). During this period, most chalcopyrite grains in the till finer than 0.5 mm and within 0.6 m of the surface have been altered to malachite plus limonite. Limonite is believed to have formed largely in place, as the insoluble residue of chalcopyrite. The occurrence of malachite as cement in unit B up to 5 cm below its contact with weathered unit C is evidence of the mobility of copper released during weathering of chalcopyrite; but most malachite is in unit C, fixed locally by carbonate ions released during weathering of ferroan dolomite and dolostone.

CONCLUSIONS AND RECOMMENDATIONS

Conclusions

1. The Quaternary units in the Lac Mistassini - Lac Waconichi area are the products of a simple glacial cycle of: major advance - recession - minor readvance - completed recession - glaciofluvial sedimentation - glaciolacustrine sedimentation - organic sedimentation. These events occurred during the Wisconsin and Holocene. The units are time-transgressive, and many of the events were partly synchronous within the area.
2. The copper-bearing dispersal trains at the Icon mine were formed by glacial erosion, transport, and deposition during the minor readvance that deposited unit C. The processes of formation of the trains were orderly, not chaotic.

3. The dispersal trains are three-dimensional bodies, the shape and lithology of which were strongly influenced by the topography and lithology of the substrate. They are ribbon or flame shaped in plan view. The Icon train has the three dimensional shape of the inverted bowl of a spoon. The trains have sharp edges and high geochemical and lithological contrast to the surrounding till. It is possible to map dispersal trains at a detailed scale.
4. It is estimated that between 7000 and 20 000 m³ of rock were eroded from the subcrop of the number one ore zone at the Icon mine by the small glacial readvance that deposited unit C. These volume estimates are equivalent to a slab of rock at least 2.8 m thick with an area between 2440 and 7140 m². Erosion is believed to have taken place mainly by quarrying of the down-ice edge of the vein subcrop.
5. Mapping the abundance of chalcopyrite-bearing pebbles in the Icon train is a more efficient guide to the location of the ore in place than geochemical analyses for copper in the soil developed on the train. Chalcopyrite is most abundant in the range 32 to 8 mm in strongly oxidized till. When clasts containing economically interesting minerals are discovered in a till, the abundance of those clasts should be mapped.
6. In the unoxidized till studied, chalcopyrite has a clast mode between 8 and 1 mm and a matrix mode from 0.063 to 0.016 mm. The clast mode developed after short transport distances, and the matrix mode required at least 100 m of transport to develop. The matrix mode should be considered for inclusion in the size range to be analyzed for copper when samples are collected from unoxidized till by subsurface sampling techniques during mineral exploration.
7. Oxidized till containing chalcopyrite plus carbonates has abundant malachite in the range 0.5 to 0.037 mm. Sampling of oxidized till for prospecting purposes should include this size range. This conclusion applies only for tills that have not been completely leached of carbonates.
8. Lodgment tills (units A and C) reflect the local bedrock lithology better than ablation till (in unit B), ice contact stratified drift (in unit B), outwash gravel (unit D), and postglacial stream or lake sediments (unit F). Lodgment tills are preferred for geochemical or lithological sampling of glacial drift in mineral exploration. Unit C contains more debris derived from the Icon ore zones than does unit A because the deposition of unit C was accompanied by strong local glacial quarrying, whereas the dominant process during deposition of unit A was probably lodgment with minor erosion of the ore zones.

Recommendations for Future Research

1. Other glacial dispersal trains should be mapped at a detailed scale to provide additional examples of the size, shape, and structure of dispersal trains. Such studies are useful for interpreting glacial processes, and they provide guidelines for mineral exploration in glaciated terrain.
2. The abundance of chalcopyrite with respect to grain size should be determined for unoxidized and oxidized tills derived from texturally and structurally different ore deposits in other areas.
3. The abundance of other ore minerals (e.g., sphalerite) with respect to grain size should be determined for unoxidized and oxidized tills in other areas.

REFERENCES

- Allan, R.J., Cameron, E.M., and Durham, C.C.
1973: Reconnaissance geochemistry using lake sediments of a 36,000-square-mile area of the northwestern Canadian Shield (Bear-Slave operation, 1972); Geological Survey of Canada, Paper 72-50, 70 p.
- Allan, R.J. and Timperley, M.H.
1975: Prospecting by use of lake sediments in areas of industrial heavy metal contamination; in *Prospecting in Areas of Glaciated Terrain, 1975*, ed. M.J. Jones, Institution of Mining and Metallurgy, London, p. 87-111.
- Allard, G.O. and Cimon, J.
1974: Minimal Pleistocene Glaciation in the Chibougamau area, Quebec; Geological Association of Canada, Mineralogical Association of Canada, Abstracts of papers presented at Annual Meeting, St. John's, Newfoundland, p. 1.
- American Society for Testing and Materials (ASTM)
1964: Procedure D422-63; in *Procedures for Testing Soils*, 4th edition; American Society for Testing and Materials, Philadelphia, p. 95-106.
- Antevs, E.
1925: Retreat of the last ice-sheet in eastern Canada; Geological Survey of Canada, Memoir 146, 142 p.
- Bergeron, R.
1957: Late Precambrian rocks of the north shore of the St. Lawrence River and of the Mistassini and Otish Mountains areas, Quebec; in *The Proterozoic of Canada*, ed. J.E. Gill, Royal Society of Canada, Special Publication No. 2, p. 124-131.
- Bostock, H.S.
1969: Physiographic regions of Canada; Geological Survey of Canada, Map 1254A, scale 1:5 000 000.
1970: Physiographic subdivisions of Canada; in *Geology and Economic Minerals of Canada*, ed. R.J.W. Douglas, Geological Survey of Canada, Economic Geology Report 1, p. 9-30.
- Boulton, G.S.
1972: The role of thermal regime in glacial sedimentation; in *Polar Geomorphology*, ed. R.J. Price and D.E. Sugden, Institute of British Geographers, Special Publication No. 4, p. 1-19.
- Bradshaw, B.C.
1951: The effect of grinding on particles; *Journal of Chemical Physics*, v. 19, p. 1057-1059.
- Bradshaw, P.M.D., ed.
1975: Conceptual models in exploration geochemistry; *Journal of Geochemical Exploration*, v. 4, p. 1-223.
- Cameron, E.M. and Durham, C.C.
1975: Soil geochemistry of the Agricola Lake massive sulphide prospect; in *Report of Activities, Part A*, Geological Survey of Canada, Paper 75-1A, p. 199-202.
- Caty, J-L.
1976: Stratigraphie et sédimentologie de la Formation de Papaskwasati de la région du Lac Mistassini, Québec; Ministère des richesses naturelles, Québec, DPV 423, 270 p.

- Caty, J.-L. et Chown, E.H.
1973: Etude géologique, région de la Baie Abatagush, Territoire de Mistassini; Ministère des richesses naturelles, Québec, DP 189, 18 p.
- Chown, E.H. and Caty, J.-L.
1973: The clastic members of the Mistassini-Otish Basin; in *Huronian Stratigraphy and Sedimentation*, ed. G.M. Young, Geological Association of Canada, Special Paper No. 12, p. 49-71.
- Coleman, A.P.
1909: Lake Ojibway: last of the great glacial lakes; Ontario Bureau of Mines, Annual Report 18, p. 284-293.
- Collins, J.A., Brown, A.C., and Smith, L.
1974: The Precambrian Mistassini Group, Grenville overthrusting and the Icon copper deposit; Geological Association of Canada, Mineralogical Association of Canada, Abstracts of papers presented at Annual Meeting, St. John's, Newfoundland, p. 19.
- Dallmeyer, R.D.
1974: $^{40}\text{Ar}/^{39}\text{Ar}$ incremental release ages of biotite and hornblende from pre-Kenoran gneisses between the Matagami-Chibougamau and Frotet-Troilus greenstone belts, Quebec; Canadian Journal of Earth Sciences, v. 11, p. 1586-1593.
- Deland, A.-N. and Sater, G.S.
1967: Duquet-McOuat area, Mistassini Territory; Quebec Department of Natural Resources, Geological Report 126, 29 p.
- DiLabio, R.N.W.
1976: Glacial dispersal of rocks and minerals in the Lac Mistassini - Lac Waconichi area, Quebec, with special reference to the Icon dispersal train; unpublished Ph.D. thesis, University of Western Ontario, London, 174 p.
- Dreimanis, A.
1956: Steep Rock iron ore boulder train; Geological Association of Canada, Proceedings, Part 1, p. 27-70.
1958: Tracing ore boulders as a prospecting method in Canada; Canadian Mining and Metallurgical Bulletin, v. 51, no. 550, p. 73-80.
1960: Geochemical prospecting for Cu, Pb, and Zn in glaciated areas, eastern Canada; 21st International Geological Congress (Norden), Pt. II, p. 7-19.
1962: Quantitative gasometric determination of calcite and dolomite by using Chittick apparatus; Journal of Sedimentary Petrology, v. 32, p. 520-529.
1976: Tills; their origin and properties; in *Glacial Till, an Interdisciplinary study*, ed. R.F. Legget, University of Toronto Press, Toronto, p. 11-49.
- Dreimanis, A. and Karrow, P.F.
1972: Glacial history of the Great Lakes-St. Lawrence region, the classification of the Wisconsin(an) Stage, and its correlatives; 24th International Geological Congress (Montreal), Section 12, p. 5-15.
- Dreimanis, A. and Vagners, U.J.
1971: Bimodal distribution of rock and mineral fragments in basal tills; in *Till/A Symposium*, ed. R.P. Goldthwait, Ohio State University Press, Columbus, p. 237-250.
- Duquette, G.
1970: Archean stratigraphy and ore relations in the Chibougamau district; Quebec Department of Natural Resources, Special Paper 8, 16 p.
1972: The Chibougamau-Chapais greenstone belt; in *Precambrian geology and mineral deposits of the Noranda-Val d'Or and Matagami-Chibougamau greenstone belts*, Quebec, ed. G.O. Allard, 24th International Geological Congress, Guidebook to Excursions A41 and C41, p. 51-70.
- Elson, J.A.
1961: The geology of tills; in *Proceedings of the 14th Canadian Soil Mechanics Conference*, ed. E. Penner and J. Butler, National Research Council of Canada, Associate Committee on Soil and Snow Mechanics, Technical Memorandum 69.
- Faribault, E.R., Gwillim, J.C., and Barlow, A.E.
1911: Geology and mineral resources of the Chibougamau region, Quebec, by the Chibougamau Mining Commission; Quebec Department of Colonization, Mines and Fisheries, 224 p.
- Fielder, F.M.
1976: Canadian Mines Handbook, 1976-1977; Northern Miner Press, Toronto, 424 p.
- Flint, R.F.
1971: *Glacial and Quaternary Geology*; John Wiley and Sons, Inc., New York, 892 p.
- Forgeron, F.D.
1971: Soil Geochemistry in the Canadian Shield; Canadian Mining and Metallurgical Bulletin, v. 64, no. 715, p. 37-42.
- Fryer, B.J.
1972: Age determinations in the Circum-Ungava Geosyncline and the evolution of Precambrian banded iron-formations; Canadian Journal of Earth Sciences, v. 9, p. 652-663.
- Gadd, N.R.
1971: Pleistocene geology of the central St. Lawrence Lowland; Geological Survey of Canada, Memoir 359, 153 p.
- Gilbert, J.E.
1958: Bignell area, Mistassini and Abitibi Territories; Quebec Department of Mines, Geological Report 79, 37 p.
- Gillett, L.B.
1962: Bedrock and Pleistocene geology of the Vienne-Blaklock area, Quebec, with observations on magnetic diabase dikes in northeast Ontario and northwest Quebec; unpublished Ph.D. thesis, Princeton University, Princeton, New Jersey, 222 p.
- Goldthwait, R.P.
1971: Introduction to till, today; in *Till/A Symposium*, ed. R.P. Goldthwait, Ohio State University Press, Columbus, p. 3-26.
- Grant, D.R.
1975: Glacial style and the Quaternary stratigraphic record in the Atlantic Provinces, Canada; in *Report of Activities, Part B, Geological Survey of Canada, Paper 75-1B*, p. 109-110.
- Gros, J.-J.
1975: Geology of south part of Poste Bay, O'Sullivan and Gauvin Townships; Quebec Ministry of Natural Resources, Preliminary Report 610, 33 p.

- Guilloux, L.
 1969: Sud-est du Canton d'O'Sullivan, Territoire de Mistassini; Ministère des richesses naturelles, Québec, DP 166, 46 p.
 1972: Geology of the Icon mine; in Precambrian geology and mineral deposits of the Noranda-Val d'Or and Matagami-Chibougamau greenstone belts, Québec, ed. G.O. Allard, 24th International Geological Congress (Montreal), Guidebook to Excursions A41 and C41, p. 83-91.
- Hageman, B.P.
 1971: Report of the Commission on the Holocene (1957); in *Etudes sur le Quaternaire dans le Monde*, v. 2, ed. M. Ters, VIII Congress INQUA, Paris, p. 679.
- Hardy, L.
 1977: La déglaciation et les épisodes lacustre et marin sur le versant québécois des basses terres de la baie de James; *Géographie physique et quaternaire*, vol. XXXI, p. 261-273.
- Hawkes, H.E. and Webb, J.S.
 1962: *Geochemistry in Mineral Exploration*; Harper and Row, New York, 415 p.
- Hyvarinen, L.
 1967: Geochemical prospecting for lead ore at Korsnas; in *Geochemical Prospecting in Fennoscandia*, ed. A. Kvalheim, Interscience, New York, p. 171-179.
- Ignatius, H.
 1958: On the late-Wisconsin deglaciation in eastern Canada; *Acta Geographica*, v. 16, no. 3, p. 1-34.
- IMM (Institution of Mining and Metallurgy)
 1977: *Prospecting in areas of glaciated terrain 1977*; Institution of Mining and Metallurgy, London, 140 p.
 1979: *Prospecting in areas of glaciated terrain 1979*; Institution of Mining and Metallurgy, London, 110 p.
- Jones, L.M., Walker, R.L., and Allard, G.O.
 1974: The rubidium-strontium whole-rock age of major units of the Chibougamau greenstone belt, Québec; *Canadian Journal of Earth Sciences*, v. 11, p. 1550-1561.
- Jones, M.J., ed.
 1973: *Prospecting in Areas of Glacial Terrain*; Institution of Mining and Metallurgy, London, 138 p.
 1975: *Prospecting in Areas of Glaciated Terrain, 1975*; Institution of Mining and Metallurgy, London, 154 p.
- Karup-Moller, S. and Brummer, J.J.
 1970: The George Lake zinc deposit, Wollaston Lake area, northeastern Saskatchewan; *Economic Geology*, v. 65, p. 862-874.
- Kauranne, L.K.
 1959: Pedogeochemical prospecting in glaciated terrain; *Commission géologique de Finlande, Bulletin* 184, p. 1-10.
 1976: Conceptual models in exploration geochemistry, Norden, 1975; *Journal of Geochemical Exploration*, v. 5, p. 173-420.
- Kelsall, D.F.
 1965: A study of breakage in a small continuous open circuit wet ball mill; in VII International Mineral Processing Congress, v. 1, ed. N. Arbiter, Gordon and Breach, New York, p. 33-42.
- Kokkola, M.
 1975: Stratigraphy of till at Hitura open-pit, Nivala, western Finland, and its bearing on geochemical prospecting; in *Prospecting in Areas of Glaciated Terrain, 1975*, ed. M.J. Jones, Institution of Mining and Metallurgy, London, p. 149-154.
- Kvalheim, A., ed.
 1967: *Geochemical Prospecting in Fennoscandia*; Interscience, New York, 350 p.
- Laurin, A.F., Co-ordinator
 1969: *Geological Map of Quebec*; Quebec Department of Natural Resources, Map.
- Levinson, A.A.
 1974: *Introduction to Exploration Geochemistry*; Applied Publishing, Calgary, 612 p.
- Long, D.G.F.
 1973: The stratigraphy and sedimentology of the Chibougamau Formation; unpublished M.Sc. thesis, University of Western Ontario, London, 305 p.
 1974: Glacial and paraglacial genesis of conglomeratic rocks of the Chibougamau Formation (Aphebian), Chibougamau, Québec; *Canadian Journal of Earth Sciences*, v. 11, p. 1236-1252.
- Low, A.P.
 1885: Report of the Mistassini Expedition, 1884-5; Geological and Natural History Survey of Canada, Annual Report, New Series, v. I, p. 1D-55D.
 1896: Report on explorations in the Labrador Peninsula along the East Main, Koksoak, Hamilton, Manicouagan and portions of other rivers in 1892-93-94-95; Geological Survey of Canada, Annual Report, New Series, v. VIII, p. 1L-387L.
 1906: Geological Report on the Chibougamau Mining Region in the northern part of the Province of Quebec; Geological Survey of Canada, Publication No. 923, 61 p.
- McDonald, B.C.
 1971: Late Quaternary stratigraphy and deglaciation in eastern Canada; in *Late Cenozoic Glacial Ages*, ed. K.K. Turekian, Yale University Press, New Haven, p. 331-353.
- McDonald, B.C. and Shilts, W.W.
 1971: Quaternary stratigraphy and events in south-eastern Quebec; *Geological Society of America Bulletin*, v. 82, p. 683-698.
- McGlynn, J.C.
 1970: Superior Province; in *Geology and Economic Minerals of Canada*, ed. R.J.W. Douglas, Geological Survey of Canada, Economic Geology Report No. 1, p. 54-71.
- Munsell Color Co.
 1971: *Munsell Soil Color Charts*; Munsell Color Company Inc., Baltimore.
- Neilson, J.M.
 1953: Albanel area, Mistassini Territory; Quebec Department of Mines, Geological Report 53, 35 p.
 1963: Lake Albanel iron range, northern Quebec; *Canadian Mining and Metallurgical Bulletin*, v. 56, no. 609, p. 35-41.
 1966: Takwa River area; Quebec Department of Natural Resources, Geological Report 124, 53 p.

- Nicol, I., Coker, W.B., Jackson, R.G., and Klassen, R.A.
 1975: Relation of lake sediment composition to mineralization in different limnological environments in Canada; in *Prospecting in Areas of Glaciated Terrain, 1975*, ed. M.J. Jones, Institution of Mining and Metallurgy, London, p. 112-125.
- Norman, G.W.H.
 1938: The last Pleistocene ice-front in the Chibougamau district, Quebec; Royal Society of Canada, *Transactions*, Section 4, v. 32, p. 69-86.
 1939: The south-eastern limit of glacial lake Barlow-Ojibway in the Mistassini Lake region Quebec; Royal Society of Canada, *Transactions*, Section 4, v. 33, p. 59-65.
 1940: Thrust faulting of Grenville gneisses northward against the Mistassini Series of Mistassini Lake, Quebec; *Journal of Geology*, v. 48, p. 512-525.
- O'Donnell, N.D.
 1973: Glacial indicator trains near Gullbridge, Newfoundland; unpublished M.Sc. thesis, University of Western Ontario, London, Ontario, 259 p.
- Prest, V.K.
 1968: Nomenclature of moraines and ice-flow features as applied to the glacial map of Canada; Geological Survey of Canada, Paper 67-57, 32 p.
 1970: Quaternary geology of Canada; in *Geology and Economic Minerals of Canada*, ed. R.J.W. Douglas, Geological Survey of Canada, Economic Geology Report No. 1, p. 675-764.
- Quirke, T.T., Jr., Goldich, S.S., and Krueger, H.W.
 1960: Composition and age of the Temiscamie iron-formation, Mistassini Territory, Quebec, Canada; *Economic Geology*, v. 55, p. 311-326.
- Richardson, J.
 1872: Report on the country north of Lake St. John; Geological Survey of Canada, Report of Progress for 1870-71, p. 283-308.
- Seguin, M.K. and Laroche, P.
 1975: Physical properties of specimens from sulphide deposits in Quebec; *Canadian Mining and Metallurgical Bulletin*, v. 68, no. 757, p. 57-66.
- Shaw, G.
 1944: Moraines of late Pleistocene ice fronts near James Bay, Quebec; Royal Society of Canada, *Transactions*, Section 4, v. 38, p. 79-85.
- Shilts, W.W.
 1971: Till studies and their application to regional drift prospecting; *Canadian Mining Journal*, v. 92, no. 4, p. 45-50.
 1973: Glacial dispersal of rocks, minerals, and trace elements in Wisconsinan till, southeastern Quebec, Canada; in *The Wisconsinan Stage*, ed. R.F. Black, R.P. Goldthwait, and H.B. Willman, Geological Society of America, Memoir 136, p. 189-219.
- Shilts, W.W. (cont'd.)
 1975: Principles of geochemical exploration for sulphide deposits using shallow samples of glacial drift; *Canadian Mining and Metallurgical Bulletin*, v. 68, no. 757, p. 73-80.
 1976: Glacial till and mineral exploration; in *Glacial Till, an Interdisciplinary Study*, ed. R.F. Legget, University of Toronto Press, Toronto, p. 205-224.
- Skinner, R.G.
 1972: Overburden study aids search for ore in Abitibi clay belt; *Northern Miner*, v. 58, no. 37, p. 62.
 1973: Quaternary stratigraphy of the Moose River basin, Ontario; Geological Survey of Canada, Bulletin 225, 77 p.
- Starkey, J.
 1970: A computer programme to prepare orientation diagrams; in *Experimental and Natural Rock Deformation*, ed. P. Paulitsch, Springer-Verlag, Berlin, p. 51-74.
- Stockwell, C.H.
 1970: Introduction to geology of the Canadian Shield; in *Geology and Economic Minerals of Canada*, ed. R.J.W. Douglas, Geological Survey of Canada, Economic Geology Report No. 1, p. 44-54.
- Szabo, N.L., Govett, G.J.S., and Lajtai, E.Z.
 1975: Dispersion trends of elements and indicator pebbles in glacial till around Mt. Pleasant, New Brunswick, Canada; *Canadian Journal of Earth Sciences*, v. 12, p. 1534-1556.
- Theimer, O.
 1952: The statistical mechanics of crushing processes; *Kolloidschrift*, v. 128, p. 1-6.
- Troop, A.J. and Darcy, G.
 1973: Geology of the Icon Sullivan Joint Venture copper deposit, Quebec; *Canadian Mining and Metallurgical Bulletin*, v. 66, no. 729, p. 89-95.
- Vagners, U.J.
 1969: Mineral distribution in tills of south-central Ontario; unpublished Ph.D. thesis, University of Western Ontario, London, 277 p.
- Vincent, J-S.
 1977: Le Quaternaire récent de la région du cours inférieur de la Grande Rivière, Québec; Commission géologique du Canada, Étude 76-19, 20 p.
- Vincent, J-S. and Hardy, L.
 1979: The evolution of glacial lakes Barlow and Ojibway in Quebec and Ontario; Geological Survey of Canada, Bulletin 316, 18 p.
- Wahl, W.G.
 1953: Temiscamie River area, Mistassini Territory; Quebec Department of Mines, Geological Report 54, 32 p.
- Warren, B.
 1974: Rapport préliminaire sur les dépôts de surface de la région de Baie du Poste; Ministère des richesses naturelles, Québec, DP 267, 8 p.
- Wennervirta, H.
 1968: Application of geochemical methods to regional prospecting in Finland; Commission Géologique du Finlande, Bulletin 234, 91 p.

APPENDIX 1

METHODS AND RESULTS OF TEXTURAL, CARBONATE, AND LITHOLOGIC ANALYSES OF QUATERNARY LITHOSTRATIGRAPHIC UNITS

Field methods

At each site, a bulk sample of approximately 1 kg of sediment was taken by channelling the sediment. At least 300 pebbles (4 to 64 mm) were collected at random from the sediment.

Till pebble orientations were measured by: (1) excavation of a horizontal bench in the till to a depth at which visually massive fresh till was met, (2) scraping of the bench surface to expose the till pebbles, and (3) measurement of the trend and plunge of the long axis of any pebble with a long to intermediate axial ratio greater than 3:2.

Laboratory analyses

Textural analysis

After air drying, each bulk sample was dry-sieved on a 4 mm sieve; the oversize was added to the pebble sample, and the undersize was retained for analysis. A subsample of 100 g of sediment finer than 4 mm was wet-sieved on a 0.037 mm sieve; the oversize was dried and retained, and the undersize was funnelled into a sedimentation cylinder for hydrometer analysis. The fraction coarser than 0.037 mm was dry-sieved to determine the weight percentage in size ranges between 4 and 0.037 mm. The hydrometer analysis procedure was similar to the ASTM procedure D422-64 (ASTM, 1964), except that a water bath was not used and the fraction coarser than 0.037 mm was not present in the sedimentation cylinder. The textural classes used were sand (4 to 0.063 mm), silt (0.063 to 0.002 mm), and clay (<0.002 mm).

Carbonate analysis

The weight percentage of calcite and dolomite in the <0.063 mm fraction of each sample was found using a modified version of the method of Dreimanis (1962). In this method, hydrochloric acid (20%) is added to a weighed sample and the volume of CO₂ evolved is recorded after 30 seconds

and about 30 minutes (or complete dissolution). The first reading is used to calculate weight per cent calcite, and both readings are used to calculate weight per cent dolomite. The modification to the method involves the use of a stopwatch instead of a time-calibrated acid burette to time the first 30 seconds.

Because the samples contained mostly dolomite and only traces of calcite, samples of 1.7 g were used. Two analyses of each sample were performed. Malachite and azurite react like dolomite (slowly) in this procedure, and samples of oxidized unit C containing abundant carbonates (Table 1.3) are those containing abundant malachite and azurite.

Pebble lithology

Each sample of pebbles (4 to 64 mm) was soaked in a dispersant solution (0.5% sodium hexametaphosphate) for about 24 hours to remove adhering matrix. The dispersant was decanted and replaced with hot hydrochloric acid (5%) for 30 seconds to complete the matrix removal. The pebbles were wet-sieved with cold water on a 4 mm sieve to complete the washing. The fraction coarser than 4 mm was dried and classified lithologically.

Tabulation of analytical results

The results of the foregoing analyses are listed in Tables 1.1 to 1.4. Texture is recorded as per cent sand (4 to 0.063 mm), silt (0.063 to 0.002 mm), and clay (<0.002 mm). Carbonate abundance (CARB) is recorded as per cent in the <0.063 mm fraction. Pebble lithology is recorded as the percentage of various rock types in the 4 to 64 mm fraction. The column headings for pebble lithology are V (total vein), CP (chalcopyrite-bearing vein, included in V), PCH (Papaskwasati plus Cheno formations), TM (Temiscamie Formation), LA (Lower Albabel Formation), UA (Upper Albabel Formation), CHB (Chibougamau Formation), IGMT (igneous and metamorphic crystallines), and NUM (number of pebbles in the sample).

Table 1.1
Texture and lithology of unit A

| SAMPLE NUMBER | TEXTURE (%) | | | CARB (%) | PEBBLE LITHOLOGY | | | | | | | | NUM |
|---------------|-------------|------|------|----------|------------------|-----|-----|-----|------|------|------|------|-----|
| | SAND | SILT | CLAY | | V | CP | PCH | TM | LA | UA | CHB | IGMT | |
| 72-1-1 | 43 | 50 | 7 | 18.9 | 0 | 0 | 1.4 | 0.3 | 62.0 | 9.2 | 0.6 | 26.5 | 347 |
| 72-1-2 | 44 | 50 | 6 | 18.6 | 0.9 | 0 | 1.7 | 0.3 | 73.2 | 6.6 | 0 | 17.3 | 347 |
| 72-1-3 | 39 | 54 | 7 | 20.8 | 0.9 | 0 | 1.5 | 0.3 | 65.1 | 11.1 | 0.3 | 20.8 | 332 |
| 72-2-1 | 50 | 44 | 6 | 16.5 | 0.6 | 0 | 1.4 | 0 | 50.4 | 6.1 | 0 | 41.5 | 359 |
| 72-2-2 | 47 | 47 | 6 | 17.8 | 0.7 | 0 | 1.3 | 0.7 | 42.1 | 10.0 | 0 | 45.3 | 309 |
| 72-2-3 | 49 | 43 | 8 | 17.8 | 0.6 | 0 | 1.5 | 0 | 55.8 | 10.4 | 0 | 31.8 | 346 |
| 72-5-2 | 45 | 49 | 6 | 18.5 | 0.3 | 0 | 1.1 | 0.3 | 56.6 | 13.5 | 1.1 | 27.2 | 364 |
| 72-6-1 | 62 | 36 | 2 | 1.4 | 0 | 0 | 2.1 | 0.6 | 15.1 | 0 | 1.5 | 80.7 | 337 |
| 72-7-1 | 61 | 34 | 5 | 1.3 | 0 | 0 | 1.0 | 0 | 19.1 | 0.2 | 11.2 | 68.4 | 418 |
| 72-7-2 | 62 | 30 | 8 | 16.1 | 0 | 0 | 0.8 | 0 | 35.7 | 3.6 | 4.0 | 55.9 | 476 |
| 72-10-1 | 70 | 27 | 3 | 1.5 | 0 | 0 | 1.2 | 0 | 5.2 | 0 | 10.4 | 83.1 | 249 |
| 72-11-1 | 65 | 30 | 5 | 1.3 | 0.3 | 0 | 1.0 | 0 | 25.5 | 0 | 4.6 | 68.6 | 389 |
| 72-13-1 | 71 | 27 | 2 | 14.5 | 0.3 | 0 | 1.6 | 0 | 53.9 | 5.9 | 3.1 | 35.3 | 388 |
| 72-14-1 | 50 | 45 | 5 | 16.7 | 0 | 0 | 0 | 0 | 71.3 | 3.6 | 0 | 25.1 | 362 |
| 72-14-2 | 52 | 42 | 6 | 18.5 | 0.3 | 0 | 0.8 | 0 | 68.3 | 2.5 | 0 | 28.1 | 398 |
| 72-14-3 | 56 | 39 | 5 | 16.3 | 0 | 0 | 0.3 | 0 | 72.0 | 3.2 | 0 | 24.5 | 372 |
| 73-1-1 | 45 | 46 | 9 | 21.1 | 0.4 | 0 | 0 | 0 | 54.3 | 2.0 | 3.2 | 40.1 | 565 |
| 73-1-2 | 42 | 49 | 9 | 22.9 | 0 | 0 | 0.4 | 0 | 66.0 | 3.8 | 1.9 | 27.8 | 468 |
| 73-2-2 | 42 | 53 | 5 | 18.5 | 0.3 | 0 | 3.0 | 0 | 59.7 | 12.8 | 0 | 24.2 | 335 |
| 73-4-1 | 52 | 43 | 5 | 28.0 | 0 | 0 | 1.8 | 0 | 74.8 | 22.1 | 0 | 1.3 | 163 |
| 73-10-1 | 47 | 49 | 4 | 19.7 | 0.6 | 0 | 2.7 | 0.2 | 61.6 | 4.9 | 0 | 30.0 | 531 |
| 73-11-1 | 43 | 50 | 7 | 16.0 | 0 | 0 | 0.8 | 0.3 | 56.3 | 8.8 | 0 | 34.0 | 400 |
| 73-12-1 | 48 | 48 | 4 | 15.1 | 0.3 | 0 | 0.8 | 0 | 59.8 | 9.8 | 0 | 29.3 | 388 |
| 73-13-1 | 47 | 45 | 8 | 20.0 | 0.2 | 0 | 2.4 | 0.2 | 49.9 | 11.8 | 0.2 | 35.3 | 425 |
| 73-13-2 | 46 | 47 | 7 | 40.4 | 0.6 | 0 | 0.2 | 0.2 | 61.7 | 6.9 | 0 | 30.4 | 493 |
| 73-14-2 | 45 | 49 | 6 | 17.3 | 0.8 | 0 | 2.0 | 0.3 | 66.8 | 12.8 | 0 | 17.3 | 397 |
| 73-15-1 | 46 | 50 | 4 | 15.5 | 0.6 | 0 | 1.5 | 0 | 51.2 | 11.8 | 0 | 25.0 | 340 |
| 73-16-1 | 49 | 46 | 5 | 17.4 | 1.1 | 0 | 0.7 | 0 | 61.0 | 7.1 | 0 | 30.1 | 451 |
| 73-17-1 | 50 | 44 | 6 | 16.7 | 0.6 | 0 | 1.5 | 0 | 59.3 | 11.2 | 0 | 27.4 | 332 |
| 73-18-1 | 49 | 46 | 5 | 13.0 | 0.6 | 0 | 4.1 | 0 | 59.7 | 9.7 | 0 | 25.9 | 340 |
| 73-19-1 | 45 | 47 | 8 | 14.9 | 0.6 | 0 | 2.3 | 0 | 60.2 | 16.1 | 0 | 20.8 | 347 |
| 73-20-1 | 37 | 57 | 6 | 17.3 | 0 | 0 | 0.9 | 0 | 70.8 | 7.1 | 0 | 21.2 | 435 |
| 73-22-1 | 46 | 47 | 7 | 17.2 | 0.5 | 0 | 1.6 | 0 | 68.8 | 8.8 | 0 | 20.3 | 365 |
| 73-23-1 | 46 | 49 | 5 | 13.7 | 0.3 | 0 | 1.3 | 0.3 | 79.2 | 9.2 | 0 | 9.7 | 303 |
| 73-24-1 | 48 | 47 | 5 | 16.0 | 0.8 | 0 | 1.0 | 0 | 66.4 | 18.1 | 0 | 13.7 | 387 |
| 73-25-1* | 20 | 52 | 28 | 3.6 | 0.3 | 0 | 1.8 | 0 | 88.4 | 8.9 | 0 | 0.6 | 395 |
| 73-26-1 | 38 | 50 | 12 | 19.4 | 0.6 | 0 | 1.1 | 0 | 75.5 | 13.2 | 0 | 9.6 | 355 |
| 73-27-1 | 30 | 58 | 12 | 19.3 | 0.5 | 0 | 0.9 | 0.2 | 80.3 | 9.5 | 0 | 8.6 | 431 |
| 73-31-1 | 29 | 61 | 10 | 25.1 | 3.7 | 0.3 | 2.0 | 0.3 | 75.3 | 13.2 | 0 | 5.4 | 295 |
| 73-32-1 | 41 | 51 | 8 | 13.7 | 5.3 | 0.3 | 2.6 | 0.6 | 64.5 | 11.4 | 0 | 15.5 | 341 |
| 73-36-1 | 50 | 42 | 8 | 17.0 | 2.0 | 0 | 2.3 | 0.3 | 50.5 | 11.6 | 0 | 33.3 | 345 |
| 73-37-1 | 54 | 37 | 9 | 17.1 | 1.3 | 0 | 2.8 | 0 | 56.0 | 12.6 | 0 | 27.3 | 396 |
| 73-67-1 | 49 | 44 | 7 | 20.2 | 0.7 | 0 | 0.7 | 0 | 69.0 | 9.2 | 0 | 20.4 | 284 |
| 73-67-2 | 47 | 46 | 7 | 21.0 | 0.2 | 0 | 0.6 | 0.4 | 58.5 | 9.1 | 0 | 31.2 | 497 |
| 73-67-3 | 42 | 50 | 8 | 20.5 | 0 | 0 | 0.8 | 0 | 56.0 | 6.1 | 0 | 37.2 | 661 |
| 73-67-4 | 43 | 50 | 7 | 20.5 | 0.2 | 0 | 1.6 | 0.2 | 57.1 | 7.4 | 0 | 33.7 | 645 |
| 73-67-5 | 45 | 47 | 8 | 19.6 | 0 | 0 | 1.7 | 0.5 | 55.3 | 7.5 | 0 | 33.4 | 637 |
| 73-69-2-4 | - | - | - | - | 1.7 | 0 | 1.7 | 1.7 | 69.0 | 15.5 | 0 | 10.4 | 58 |
| 73-69-6 | - | - | - | - | 6.5 | 0 | 3.2 | 0 | 74.2 | 9.7 | 0 | 6.5 | 31 |
| 73-73-1 | 53 | 42 | 5 | 19.0 | 0 | 0 | 0.8 | 0 | 44.4 | 4.9 | 17.7 | 32.2 | 388 |
| 74-13-1 | 25 | 61 | 14 | 20.0 | - | - | - | - | - | - | - | - | - |

*Colluvium

Table 1.2
Texture and lithology of unit B

| SAMPLE NUMBER | TEXTURE (%) | | | CARB (%) | PEBBLE LITHOLOGY | | | | | | | | NUM |
|---|-------------|------|------|----------|------------------|-----|------|-----|------|------|------|------|------|
| | SAND | SILT | CLAY | | V | CP | PCH | TM | LA | UA | CHB | IGMT | |
| <u>Till in unit B at the Icon mine</u> | | | | | | | | | | | | | |
| 72-12ALO6 | 60 | 34 | 6 | 23.2 | 0 | 0 | 5.5 | 0 | 65.6 | 10.2 | 0 | 18.7 | 343 |
| 72-12BLO6 | 64 | 28 | 8 | 22.0 | 0 | 0 | 4.5 | 0 | 67.2 | 12.3 | 0 | 16.0 | 399 |
| 72-12BL2 | 61 | 32 | 7 | 22.5 | 1.0 | 0.3 | 4.3 | 0 | 63.0 | 11.2 | 0 | 20.4 | 392 |
| 72-12BL4 | 67 | 28 | 5 | 37.7 | 0.5 | 0 | 3.8 | 0.7 | 70.9 | 7.8 | 0 | 16.4 | 426 |
| 72-12CLO6 | 60 | 33 | 7 | 19.2 | 2.3 | 0.2 | 8.3 | 0.2 | 59.3 | 12.2 | 0 | 17.7 | 435 |
| 72-12CL2 | 64 | 26 | 10 | 21.6 | 0 | 0 | 11.8 | 0.3 | 59.8 | 7.4 | 0 | 20.8 | 366 |
| 72-12CL4 | 63 | 30 | 7 | 26.6 | 4.4 | 0 | 4.1 | 0.5 | 62.5 | 12.1 | 0 | 16.5 | 413 |
| 72-12DLO6 | 64 | 30 | 6 | 19.9 | 0 | 0 | 14.6 | 0.3 | 59.2 | 7.4 | 0.3 | 18.2 | 390 |
| 72-12DL2 | 63 | 32 | 5 | 18.9 | 0.3 | 0 | 11.3 | 0 | 62.0 | 8.4 | 0 | 18.1 | 382 |
| 72-12DL4 | 63 | 33 | 4 | 20.6 | 1.5 | 0 | 9.9 | 0.3 | 61.8 | 7.6 | 0 | 19.0 | 406 |
| 72-12EL1 | 52 | 40 | 8 | 18.0 | 0 | 0 | 7.8 | 0 | 63.7 | 8.8 | 0 | 19.7 | 295 |
| 72-12EL3 | 60 | 34 | 6 | 20.4 | 0 | 0 | 10.9 | 0 | 59.3 | 9.9 | 0.5 | 19.4 | 396 |
| 72-12GLO6 | 67 | 27 | 6 | 19.7 | 0 | 0 | 18.7 | 0 | 39.6 | 6.1 | 0 | 35.7 | 311 |
| 2S-5E-F | - | - | - | - | 1.3 | 0 | 7.0 | 0 | 58.9 | 12.0 | 0 | 20.9 | 158 |
| 6S-8E-F | 61 | 36 | 3 | 23.9 | 0.8 | 0 | 3.8 | 0.4 | 79.3 | 5.9 | 0 | 9.7 | 237 |
| 71-3 | 66 | 30 | 4 | 21.0 | 0 | 0 | 14.6 | 0 | 55.1 | 8.4 | 0 | 21.9 | 356 |
| 71-15 | - | - | - | - | 0.8 | 0 | 4.6 | 0 | 76.4 | 0 | 0 | 18.2 | 259 |
| 71-18 | - | - | - | - | 0.7 | 0 | 19.9 | 0 | 50.3 | 8.0 | 0 | 21.1 | 302 |
| 73-61-1 | 41 | 54 | 5 | 20.3 | 0.3 | 0 | 1.2 | 0 | 83.6 | 5.1 | 0 | 9.8 | 604 |
| 74-9-1 | 65 | 30 | 5 | 21.6 | 0.5 | 0 | 7.7 | 0.5 | 58.3 | 6.0 | 0 | 27.0 | 182 |
| 71-4 | 62 | 35 | 3 | 17.3 | 0.9 | 0 | 16.4 | 0.9 | 48.3 | 6.9 | 0 | 26.7 | 116 |
| 73-64-15-17 | - | - | - | - | 0.5 | 0 | 2.7 | 0 | 70.7 | 11.2 | 0 | 14.9 | 402 |
| 73-65-23 | - | - | - | - | 0.1 | 0 | 6.4 | 0.3 | 70.3 | 11.3 | 0 | 11.7 | 1140 |
| 71-30 | 60 | 37 | 2 | 25.4 | 0.3 | 0 | 4.8 | 0.6 | 71.5 | 9.8 | 0 | 13.1 | 337 |
| 71-31 | 41 | 56 | 3 | 19.6 | 0.9 | 0.9 | 0 | 0 | 80.5 | 8.9 | 0 | 9.7 | 113 |
| 74-5-2 | 57 | 39 | 4 | 39.0 | - | - | - | - | - | - | - | - | - |
| 6S-11E-E | - | - | - | - | 0 | 0 | 0 | 0 | 92.6 | 3.3 | 0 | 4.1 | 122 |
| 10S-12E-D | - | - | - | - | 0 | 0 | 2.0 | 2.0 | 78.2 | 11.6 | 0 | 6.2 | 147 |
| 10S-12E-E | 8 | 84 | 8 | 4.5 | 0 | 0 | 0 | 0 | 89.8 | 3.4 | 0 | 6.8 | 59 |
| <u>Ice contact stratified drift in unit B at the Icon mine</u> | | | | | | | | | | | | | |
| 2S-3D-E | - | - | - | - | 1.1 | 0 | 1.6 | 0 | 81.5 | 4.9 | 0 | 10.9 | 184 |
| 73-62-9-11 | - | - | - | - | 0.6 | 0 | 2.2 | 0 | 85.1 | 6.5 | 0 | 5.6 | 321 |
| 73-62-18 | - | - | - | - | 0 | 0 | 1.9 | 0 | 87.4 | 5.1 | 0 | 5.6 | 214 |
| 73-64-13,14 | - | - | - | - | 0 | 0 | 2.5 | 0.2 | 81.8 | 5.3 | 0 | 10.3 | 610 |
| 73-64-19 | - | - | - | - | 0.4 | 0 | 5.6 | 0 | 68.9 | 10.1 | 0 | 15.0 | 1351 |
| 73-64-20 | - | - | - | - | 0 | 0 | 0.6 | 0.1 | 84.2 | 6.7 | 0 | 8.4 | 1163 |
| 74-5-1 | 89 | 9 | 2 | 35.9 | 0 | 0 | 18.0 | 0 | 54.5 | 5.6 | 0 | 21.9 | 517 |
| 72-12F2 | 85 | 13 | 2 | 30.8 | - | - | - | - | - | - | - | - | - |
| 72-12FO6 | 45 | 51 | 4 | 15.7 | - | - | - | - | - | - | - | - | - |
| 72-12G2 | 57 | 39 | 4 | 14.7 | - | - | - | - | - | - | - | - | - |
| 73-66-2 | 61 | 37 | 2 | 20.3 | - | - | - | - | - | - | - | - | - |
| 73-62-19 | - | - | - | - | 0.5 | 0 | 1.8 | 0 | 86.7 | 4.6 | 0 | 6.4 | 218 |
| <u>Till in unit B elsewhere in the study area</u> | | | | | | | | | | | | | |
| 72-5-1 | 80 | 18 | 2 | 16.4 | 0.2 | 0 | 0.9 | 0.2 | 46.4 | 6.5 | 11.3 | 34.7 | 681 |
| 72-8-1 | - | - | - | - | 0 | 0 | 1.2 | 0 | 38.7 | 8.8 | 14.7 | 36.7 | 251 |
| 72-8-2 | - | - | - | - | 0.4 | 0 | 2.7 | 0 | 44.1 | 3.5 | 16.4 | 32.8 | 256 |
| 73-63-1 | - | - | - | - | 0 | 0 | 1.1 | 0 | 18.3 | 0 | 4.4 | 76.2 | 1041 |
| 73-72-1 | - | - | - | - | 0 | 0 | 1.3 | 0 | 44.6 | 2.8 | 2.8 | 48.5 | 634 |
| <u>Ice contact stratified drift in unit B elsewhere in the study area</u> | | | | | | | | | | | | | |
| 72-3-1 | 81 | 17 | 2 | 23.6 | 0.4 | 0 | 1.2 | 0.3 | 45.0 | 8.6 | 0.1 | 44.3 | 733 |
| 72-4-1 | 85 | 14 | 1 | 28.3 | 0.5 | 0 | 2.9 | 0 | 44.0 | 9.9 | 0 | 42.8 | 587 |
| 72-9-1 | - | - | - | - | 0.4 | 0 | 0.8 | 0 | 46.2 | 8.8 | 12.5 | 31.3 | 249 |
| 73-53-1 | - | - | - | - | 0 | 0 | 1.2 | 0.1 | 43.5 | 6.0 | 0.4 | 48.8 | 1147 |
| 73-43-1 | - | - | - | - | 1.0 | 0 | 2.4 | 0.1 | 52.2 | 13.6 | 0 | 30.7 | 1436 |
| 73-44-1 | - | - | - | - | 1.1 | 0 | 3.4 | 0.6 | 51.5 | 15.2 | 0 | 28.3 | 1493 |
| 73-45-1 | - | - | - | - | 0.2 | 0 | 2.7 | 0 | 76.6 | 15.2 | 0 | 5.3 | 1332 |
| 73-46-1 | - | - | - | - | 0.2 | 0 | 3.8 | 0.2 | 76.9 | 12.0 | 0 | 6.9 | 1289 |
| 73-41-1 | - | - | - | - | 1.7 | 0 | 7.9 | 0 | 28.5 | 10.3 | 0 | 51.6 | 808 |
| 73-42-1 | - | - | - | - | 0.9 | 0 | 3.6 | 0.1 | 43.0 | 14.6 | 0 | 37.8 | 1435 |

Table 1.3
Texture and lithology of unit C

| SAMPLE NUMBER | TEXTURE (%) | | | CARB (%) | PEBBLE LITHOLOGY | | | | | | | | NUM |
|-------------------|-------------|------|------|----------|------------------|------|-----|-----|------|-----|-----|------|------|
| | SAND | SILT | CLAY | | V | CP | PCH | TM | LA | UA | CHB | IGMT | |
| <u>Unoxidized</u> | | | | | | | | | | | | | |
| 71-2 | 63 | 30 | 7 | 35.4 | 100.0 | 36.6 | 0 | 0 | 0 | 0 | 0 | 0 | 172 |
| 71-42 | 50 | 45 | 5 | 24.0 | 86.8 | 22.4 | 0 | 0 | 12.3 | 0.6 | 0 | 0.3 | 357 |
| 71-43 | 59 | 37 | 4 | 22.3 | 48.2 | 30.2 | 1.4 | 0 | 43.7 | 2.7 | 0 | 4.1 | 222 |
| 71-44 | 45 | 51 | 4 | 26.6 | 0.6 | 0 | 0 | 0 | 97.9 | 0.9 | 0 | 0.6 | 337 |
| 73-54-1 | 59 | 36 | 5 | 27.0 | 56.9 | 4.2 | 0.1 | 0 | 38.7 | 0.2 | 0 | 4.1 | 1799 |
| 73-55-1 | 72 | 21 | 7 | 26.0 | 96.4 | 3.1 | 0 | 0 | 3.6 | 0 | 0 | 0 | 2421 |
| 73-56 | 56 | 40 | 4 | 24.6 | - | - | - | - | - | - | - | - | - |
| 73-57 | 53 | 44 | 3 | 23.3 | - | - | - | - | - | - | - | - | - |
| 73-58 | 61 | 34 | 5 | 25.1 | - | - | - | - | - | - | - | - | - |
| 73-74 | 70 | 26 | 4 | 25.4 | - | - | - | - | - | - | - | - | - |
| 74-4-1 | 51 | 41 | 8 | 16.4 | 51.7 | 0.5 | 0 | 0 | 48.0 | 0 | 0 | 0.3 | 367 |
| 74-12-2 | 65 | 26 | 9 | 17.2 | 77.6 | 4.7 | 0.1 | 0 | 22.2 | 0 | 0 | 0.1 | 817 |
| 74-14-1 | 67 | 27 | 6 | 14.5 | 88.8 | 11.0 | 0 | 0 | 11.2 | 0 | 0 | 0 | 975 |
| 73-69-1 | - | - | - | - | 67.5 | 2.5 | 0.8 | 0 | 30.8 | 0 | 0 | 0.8 | 120 |
| 73-69-5 | - | - | - | - | 52.6 | 17.1 | 0 | 0 | 43.4 | 1.3 | 0 | 2.6 | 76 |
| 73-69-7 | - | - | - | - | 97.5 | 35.3 | 0 | 0 | 2.5 | 0 | 0 | 0 | 122 |
| 73-69-8 | - | - | - | - | 74.5 | 36.4 | 0 | 0 | 25.1 | 0 | 0 | 0.4 | 247 |
| 73-69-9 | - | - | - | - | 13.8 | 0.7 | 0 | 0 | 86.2 | 0 | 0 | 0 | 290 |
| 73-69-10 | - | - | - | - | 55.8 | 27.9 | 0 | 0 | 43.0 | 1.2 | 0 | 0 | 86 |
| 73-68-3 | - | - | - | - | 41.4 | 19.0 | 3.4 | 0 | 53.5 | 0 | 0 | 1.7 | 58 |
| 73-68-4 | - | - | - | - | 42.0 | 12.4 | 1.2 | 0 | 53.1 | 1.2 | 0 | 2.5 | 81 |
| 73-68-5 | - | - | - | - | 49.3 | 18.7 | 0 | 0 | 50.7 | 0 | 0 | 0 | 75 |
| 71-8 | 36 | 49 | 15 | 13.0 | 0 | 0 | 0.4 | 0 | 93.5 | 3.0 | 0 | 3.0 | 263 |
| 71-9 | 64 | 29 | 7 | 23.4 | 0.5 | 0 | 2.1 | 0 | 88.0 | 3.2 | 0 | 6.1 | 376 |
| 71-10 | 70 | 23 | 7 | 23.8 | 0.5 | 0 | 1.1 | 0.3 | 89.5 | 3.0 | 0 | 5.7 | 371 |
| 74-12-1 | - | - | - | - | 100.0 | 39.0 | 0 | 0 | 0 | 0 | 0 | 0 | 308 |
| <u>Oxidized</u> | | | | | | | | | | | | | |
| 71-1 | 64 | 33 | 3 | 9.3 | 77.4 | 4.8 | 0 | 0 | 22.1 | 0 | 0 | 0.5 | 208 |
| 71-14 | - | - | - | - | 6.7 | 0 | 0.5 | 0 | 87.1 | 0 | 0 | 5.8 | 224 |
| 71-17 | - | - | - | - | 52.3 | 0 | 0.9 | 0 | 39.5 | 0 | 0 | 7.3 | 109 |
| 71-19 | - | - | - | - | 30.1 | 0.8 | 1.6 | 0 | 61.0 | 0 | 0 | 7.3 | 123 |
| 71-20 | - | - | - | - | 0 | 0 | 4.3 | 0 | 77.4 | 0 | 0 | 18.3 | 115 |
| 71-21 | - | - | - | - | 2.6 | 0 | 2.0 | 0 | 77.3 | 0 | 0 | 18.1 | 343 |
| 71-22 | - | - | - | - | 2.0 | 0 | 0 | 0.7 | 92.7 | 0 | 0 | 4.6 | 151 |
| 71-23 | - | - | - | - | 0.5 | 0 | 0 | 0 | 98.4 | 0 | 0 | 1.1 | 184 |
| 72-12AU2 | 74 | 23 | 3 | 28.9 | 62.8 | 7.0 | 0.4 | 0 | 31.2 | 3.0 | 0 | 2.7 | 529 |
| 72-12AU4 | 80 | 17 | 3 | 8.7 | 94.1 | 3.6 | 0 | 0 | 5.6 | 0 | 0 | 0.3 | 609 |
| 72-12AU6 | 63 | 33 | 4 | 8.6 | 74.0 | 9.7 | 0 | 0 | 26.0 | 0 | 0 | 0 | 381 |
| 72-12BU6 | 64 | 32 | 4 | 5.4 | 69.3 | 7.4 | 0 | 0 | 30.7 | 0 | 0 | 0 | 501 |
| 72-12CU6 | 67 | 29 | 4 | 11.3 | 69.9 | 5.2 | 0 | 0 | 29.6 | 0 | 0 | 0.5 | 601 |
| 72-12DU5 | 69 | 28 | 3 | 4.2 | 74.5 | 5.7 | 0 | 0 | 25.3 | 0 | 0 | 0.2 | 597 |
| 72-12EU46 | 68 | 27 | 5 | 11.4 | 84.7 | 8.2 | 0.3 | 0 | 13.8 | 0.5 | 0 | 0.7 | 588 |
| 72-12EU56 | 70 | 27 | 3 | 4.3 | 71.0 | 15.8 | 0 | 0 | 29.0 | 0 | 0 | 0 | 590 |
| 72-12FU3 | 71 | 25 | 4 | 14.4 | 86.2 | 5.1 | 0.4 | 0 | 11.8 | 0.4 | 0 | 1.2 | 507 |
| 72-12FU4 | 58 | 38 | 4 | 2.8 | 76.4 | 9.5 | 0 | 0 | 23.6 | 0 | 0 | 0 | 454 |
| 72-12GU36 | 74 | 22 | 4 | 5.4 | 93.2 | 5.4 | 0 | 0 | 6.8 | 0 | 0 | 0 | 636 |
| 73-33-1 | 16 | 69 | 15 | 6.5 | 82.8 | 2.0 | 0 | 0 | 16.3 | 0 | 0 | 0.9 | 449 |
| 73-34-1 | 34 | 59 | 7 | 14.6 | 73.2 | 10.9 | 0.3 | 0 | 22.9 | 2.1 | 0 | 1.5 | 671 |
| 73-62-17 | 51 | 46 | 3 | 6.9 | 14.8 | 0.5 | 0.4 | 0 | 83.9 | 0 | 0 | 0.9 | 569 |
| 73-64-18 | 54 | 43 | 3 | 5.0 | 89.3 | 3.0 | 0 | 0 | 9.8 | 0 | 0 | 0.9 | 346 |
| 73-66-1 | 56 | 41 | 3 | 28.1 | - | - | - | - | - | - | - | - | - |
| 74-10-1 | 67 | 27 | 6 | 14.1 | 97.7 | 3.8 | 0 | 0 | 2.3 | 0 | 0 | 0 | 686 |
| 73-65-22 | - | - | - | - | 73.5 | 2.4 | 0.7 | 0 | 24.3 | 0 | 0 | 1.4 | 805 |
| 73-70-3 | - | - | - | - | 98.5 | 7.9 | 0 | 0 | 1.5 | 0 | 0 | 0 | 192 |
| 73-68-6 | - | - | - | - | 1.0 | 0 | 0 | 0 | 98.0 | 0 | 0 | 1.0 | 100 |
| 73-68-7 | - | - | - | - | 0 | 0 | 0 | 0 | 98.6 | 1.4 | 0 | 0 | 69 |
| 73-68-8 | - | - | - | - | 3.0 | 1.5 | 0 | 0 | 97.0 | 0 | 0 | 0 | 66 |
| 73-68-9 | - | - | - | - | 0 | 0 | 0 | 0 | 97.7 | 0 | 0 | 2.3 | 86 |
| 73-68-10 | - | - | - | - | 1.9 | 0 | 0 | 0 | 96.2 | 0 | 0 | 1.9 | 52 |
| 73-68-11 | - | - | - | - | 1.5 | 0 | 0 | 0 | 97.0 | 0 | 0 | 1.5 | 68 |

Table 1.3 (cont.)

| SAMPLE NUMBER | TEXTURE (%) | | | CARB (%) | PEBBLE LITHOLOGY | | | | | | | | |
|---|-------------|------|------|----------|------------------|-----|-----|-----|------|-----|-----|------|-----|
| | SAND | SILT | CLAY | | V | CP | PCH | TM | LA | UA | CHB | IGMT | NUM |
| Oxidized samples from the grid shown in Figures 30, 35. The site in the northwest corner of the grid is OS-OE and the most southwesterly site is 20S-1E | | | | | | | | | | | | | |
| 6S-5E-E | 33 | 65 | 2 | 2.0 | 23.7 | 0 | 1.8 | 0.9 | 67.6 | 2.6 | 0 | 3.5 | 114 |
| 6S-8E-E | 49 | 46 | 5 | 0.0 | 47.3 | 2.0 | 2.7 | 0 | 41.9 | 0.7 | 0 | 7.4 | 148 |
| 8S-8E-E | 15 | 71 | 14 | 0.0 | 66.7 | 6.7 | 0 | 0 | 33.3 | 0 | 0 | 0 | 30 |
| 12S-8E-E* | 22 | 73 | 5 | 4.2 | 10.5 | 1.2 | 2.3 | 0 | 80.2 | 0 | 0 | 7.0 | 86 |
| 14S-10E-E | 38 | 58 | 4 | 10.2 | 16.7 | 0.2 | 0.7 | 0 | 74.8 | 0.2 | 0 | 7.6 | 564 |
| 14S-11E-E | 57 | 41 | 2 | 24.9 | 3.8 | 0.2 | 1.4 | 0.2 | 82.0 | 6.4 | 0 | 6.2 | 629 |
| 16S-9E-E | 51 | 46 | 3 | 24.7 | 12.6 | 0 | 0.5 | 0 | 75.6 | 5.3 | 0 | 6.0 | 398 |

| SAMPLE NUMBER | PEBBLE LITHOLOGY | | | | | | | | | |
|---|------------------|-----|------|-----|------|-----|-----|------|-----|--|
| | V | CP | PCH | TM | LA | UA | CHB | IGMT | NUM | |
| Oxidized samples from the grid, pebble lithology only | | | | | | | | | | |
| OS-OE-D | 0 | 0 | 0.6 | 0 | 93.3 | 0 | 0 | 6.1 | 163 | |
| 2S-OE-D | 0 | 0 | 1.5 | 0 | 89.5 | 0 | 0 | 9.0 | 134 | |
| 2S-1E-D | 0.8 | 0 | 0.8 | 0 | 95.9 | 0 | 0 | 2.5 | 121 | |
| 2S-3E-D | 18.8 | 0.9 | 0.9 | 0 | 79.5 | 0 | 0 | 0.9 | 117 | |
| 2S-5E-E | 31.7 | 1.7 | 0 | 0 | 65.8 | 0 | 0 | 2.5 | 120 | |
| 2S-6E-D | 24.6 | 0.9 | 0 | 0 | 75.4 | 0 | 0 | 0 | 110 | |
| 2S-7E-D | 79.8 | 0 | 0 | 0 | 20.2 | 0 | 0 | 0 | 114 | |
| 4S-OE-D | 3.5 | 0.7 | 1.4 | 0 | 91.6 | 0 | 0 | 3.5 | 144 | |
| 4S-1E-D | 0 | 0 | 0 | 0 | 98.4 | 0 | 0 | 1.6 | 127 | |
| 4S-2E-D | 3.3 | 0 | 1.6 | 0 | 87.7 | 0 | 0 | 7.4 | 122 | |
| 4S-3E-D | 1.4 | 0 | 3.6 | 0.7 | 85.7 | 0 | 0 | 8.6 | 139 | |
| 4S-4E-D | 10.2 | 0.9 | 3.7 | 0 | 83.3 | 0 | 0 | 2.8 | 108 | |
| 4S-5E-D | 51.6 | 0.8 | 1.6 | 0 | 44.3 | 0 | 0 | 2.5 | 122 | |
| 4S-6E-D | 46.0 | 0.7 | 0 | 0 | 48.9 | 0 | 0 | 5.1 | 137 | |
| 4S-7E-D* | 33.9 | 0 | 14.2 | 0 | 32.3 | 0 | 0 | 19.7 | 127 | |
| 4S-7E-E | 29.8 | 2.1 | 2.8 | 0 | 61.7 | 0 | 0 | 5.7 | 141 | |
| 4S-8E-D | 93.1 | 2.6 | 0 | 0 | 6.0 | 0 | 0 | 0.9 | 116 | |
| 4S-9E-D | 63.7 | 0 | 0 | 0 | 36.3 | 0 | 0 | 0 | 102 | |
| 6S-OE-D | 0 | 0 | 4.4 | 0.7 | 87.1 | 0.7 | 0 | 7.1 | 140 | |
| 6S-1E-D | 0.6 | 0 | 4.3 | 0 | 86.5 | 0 | 0 | 8.6 | 163 | |
| 6S-2E-D | 2.1 | 0 | 0.7 | 0 | 95.1 | 0 | 0 | 2.1 | 142 | |
| 6S-3E-D | 2.9 | 0 | 0.7 | 0 | 87.8 | 0 | 0 | 8.6 | 139 | |
| 6S-4E-D | 24.0 | 0 | 0.8 | 0 | 72.1 | 0 | 0 | 3.1 | 129 | |
| 6S-4E-E | 26.3 | 0 | 1.9 | 0 | 66.2 | 0 | 0 | 5.6 | 160 | |
| 6S-5E-D | 31.9 | 1.3 | 3.1 | 0 | 57.5 | 0 | 0 | 7.5 | 160 | |
| 6S-6E-D | 54.4 | 0.7 | 2.0 | 0 | 42.3 | 0 | 0 | 1.3 | 149 | |
| 6S-7E-D | 37.3 | 1.8 | 3.0 | 0 | 56.1 | 0 | 0 | 3.6 | 169 | |
| 6S-8E-D | 65.5 | 1.8 | 0 | 0 | 27.5 | 3.5 | 0 | 3.5 | 113 | |
| 6S-9E-D | 80.5 | 7.1 | 0 | 0 | 19.5 | 0 | 0 | 0 | 113 | |
| 6S-10E-D | 66.3 | 8.9 | 1.2 | 0 | 32.5 | 0 | 0 | 0 | 169 | |
| 6S-11E-D | 2.5 | 0 | 1.7 | 0 | 93.3 | 1.7 | 0 | 0.8 | 120 | |
| 8S-OE-D | 0.8 | 0 | 1.6 | 0 | 92.8 | 0 | 0 | 4.8 | 125 | |
| 8S-1E-D | 0 | 0 | 0 | 0 | 97.9 | 0.7 | 0 | 1.4 | 147 | |
| 8S-2E-D | 0 | 0 | 0.9 | 0 | 95.6 | 2.6 | 0 | 0.9 | 117 | |
| 8S-3E-D | 7.1 | 0.7 | 0.7 | 0 | 87.2 | 0 | 0 | 5.0 | 140 | |
| 8S-4E-D | 21.9 | 0 | 0.6 | 0 | 76.6 | 0 | 0 | 1.9 | 155 | |
| 8S-5E-D | 43.0 | 0 | 4.4 | 0.6 | 46.2 | 0 | 0 | 5.8 | 158 | |
| 8S-6E-D* | 12.2 | 0.6 | 3.0 | 0 | 70.8 | 6.7 | 0 | 7.3 | 165 | |
| 8S-7E-D* | 31.1 | 0.7 | 0.7 | 0 | 55.4 | 5.4 | 0 | 7.4 | 148 | |
| 8S-8E-D | 26.6 | 0 | 0.8 | 0 | 66.1 | 0 | 0 | 6.5 | 124 | |
| 8S-9E-D | 42.9 | 0 | 0 | 0 | 50.7 | 1.6 | 0 | 4.8 | 126 | |
| 8S-10E-D | 68.3 | 8.1 | 0.8 | 0 | 27.6 | 0 | 0 | 3.3 | 123 | |
| 8S-11E-D | 4.9 | 0 | 0.6 | 0 | 87.3 | 0 | 0 | 7.2 | 166 | |
| 8S-12E-D | 0.8 | 0 | 1.5 | 0 | 90.0 | 0.8 | 0 | 6.9 | 132 | |
| 10S-1W-D | 0.8 | 0 | 0 | 0 | 95.4 | 0 | 0 | 3.8 | 130 | |
| 10S-OE-D | 4.1 | 0 | 0 | 0 | 87.6 | 0 | 1.4 | 6.9 | 145 | |
| 10S-1E-D | 3.9 | 0 | 3.9 | 0 | 89.4 | 0 | 0 | 2.8 | 180 | |
| 10S-2E-D | 3.8 | 0 | 1.5 | 0.8 | 89.4 | 0 | 0 | 4.5 | 132 | |
| 10S-3E-D | 1.5 | 0 | 2.5 | 0 | 90.1 | 0.5 | 0 | 5.4 | 203 | |
| 10S-4E-D | 39.3 | 0 | 0.9 | 0 | 56.4 | 0 | 0 | 3.4 | 117 | |
| 10S-5E-D | 60.3 | 0.8 | 0 | 0 | 34.8 | 0 | 0 | 4.1 | 121 | |

*Incorporation of unit B in unit C

Table 1.3 (cont.)

| SAMPLE NUMBER | PEBBLE LITHOLOGY | | | | | | | | NUM |
|---------------|------------------|-----|-----|-----|------|-----|-----|------|-----|
| | V | CP | PCH | TM | LA | UA | CHB | IGMT | |
| 10S-6E-D | 45.4 | 4.3 | 5.7 | 0 | 41.1 | 0 | 0 | 7.8 | 141 |
| 10S-7E-D | 23.3 | 1.5 | 5.3 | 0 | 61.6 | 0 | 0 | 9.8 | 133 |
| 10S-8E-D | 22.7 | 2.5 | 3.4 | 0 | 57.0 | 3.4 | 0 | 13.5 | 119 |
| 10S-9E-D | 5.8 | 0 | 1.3 | 0 | 88.4 | 0 | 0 | 4.5 | 155 |
| 10S-10E-D | 39.3 | 3.3 | 0 | 0 | 60.0 | 0 | 0 | 0.7 | 150 |
| 10S-13E-D | 0 | 0 | 0.6 | 0 | 95.0 | 0 | 0 | 4.4 | 159 |
| 12S-OE-D | 1.1 | 0 | 3.4 | 0 | 91.0 | 0 | 0 | 4.5 | 179 |
| 12S-1E-D | 2.7 | 0 | 0.7 | 0 | 93.2 | 0 | 0 | 3.4 | 148 |
| 12S-2E-D | 0.7 | 0 | 0 | 0.7 | 90.0 | 4.3 | 0 | 4.3 | 138 |
| 12S-3E-D | 33.1 | 0 | 1.4 | 0 | 60.0 | 0 | 0 | 5.5 | 145 |
| 12S-4E-D* | 23.1 | 0 | 5.4 | 0 | 64.6 | 0 | 0 | 6.9 | 130 |
| 12S-5E-D | 15.8 | 0.8 | 2.4 | 0 | 77.8 | 0.8 | 0 | 3.2 | 127 |
| 12S-6E-D | 36.5 | 6.1 | 6.1 | 0 | 46.1 | 0 | 0 | 11.3 | 115 |
| 12S-7E-D | 11.9 | 0.6 | 3.4 | 0.6 | 65.9 | 2.3 | 0 | 15.9 | 176 |
| 12S-8E-D* | 4.8 | 0 | 9.7 | 0 | 75.0 | 4.0 | 0 | 6.5 | 124 |
| 12S-11E-D | 37.7 | 0 | 0 | 0 | 56.1 | 0.9 | 0 | 5.3 | 114 |
| 12S-12E-D | 0.7 | 0 | 2.9 | 0 | 85.0 | 2.1 | 0 | 9.3 | 140 |
| 14S-OE-D | 1.3 | 0 | 0.7 | 0 | 96.0 | 0 | 0 | 2.0 | 153 |
| 14S-1E-D | 2.1 | 0 | 0.7 | 0 | 92.9 | 0 | 0 | 4.3 | 140 |
| 14S-2E-D | 0 | 0 | 0 | 0 | 67.2 | 0 | 0 | 32.8 | 116 |
| 14S-3E-D | 1.4 | 0 | 0.7 | 0 | 90.0 | 1.4 | 0 | 5.6 | 143 |
| 14S-4E-D | 23.9 | 0 | 2.9 | 0 | 65.4 | 0 | 0 | 7.8 | 138 |
| 14S-5E-D | 8.2 | 4.1 | 3.4 | 0 | 79.6 | 0 | 0 | 8.8 | 147 |
| 14S-6E-D | 9.9 | 0.8 | 4.1 | 0.8 | 65.4 | 3.3 | 0 | 16.5 | 121 |
| 14S-7E-D | 19.7 | 0.8 | 5.5 | 0 | 54.3 | 0.8 | 0 | 19.7 | 127 |
| 14S-9E-D | 10.4 | 0 | 2.6 | 0 | 81.8 | 0 | 0 | 5.2 | 116 |
| 14S-10E-D | 22.5 | 0.7 | 0.7 | 0 | 70.7 | 0.7 | 0 | 5.4 | 147 |
| 14S-11E-D | 11.0 | 2.2 | 0 | 0 | 83.2 | 2.2 | 0 | 3.6 | 137 |
| 16S-OE-D | 1.5 | 0 | 2.3 | 0 | 90.9 | 0 | 0 | 5.3 | 132 |
| 16S-1E-D | 3.2 | 0 | 0 | 0 | 90.3 | 0 | 0 | 6.5 | 124 |
| 16S-2E-D | 0 | 0 | 2.7 | 0 | 93.8 | 0 | 0 | 3.5 | 113 |
| 16S-3E-D | 10.2 | 0.8 | 0.8 | 0 | 74.2 | 0 | 0 | 14.8 | 128 |
| 16S-4E-D | 3.2 | 0 | 1.6 | 0 | 55.2 | 0 | 0 | 40.0 | 125 |
| 16S-5E-D | 11.5 | 1.5 | 1.5 | 0 | 65.6 | 0.8 | 0 | 20.6 | 131 |
| 16S-6E-D | 21.3 | 1.6 | 2.4 | 0 | 55.9 | 0 | 0 | 22.8 | 127 |
| 16S-7E-D | 14.9 | 0 | 4.1 | 0 | 71.9 | 0 | 0 | 9.1 | 121 |
| 16S-9E-D | 22.8 | 1.0 | 1.0 | 0 | 75.2 | 0 | 0 | 1.0 | 101 |
| 16S-12E-D | 0 | 0 | 1.2 | 0 | 79.2 | 4.3 | 0.6 | 14.7 | 163 |
| 18S-OE-D | 0.7 | 0 | 0.7 | 0 | 97.2 | 0 | 0 | 1.4 | 147 |
| 18S-2E-D | 0 | 0 | 0 | 0.9 | 69.3 | 0 | 0 | 29.8 | 114 |
| 18S-3E-D | 3.7 | 0 | 0 | 0 | 91.3 | 0 | 0 | 5.0 | 161 |
| 18S-4E-D | 0 | 0 | 0.7 | 0 | 42.6 | 0 | 0 | 56.7 | 141 |
| 18S-8E-D | 0.7 | 0 | 0.7 | 0 | 81.5 | 0 | 0 | 17.1 | 140 |
| 20S-1E-D | 3.2 | 0 | 6.4 | 0 | 81.5 | 0 | 0 | 8.9 | 124 |
| 20S-3E-D | 0 | 0 | 0 | 0 | 95.6 | 0.7 | 0 | 3.7 | 136 |
| 20S-4E-D | 0.8 | 0 | 0 | 0 | 38.5 | 0 | 0 | 60.7 | 122 |
| 20S-6E-D | 8.9 | 0 | 2.0 | 0 | 64.3 | 0 | 0 | 24.8 | 101 |

*Incorporation of unit B in unit C

Table 1.4
Texture and lithology of units D, E, and F

| SAMPLE NUMBER | TEXTURE (%) | | | CARB (%) | PEBBLE LITHOLOGY | | | | | | | | NUM |
|--|-------------|------|------|----------|------------------|----|-----|-----|------|-----|-----|------|-----|
| | SAND | SILT | CLAY | | V | CP | PCH | TM | LA | UA | CHB | IGMT | |
| <u>Unit D, proximal outwash gravel</u> | | | | | | | | | | | | | |
| 71-13 | 67 | 31 | 2 | 18.6 | 0 | 0 | 1.3 | 0 | 78.8 | 3.4 | 0 | 16.5 | 236 |
| 71-25 | - | - | - | - | 1.3 | 0 | 0.7 | 0 | 83.3 | 4.7 | 0 | 10.0 | 150 |
| 71-26 | - | - | - | - | 0.4 | 0 | 1.1 | 0 | 84.1 | 4.8 | 0 | 9.6 | 271 |
| 71-27 | - | - | - | - | 0.6 | 0 | 0.6 | 0 | 84.0 | 5.5 | 0 | 9.3 | 343 |
| 71-32 | 57 | 40 | 3 | 23.0 | 0 | 0 | 0.5 | 0.3 | 84.8 | 1.8 | 0 | 12.6 | 388 |
| 71-33 | 61 | 34 | 5 | 26.1 | 0 | 0 | 0.3 | 0.6 | 84.9 | 3.0 | 0 | 11.2 | 338 |
| 71-34 | 70 | 26 | 4 | 19.1 | 0.8 | 0 | 1.6 | 0.3 | 84.7 | 4.3 | 0 | 8.3 | 373 |
| 71-37 | 48 | 49 | 3 | 21.1 | 0 | 0 | 0.4 | 0 | 87.0 | 2.9 | 0 | 9.8 | 246 |
| 71-39 | 54 | 43 | 3 | 18.9 | 0.5 | 0 | 2.0 | 0 | 60.6 | 4.4 | 0 | 32.5 | 203 |
| 71-41 | 53 | 44 | 3 | 19.8 | 0 | 0 | 0.4 | 0 | 56.6 | 2.7 | 0 | 40.2 | 256 |
| <u>Unit E, lacustrine silts</u> | | | | | | | | | | | | | |
| 71-11 | 0 | 78 | 22 | 7.6 | - | - | - | - | - | - | - | - | - |
| 71-28 | 0 | 89 | 11 | 10.3 | - | - | - | - | - | - | - | - | - |
| 71-36 | 0 | 82 | 18 | 11.3 | - | - | - | - | - | - | - | - | - |
| <u>Unit F, alluvium</u> | | | | | | | | | | | | | |
| 71-29 | 5 | 91 | 4 | 7.3 | - | - | - | - | - | - | - | - | - |

APPENDIX 2

TRUE DISTRIBUTION OF CHALCOPYRITE IN UNOXIDIZED TILL

Vagners (1969, p. 4-7) described the concept of true and apparent distribution of a mineral in till as follows:

"In most ... till studies, the percentages of each mineral have been determined for each grain size fraction separately, and then presented in a table or as a histogram ... This is an apparent distribution because it is valid only for each particle size fraction, but does not give the true distribution of the mineral throughout the entire till sample.

The true distribution of each mineral in the entire till sample depends upon two factors:

1. the abundance of the mineral in each particle size fraction
2. the relative percentage of all mineral matter in each particle size fraction in relation to the total till sample, i.e. - the granulometric composition of the till...

If these two factors are considered, then the true distribution of a mineral ... may be determined as follows. First the true percentage of each mineral, in relationship to the total till sample, has to be determined. The true percentage (Tp) of a mineral in each grain size fraction is calculated using the basic formula:

$$Tp = Ap \times \frac{Gp}{100}$$

where Ap is the percentage of the mineral in the grain size considered (from the apparent distribution), and Gp is the percentage of all mineral matter present in the same grain size fraction in relation to the total till sample (from the granulometric composition of the till).

Because the sums of the true percentages of each mineral for all grain size fractions are not constant in all the till samples, it is difficult to compare the distributions of the minerals and impossible to calculate percentages for their average distributions. Therefore relative percentages have to be determined for each grain size, considering the sum of these percentages for all the grain size fractions of each mineral as one hundred per cent. The following formula is used for this calculation:

$$\text{Relative true percentage (Trp)} = \frac{Tp \times 100}{STp}$$

where Tp is the true percentage of a mineral in a grain size fraction and STp is the sum of the true percentages of the mineral in all the grain sizes of the sample investigated. The distribution of these relative percentages in all the grain sizes is termed true distribution of each mineral investigated."

Table 2.1 lists the Ap, Gp, Tp, and Trp for the four bulk samples of unoxidized chalcopyrite-bearing till (unit C).

Table 2.1
Abundance of chalcopyrite with respect to grain size
in unoxidized till samples

| Sample 73-56 | | Sample 73-57 | | Sample 73-58 | | Sample 73-74 | | Totals | | | | | | | | |
|---------------|----------|--------------|--------|---------------|----------|--------------|--------|---------------|----------|--------|--------|---------------|----------|--------|--------|--------|
| Fraction (mm) | Ap | Gp | Trp | Fraction (mm) | Ap | Gp | Trp | Fraction (mm) | Ap | Gp | Trp | Fraction (mm) | Ap | Gp | Trp | Totals |
| 128 | 28.3 | 2.04 | 3.42 | 128 | 24.8 | 1.84 | 1.96 | 128 | 0.0 | 3.04 | 0.0 | 128 | 24.8 | 1.84 | 1.96 | 100.02 |
| 64 | 31.2 | 4.44 | 9.71 | 64 | 40.9 | 3.50 | 6.14 | 64 | 1.56 | 7.70 | 0.120 | 64 | 40.9 | 3.50 | 6.14 | 3.483 |
| 32 | 27.1 | 5.02 | 9.50 | 32 | 21.7 | 7.47 | 6.96 | 32 | 2.18 | 10.12 | 0.220 | 32 | 21.7 | 7.47 | 6.96 | |
| 16 | 30.8 | 4.79 | 10.34 | 16 | 27.2 | 7.00 | 8.16 | 16 | 2.95 | 8.94 | 1.90 | 16 | 27.2 | 7.00 | 8.16 | |
| 8 | 36.8 | 3.63 | 9.36 | 8 | 35.3 | 7.21 | 10.95 | 8 | 4.06 | 7.94 | 2.55 | 8 | 35.3 | 7.21 | 10.95 | |
| 4 | 38.6 | 5.30 | 14.32 | 4 | 23.7 | 10.79 | 10.99 | 4 | 1.57 | 8.80 | 0.138 | 4 | 23.7 | 10.79 | 10.99 | |
| 2 | 33.2 | 5.75 | 13.34 | 2 | 24.1 | 14.49 | 14.98 | 2 | 2.60 | 11.21 | 0.291 | 2 | 24.1 | 14.49 | 14.98 | |
| 1 | 31.2 | 4.85 | 10.55 | 1 | 25.9 | 9.10 | 10.13 | 1 | 0.5 | 7.47 | 0.264 | 1 | 25.9 | 9.10 | 10.13 | |
| 0.5 | 13.2 | 6.77 | 6.22 | 0.5 | 22.3 | 7.19 | 6.87 | 0.5 | 0.25 | 6.56 | 0.222 | 0.5 | 22.3 | 7.19 | 6.87 | |
| 0.25 | 6.3 | 8.46 | 3.77 | 0.25 | 16.6 | 6.77 | 4.81 | 0.25 | 0.125 | 5.56 | 0.146 | 0.25 | 16.6 | 6.77 | 4.81 | |
| 0.125 | 4.8 | 7.44 | 2.52 | 0.125 | 20.4 | 3.81 | 3.35 | 0.125 | 0.063 | 3.07 | 0.190 | 0.125 | 20.4 | 3.81 | 3.35 | |
| 0.063 | 3.7 | 10.33 | 2.65 | 0.063 | 18.7 | 8.32 | 6.70 | 0.063 | 0.032 | 5.54 | 0.377 | 0.063 | 18.7 | 8.32 | 6.70 | |
| 0.032 | 2.5 | 8.25 | 1.40 | 0.032 | 18.2 | 3.43 | 2.68 | 0.032 | 0.016 | 5.42 | 0.350 | 0.032 | 18.2 | 3.43 | 2.68 | |
| 0.016 | 3.0 | 7.21 | 1.54 | 0.016 | 17.2 | 2.70 | 1.99 | 0.016 | 0.0078 | 4.17 | 0.236 | 0.016 | 17.2 | 2.70 | 1.99 | |
| 0.0078 | 2.6 | 3.84 | 0.70 | 0.0078 | 14.4 | 2.98 | 1.67 | 0.0078 | 0.0039 | 3.24 | 0.170 | 0.0078 | 14.4 | 2.98 | 1.67 | |
| 0.0039 | 2.1 | 2.08 | 0.30 | 0.0039 | 10.2 | 1.61 | 0.70 | 0.0039 | 0.0016 | 2.43 | 0.021 | 0.0039 | 10.2 | 1.61 | 0.70 | |
| <0.002 | Est. 1.5 | 3.52 | 0.36 | <0.002 | Est. 7.8 | 2.99 | 0.97 | <0.002 | Est. 4.4 | 3.42 | 0.15 | <0.002 | Est. 7.8 | 2.99 | 0.97 | |
| Totals | 93.72 | 14.32 | 100.00 | Totals | 100.63 | 23.292 | 100.01 | Totals | 100.92 | 23.292 | 100.01 | Totals | 100.92 | 23.292 | 100.01 | |

APPENDIX 3

**DISTRIBUTION OF HEAVY MINERALS AND CHALCOPYRITE
IN OXIDIZED TILL**

The results of the analyses of the oxidized chalcopyrite-bearing till are listed in Table 3.1. The calculations performed are the same as for the unoxidized samples (Appendix 2); for explanations of Ap, Gp, Tp, and Trp see Appendix 2. Hp is the weight percentage of heavy minerals (chalcopyrite, malachite, and limonite). ND means not determined.

Table 3.1
Abundance of heavy minerals and chalcopyrite in oxidized till samples

| Sample 72-12BU6 | Fraction (mm) | Hp | Ap | Gp | Tp | Trp |
|-----------------|------------------|------|------|--------------|-------------|-------------|
| | 64 - 32 | 0.0 | 0.0 | 0.0 | 0.0 | 0.0 |
| | 32 - 16 | 13.7 | 13.7 | 35.0 | 4.80 | 49.4 |
| | 16 - 8 | 6.2 | 6.2 | 17.6 | 1.09 | 11.2 |
| | 8 - 4 | 8.6 | 8.6 | 9.1 | 0.78 | 8.0 |
| | 4 - 2 | 12.7 | 10.0 | 5.5 | 0.55 | 5.7 |
| | 2 - 1 | 17.5 | 14.1 | 5.9 | 0.83 | 8.6 |
| | 1 - 0.5 | 22.7 | 15.8 | 4.2 | 0.66 | 6.8 |
| | 0.5 - 0.25 | 25.3 | 13.9 | 3.3 | 0.46 | 4.7 |
| | 0.25 - 0.125 | 33.0 | 9.6 | 3.4 | 0.33 | 3.4 |
| | 0.125 - 0.063 | 32.8 | 6.4 | 2.3 | 0.15 | 1.5 |
| | 0.063 - 0.037 | 31.0 | 2.1 | 2.6 | 0.06 | 0.6 |
| | <0.037 | ND | ND | 11.2 | ND | ND |
| Totals | | | | 100.1 | 9.71 | 99.9 |

Sample 72-12EU46

| | | | | | | |
|---------------|---------------|------|-----|--------------|-------------|--------------|
| | 64 - 32 | 0.0 | 0.0 | 5.0 | 0.0 | 0.0 |
| | 32 - 16 | 0.0 | 0.0 | 18.8 | 0.0 | 0.0 |
| | 16 - 8 | 0.0 | 0.0 | 19.5 | 0.0 | 0.0 |
| | 8 - 4 | 6.4 | 6.4 | 11.9 | 0.76 | 27.2 |
| | 4 - 2 | 9.5 | 7.4 | 6.7 | 0.50 | 17.9 |
| | 2 - 1 | 8.8 | 7.2 | 6.4 | 0.46 | 16.5 |
| | 1 - 0.5 | 10.9 | 8.2 | 5.2 | 0.43 | 15.4 |
| | 0.5 - 0.25 | 10.6 | 7.2 | 4.7 | 0.34 | 12.2 |
| | 0.25 - 0.125 | 12.3 | 4.1 | 4.4 | 0.18 | 6.5 |
| | 0.125 - 0.063 | 14.5 | 2.7 | 2.9 | 0.08 | 2.9 |
| | 0.063 - 0.037 | 15.7 | 1.3 | 3.1 | 0.04 | 1.4 |
| | <0.037 | ND | ND | 11.4 | ND | ND |
| Totals | | | | 100.0 | 2.79 | 100.0 |

Sample 72-12EU56

| | | | | | | |
|---------------|---------------|------|------|--------------|--------------|-------------|
| | 64 - 32 | 0.0 | 0.0 | 4.0 | 0.0 | 0.0 |
| | 32 - 16 | 21.1 | 21.1 | 37.2 | 7.85 | 49.1 |
| | 16 - 8 | 18.5 | 18.5 | 21.2 | 3.92 | 24.5 |
| | 8 - 4 | 16.8 | 16.8 | 8.7 | 1.46 | 9.1 |
| | 4 - 2 | 21.4 | 16.2 | 4.4 | 0.71 | 4.4 |
| | 2 - 1 | 24.2 | 17.3 | 4.8 | 0.83 | 5.2 |
| | 1 - 0.5 | 25.6 | 14.9 | 3.3 | 0.49 | 3.1 |
| | 0.5 - 0.25 | 29.4 | 12.1 | 2.8 | 0.34 | 2.1 |
| | 0.25 - 0.125 | 36.6 | 7.9 | 3.0 | 0.24 | 1.5 |
| | 0.125 - 0.063 | 33.0 | 5.3 | 1.9 | 0.10 | 0.6 |
| | 0.063 - 0.037 | 31.5 | 2.4 | 2.0 | 0.05 | 0.3 |
| | <0.037 | ND | ND | 6.8 | ND | ND |
| Totals | | | | 100.1 | 15.99 | 99.9 |

Table 3.1 (cont.)

| Sample 72-12GU36 | | Fraction (mm) | Hp | Ap | Gp | Tp | Trp |
|------------------|---------|------------------|------|-----|-------|------|-------|
| 64 | - 32 | | 0.0 | 0.0 | 0.0 | 0.0 | 0.0 |
| 32 | - 16 | | 0.0 | 0.0 | 32.3 | 0.0 | 0.0 |
| 16 | - 8 | | 0.9 | 0.9 | 20.6 | 0.19 | 16.4 |
| 8 | - 4 | | 2.2 | 2.2 | 10.1 | 0.22 | 19.0 |
| 4 | - 2 | | 2.3 | 1.9 | 7.5 | 0.14 | 12.1 |
| 2 | - 1 | | 3.4 | 2.7 | 6.9 | 0.19 | 16.4 |
| 1 | - 0.5 | | 5.4 | 3.7 | 4.5 | 0.17 | 14.7 |
| 0.5 | - 0.25 | | 6.6 | 3.1 | 3.3 | 0.10 | 8.6 |
| 0.25 | - 0.125 | | 12.7 | 2.8 | 3.0 | 0.08 | 6.9 |
| 0.125 | - 0.063 | | 14.1 | 2.1 | 1.9 | 0.04 | 3.5 |
| 0.063 | - 0.037 | | 13.8 | 1.5 | 2.1 | 0.03 | 2.6 |
| | <0.037 | | ND | ND | 7.8 | ND | ND |
| Totals | | | | | 100.0 | 1.16 | 100.2 |

Sample 72-12FU3

| | | | | | | | |
|--------|---------|--|------|-----|-------|------|-------|
| 64 | - 32 | | 0.0 | 0.0 | 0.0 | 0.0 | 0.0 |
| 32 | - 16 | | 0.0 | 0.0 | 30.8 | 0.0 | 0.0 |
| 16 | - 8 | | 1.2 | 1.2 | 24.7 | 0.30 | 14.3 |
| 8 | - 4 | | 4.7 | 4.7 | 8.2 | 0.39 | 18.6 |
| 4 | - 2 | | 6.1 | 5.4 | 4.8 | 0.26 | 12.4 |
| 2 | - 1 | | 7.9 | 6.5 | 5.3 | 0.35 | 16.7 |
| 1 | - 0.5 | | 11.0 | 7.5 | 4.7 | 0.35 | 16.7 |
| 0.5 | - 0.25 | | 10.1 | 5.0 | 4.3 | 0.22 | 10.5 |
| 0.25 | - 0.125 | | 14.8 | 3.8 | 3.9 | 0.15 | 7.1 |
| 0.125 | - 0.063 | | 13.3 | 2.2 | 2.7 | 0.06 | 2.9 |
| 0.063 | - 0.037 | | 13.0 | 0.5 | 3.1 | 0.02 | 1.0 |
| | <0.037 | | ND | ND | 7.5 | ND | ND |
| Totals | | | | | 100.0 | 2.10 | 100.2 |

Sample 72-12FU4

| | | | | | | | |
|--------|---------|--|------|------|-------|-------|-------|
| 64 | - 32 | | 0.0 | 0.0 | 0.0 | 0.0 | 0.0 |
| 32 | - 16 | | 1.6 | 1.6 | 35.6 | 0.57 | 14.5 |
| 16 | - 8 | | 3.5 | 3.5 | 27.8 | 0.97 | 24.7 |
| 8 | - 4 | | 8.5 | 8.5 | 7.1 | 0.60 | 15.3 |
| 4 | - 2 | | 19.0 | 13.3 | 3.4 | 0.45 | 11.5 |
| 2 | - 1 | | 17.3 | 13.5 | 3.6 | 0.49 | 12.5 |
| 1 | - 0.5 | | 18.6 | 12.6 | 3.0 | 0.38 | 9.7 |
| 0.5 | - 0.25 | | 17.7 | 8.4 | 2.6 | 0.22 | 5.6 |
| 0.25 | - 0.125 | | 20.6 | 5.4 | 2.4 | 0.14 | 3.6 |
| 0.125 | - 0.063 | | 16.6 | 3.9 | 1.9 | 0.074 | 1.9 |
| 0.063 | - 0.037 | | 15.3 | 1.4 | 2.5 | 0.035 | 0.9 |
| | <0.037 | | ND | ND | 9.9 | ND | ND |
| Totals | | | | | 100.0 | 3.929 | 100.2 |

Sample 72-12-CU6

| | | | | | | | |
|--------|---------|--|------|------|-------|------|-------|
| 64 | - 32 | | 0.0 | 0.0 | 0.0 | 0.0 | 0.0 |
| 32 | - 16 | | 0.0 | 0.0 | 33.8 | 0.0 | 0.0 |
| 16 | - 8 | | 10.8 | 10.8 | 19.6 | 2.12 | 45.0 |
| 8 | - 4 | | 6.2 | 6.2 | 10.1 | 0.63 | 13.4 |
| 4 | - 2 | | 9.7 | 8.3 | 6.2 | 0.51 | 10.8 |
| 2 | - 1 | | 11.6 | 9.3 | 5.3 | 0.49 | 10.4 |
| 1 | - 0.5 | | 14.4 | 10.4 | 3.7 | 0.38 | 8.1 |
| 0.5 | - 0.25 | | 16.5 | 8.9 | 3.2 | 0.28 | 5.9 |
| 0.25 | - 0.125 | | 17.6 | 5.6 | 3.4 | 0.19 | 4.0 |
| 0.125 | - 0.063 | | 18.9 | 2.7 | 2.3 | 0.06 | 1.3 |
| 0.063 | - 0.037 | | 20.0 | 1.8 | 2.6 | 0.05 | 1.1 |
| | <0.037 | | ND | ND | 9.8 | ND | ND |
| Totals | | | | | 100.0 | 4.71 | 100.0 |